Vine Nutrition

VITI DOC

DIAGNOSE

FINAL REPORT TO WINE AUSTRALIA

Project Number: **CSU 1702-3**

Principal Investigator: **Suzy Y Rogiers**

Research Organisations: **National Wine & Grape Industry Centre/ NSW Department of Primary Industries/ Charles Sturt University**

Date: **15.12.2021**

Vine Nutrition: A Diagnostic App for Nutrient Disorder Assessment

CSU 1702-3

Suzy Rogiers, Lihong Zheng, Alex Oczkowski, Motiur Rahaman, Manoranjan Paul,
Tintu Baby, Krista Mentjox, Leigh Schmidtke, Rob Walker, Bruno Holzapfel

Copyright Statement:

© State of New South Wales through the Department of Regional NSW 2021. The information contained in this publication is based on knowledge and understanding at the time of writing (December 2021). However, because of advances in knowledge, users are reminded of the need to ensure that the information upon which they rely is up to date and to check the currency of the information with the appropriate officer of the Department of Primary Industries or the user's independent adviser.

Disclaimer:

The State of New South Wales, including the NSW Department of Industry (" the Department"), does not give any warranty, guarantee or representation about the accuracy, currency or completeness of any information contained in this document [or DVD, film, material, etc.] (including, without limitation, any information included in the document which was provided by third parties). The State of New South Wales (including the Department) provides this document [or DVD, film, material, etc.] without assumption of a duty of care to any person.

To the fullest extent permitted by law, the State of New South Wales (including the Department) excludes all liability in relation to the information contained in this document [or DVD, film, material, etc.] or for any injury, expense loss, or damage whatsoever (including without limitation liability for negligence and consequential losses) suffered or incurred.

The product trade names in this publication are supplied on the understanding that no preference between equivalent products is intended and that the inclusion of a product name does not imply endorsement by the department over any equivalent product from another manufacturer.

Table of Contents

..... 1

FINAL REPORT TO WINE AUSTRALIA 1

1. Executive summary 4

2. Background 5

3. Project Aims 6

4. Methods/Results/Discussion 6

Chapter 1- Development of a Diagnostic App for Nutritional Disorders 6

1. Regional Survey 6
2. One-on-one Interviews 7
3. Nutritional Disorder Symptom Formation for Image Database 10
4. Algorithm development 19
5. Prototyping and testing 19

Chapter 2- Hyperspectral Imaging of leaves to detect nutrient disorders 29

Introduction 29

Method 30

Results 31

Discussion 50

Chapter 3- Grapevine Tissue Sampling for Nutrient Analysis 52

Introduction 52

Methods 53

Results 56

Discussion 71

5 Conclusions/Outcomes 74

6 Recommendations 75

7 Appendix 1: Communication 76

8 Appendix 2: Intellectual Property 77

9 Appendix 3: References 78

References for Chapter 2 78

References for Chapter 3 81

10 Appendix 4: Staff 84

11 Appendix 5: Survey questions 85

12 Appendix 6: Acknowledgements 86

Abstract

A smartphone app was developed for the diagnosis of nutritional disorders in grapevines using visual leaf symptoms. The app uses artificial intelligence (AI) to assess images captured by the user using a standard camera on a smartphone. To develop the symptom database, glasshouse Chardonnay and Shiraz vines were grown hydroponically in various nutrient solutions and RGB images were captured of leaves as symptoms developed and progressed. The image database includes symptoms for nitrogen, potassium, magnesium, calcium and iron deficiency. Machine learning was used to process the images and a model with high accuracy and rapid processing times was incorporated into the app. However, outdoor image acquisition of leaves on field vines resulted in lower accuracy and further development is therefore necessary. In a separate study, hyperspectral imaging accompanied by machine learning also proved effective in identifying leaf age-based differences and individual nutrient disorders. Lastly, based on gradients in nutrients along the petiole, tissue sampling protocols for nutrient assessment were refined.

1. Executive summary

Optimum grapevine nutrition is required for long-term plant resilience against biotic and abiotic stresses, and for achieving the desired yield and berry composition. The most accurate method to determine vine nutrient status is through a chemical analysis of sampled tissues. Obvious visual leaf symptoms can also be useful in diagnosing nutrient disorders but reference images provided in field manuals are often not clear, not cultivar specific and don't show the progression of symptoms. Better methods are required to use these visual leaf symptoms to optimum benefit. This project had 3 objectives. The first objective was to develop a smartphone diagnostic app that provides information to growers on nutritional disorders in grapevines using visual symptoms. The second objective was to assess hyperspectral imaging as a method for diagnosing early-stage nutritional disorders. The third objective was to assess various tissue sampling protocols for vine nutrient assessment.

Diagnostic App

The advancement of image processing and machine learning has made it feasible to develop rapid tools to assess grapevine nutritional disorders using visual symptoms. We therefore set out to develop a smartphone app to capture and analyse images of vine leaves displaying symptoms of particular nutritional disorders. This tool uses underlying customised machine learning and computer vision techniques to assist identification of nutrient deficiencies. The app also contains an image library of symptomatic leaves for various nutrient disorders to assist growers in making in-field assessments. Finally, the app contains links to information on how to remedy the specific nutritional disorder. Limited field testing has indicated that non-uniform light and complex backgrounds decreases the app's accuracy and therefore further development is required. The app is useful only after visual symptoms appear and is not intended as a replacement for plant tissue tests.

Hyperspectral Imaging Study

Hyperspectral (HS) imaging is a potential method to detect early indicators of plant stress, invisible to the human eye. In this study, HS imaging was successfully employed in the 380 nm to 1000 nm wavelength range to investigate the efficacy of detecting age, healthiness and individual nutrient deficiency of grapevine leaves collected from vineyards located in central west NSW, Australia. Several features were employed across the Ultraviolet (UV), Visible (VIS) and Near Infrared (NIR) regions including mean brightness, mean 1st derivative brightness, variation index, mean spectral ratio, normalised difference vegetation index (NDVI) and standard deviation (SD). Experimental results demonstrate that these features could be utilised with a high degree of effectiveness to compare age, identify unhealthy samples and not only to distinguish between control and nutrient deficient leaves

but also to identify specific nutrient deficiencies. Therefore, our work corroborated that HS imaging has excellent potential as a non-destructive as well as a non-contact method to detect age, healthiness and specific nutrient deficiencies of grapevine leaves. With further development, this technique could allow frequent assessment of nutrient status across a block and allow the development of nutritional maps at several time points across a growing season.

Tissue Sampling Study
Leaf tissue nutrient concentration is useful for determining grapevine nutritional status and managing vineyard nutrition. Current Australian guidelines are based on the analysis of petioles at flowering or leaf blades at veraison, sampled adjacent to the basal inflorescence and bunch. Our data indicate that nutrient concentrations were non-uniform along the length of the petiole. The concentrations of some nutrients within the leaf blade were correlated with those of the petiole but this was dependent on the cultivar and the time of sampling. The nutrient concentrations of the bunchstem were more closely correlated to the petiole than the blade. Cultivar differences were also apparent, but this depended on the individual nutrient and the sampling time. Therefore, tissue nutrient analysis will be meaningful only if sampling is consistent across these variables. These results suggest that the entire petiole should be sampled and that vineyard specific historical databases with consistent sampling procedures will be most meaningful for nutrition assessments.

This work was carried out in a close collaboration between Regional NSW, the Department of Computing and Mathematics at Charles Sturt University, and the National Wine & Grape Industry Centre with strong support from the NSW Wine Industry. Further support was provided by the GATE during the commercialisation phase of the app.

2. Background

Plant nutrition is a cornerstone of grapevine health and productivity regardless of growing region or climatic zone. It can be a very significant cost to the management of a vineyard, and if not handled correctly, yield and quality will suffer. If severe enough, nutrient deficiency or toxicity can result in deformity, discoloration and even death of tissues. These disorders also increase risk to pathogens and abiotic stresses such as frost and heat. The nutrient profile of plants is most commonly assessed through a tissue element analysis. A number of leaf petioles or blades are collected across a representative area of the block and these are sent to a diagnostic laboratory for analysis. The results are then compared to reference standards to determine any deficiencies or toxicities. Correct tissue sampling is imperative to generating data that is meaningful. The leaf blade, leaf petiole or bunch stem may be sampled but it is uncertain how meaningful each of these tissues are in relation to whole vine nutritional status at any particular phenological stage. A detailed assessment of these tissues in relation to each other may offer some clues as the best tissue to sample at any particular time.

Visual symptoms of nutrient disorders can also be informative, however they are particularly difficult to diagnose. There are few clear reference images available in the literature or field manuals. Moreover, these images do not show symptom progression or cultivar differences. Combining advances in mobile device camera quality, image processing and machine learning opens up avenues for the accurate diagnosis of these symptoms using AI. Smartphones are relatively cheap and easily transportable to the field, and so offer a readily available tool to carry out rapid assessments of symptoms that are already visually apparent.

Ideally, the identification of stresses should occur prior to visible physical damage. Hyperspectral imaging may be useful in this regard. RGB sensors detect the reflected red, green, blue wavelengths of the light spectrum (390 to 750 nm) while multispectral and hyperspectral sensors range usually in the near and shortwave infrared region from 0.4 to 2.5 um. Usually, signature wavelengths are

identified for each particular stress. It is possible to discern each nutrient disorder through changes in unique biochemical changes and thus reflectance spectra. This technology can be combined with machine learning to allow for precise diagnosis at the individual leaf level, and beyond to the whole block level. Hyperspectral imaging is advancing rapidly in many crops and may be applied successfully to viticulture as a non-destructive and non-invasive method for monitoring nutrient status.

The overall objective of this work was to optimise plant nutrition assessments through three different approaches: traditional tissue assessment protocols, visual symptom assessment and hyperspectral imaging.

3. Project Aims

I. Aim: Develop an app that provides information to growers on nutritional disorders in a white and red variety.

Deliverable: A user-friendly app that provides an assessment of disorders in grapevine nutrition using (a) intelligent image capture and intelligent analytics of the image; and (b) a digital image database that growers can refer to for their own assessments.

II. Aim: Develop the capacity to assess vine nutrient status using a deep learning framework based on a hyperspectral image library

Deliverable: Deep learning framework using hyperspectral images for leaf nutrient classification.

III. Aim: Provide a refined tissue sampling protocol by determining which leaf tissue is the most appropriate indicator for vine macro and micronutrient status.

Deliverable: Revised sampling protocol for the assessment of vine nutrient status.

4. Methods/Results/Discussion

Chapter 1- Development of a Diagnostic App for Nutritional Disorders

1. Regional Survey

The objective of the survey was two-fold: 1) to assess current practise in assessing disorders, and (2) to determine if industry would be interested in using a diagnostic app for nutritional disorders. The questionnaire was paper based and administered to 4 growing regions: Swan Hill, Mildura, Griffith and Tumbarumba during the AWRI Pre-season Pest and Disease Workshop (August 2019) and NWGIC Spring Vine Health Field Days (September 2019). It consisted of 17 questions.

Results

- Most respondents use a combination of resources to diagnose disorders. About 65% relied on experience but also other methods: half used manuals, half used diagnostic labs. Only 1 used Google and only 1 used a viticulturist.
- All respondents except one have sent their samples to a diagnostic lab for nutritional analyses. About half the respondents conducted the test every year and the other half less frequently than this. Only half have used an entomology or pathology lab for the diagnosis of other disorders.
- 100% of the respondents indicated that they would use an app to help with pest/disease/nutritional diagnosis. Only 15% said they were currently using another app. This included Pmapp and Pest ID.
- 100% of the respondents wanted the app to be able to address all three: pest, disease and nutrition.
- Most of the respondents were unsure and did not respond to the question regarding the minimum acceptable accuracy for the correct diagnosis. Of the 7 that responded, half indicated that 80% was acceptable, half indicated that 90% was acceptable, and one wanted 100% accuracy.
- The maximum processing time users were willing to wait ranged widely from immediate to 1 day.
- Most (70%) of the respondents would prefer to take the pictures in the vineyard and only one preferred to take the pictures indoors. One respondent indicated a preference for both options and two respondents thought either option was acceptable.
- All of the respondents wanted to be able to tag the geolocation.
- All of the respondents wanted to have links to fact sheets and other resources.
- All of the respondents wanted real time incidence information for their region.
- All of the respondents, except one, wanted to create a historical database of their blocks.
- The internet connection available to the respondents was assessed as acceptable (70%). Only 10% of the respondents found it poor. The rest found it variable.
- 60% of the respondents wanted further information about the app as it developed.

2. One-on-one Interviews

We wanted to gain a deeper understanding of what the major challenges were for the industry in terms of vine nutrition and to gain insights into the potential user's world to help guide how we might design the app. We thus carried out 10 one-on-one interviews covering small, intermediate and large companies from the major viticultural regions across Australia (1 hour each). We interviewed 4 small, 2 intermediate and 4 large operations. We spoke to 4 on the ground vineyard personnel and 4 technical specialists or managers. 6 were male and 4 were female.

We asked about their productivity goals and motivations, how they manage vine nutrition, what systems they use to manage their vineyard, what sort of devices they use, how they manage their data, how they view R&D and industry information from different sources, and how they keep up to date with the latest developments in the industry.

Figure 1. Topics explored in one-on-one interviews

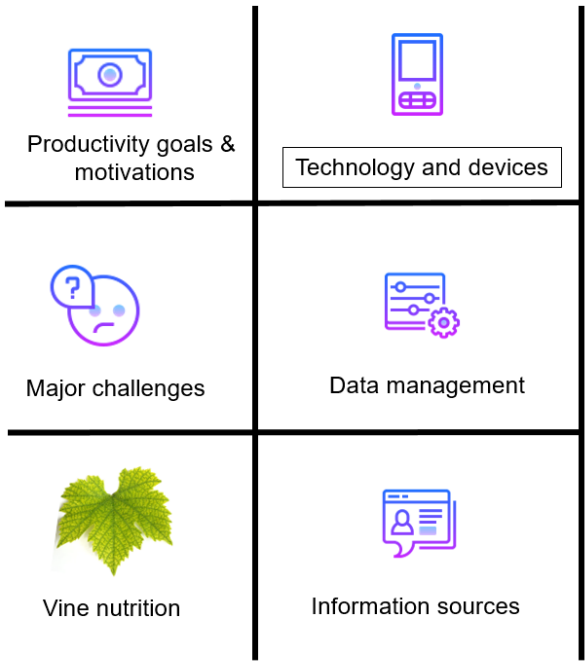


Figure 2. We used affinity mapping to organise data from all ten interviews. We had more than 100 insights which enabled us to draw out key challenges.

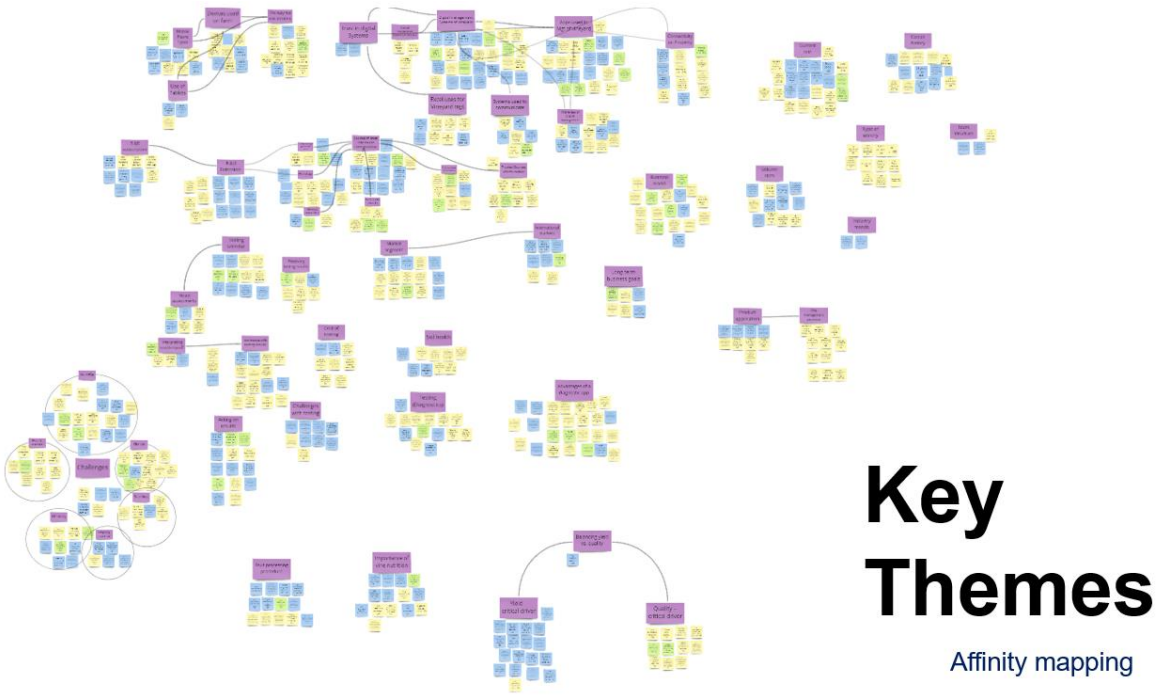


Figure 3. Interview responses according to affiliation with small or large operations

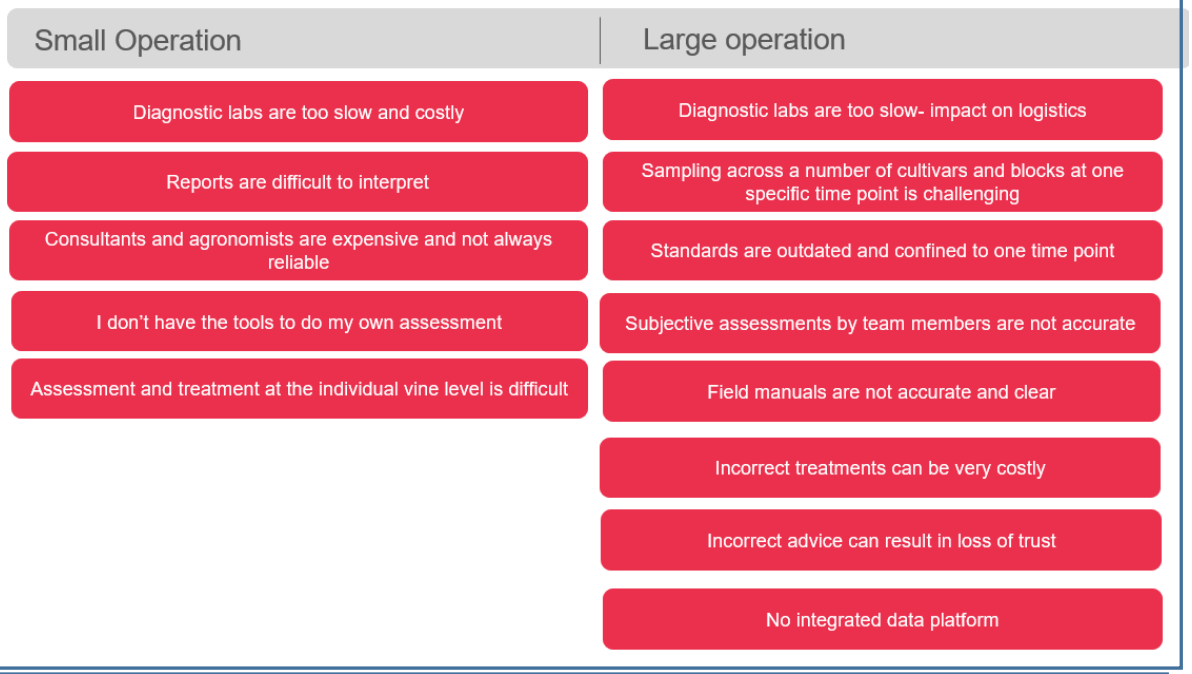
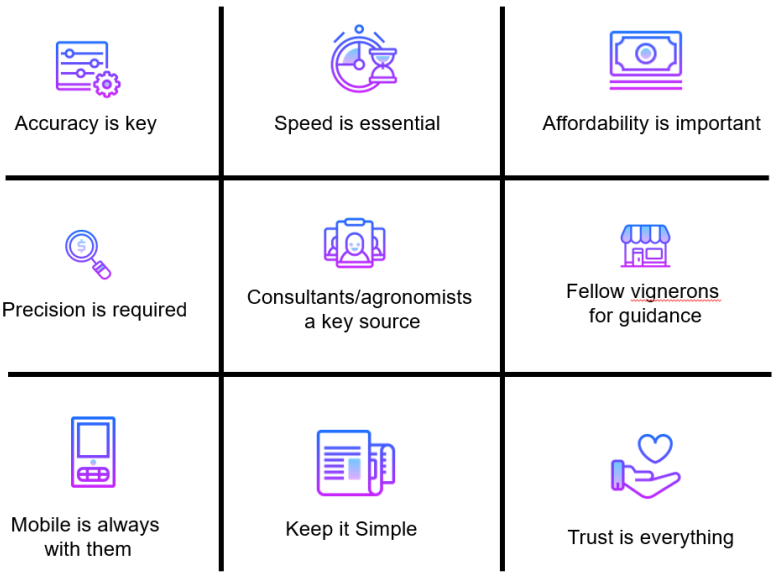


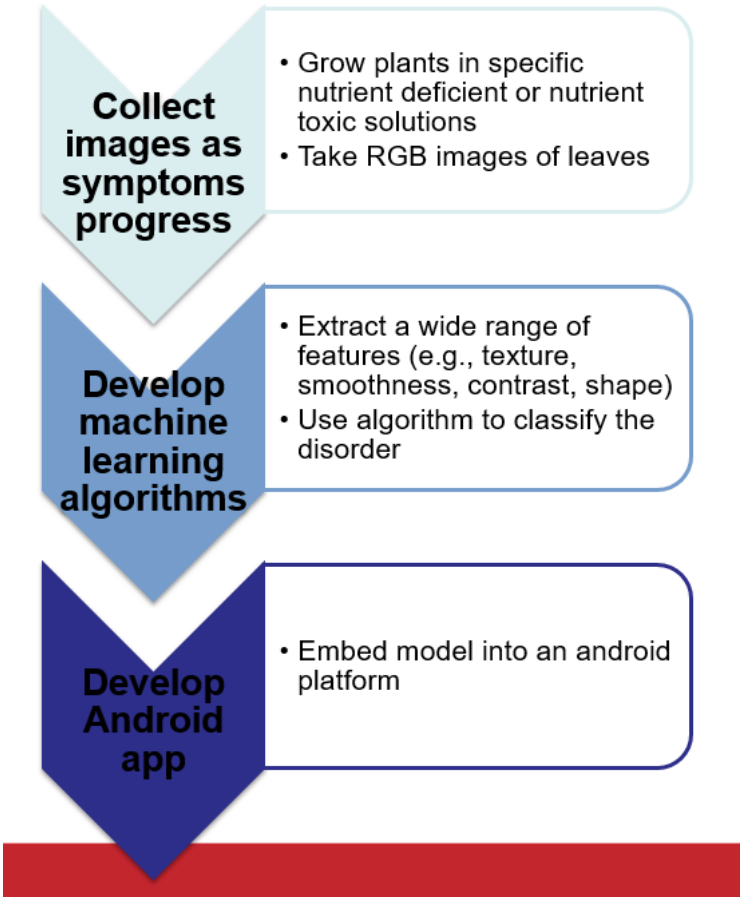
Figure 4. Summary of feedback from industry members regarding current and potential new methods and tools for vine symptom identification.



This feedback gave us confidence that a simple and affordable Smartphone app with the capability to analyse nutrient disorders with accuracy and speed would likely have high adoption by the industry.

3. Nutritional Disorder Symptom Formation for Image Database

Figure 5. Overall approach to developing a diagnostic app.



Extensive method development was undertaken to ensure that visual symptoms were specific to a particular nutrient deficiency. Initially 3-year-old rooted cuttings were grown in a sand culture outdoors but leaves did not show symptoms over the entire season because the vines were quite large and had ample nutrient reserves to compensate for the absence of nutrients in the sand. We then progressed to a hydroponic system using short canes. Symptoms may be different between a red and white variety and therefore we focussed on both Shiraz and Chardonnay. Details of the method are as follows:

After five weeks of rooting, one-year-old dormant cuttings of Chardonnay and Shiraz vines were potted into 2.5 L pots containing perlite and established in greenhouse conditions under natural light with an average air temperature of 25°C during the day and 15°C during the night. The vines were placed in a randomised block design across 3 tables with each table supporting 3 vines of each treatment. One shoot was retained on each plant and staked vertically. Nutrient treatments were applied manually to the point of run-off. The control was a full nutrient treatment based on modified half-strength Hoagland's solution (Baby et al., 2014). The other deficiency treatments were the same nutrients except with the elimination of the nutrient of interest. Petioles were collected at the 10-leaf stage from 8 replicate plants, dried, ground and assessed by ICP-OES at a commercial diagnostic lab (Charles Sturt University,

Wagga Wagga, NSW). N was determined on a 50-mg sample with a VarioMAX combustion analyser (Elementar, Hanau, Germany).

Figure 6. Vines were developed from short single node cuttings to minimise nutrient mobilisation from the perennial woody components. Upon adequate root formation, plants were potted into perlite and transferred to a temperature-controlled glasshouse where a specific nutrient solution was administered to each pot.





Chardonnay Symptoms

Figure 7. Progression of N (nitrogen) deficiency in Chardonnay from left to right. Symptoms: uniform loss of greenness and yellowing across the leaf blade. The veins do not remain bright green. Mature leaves are usually more yellow than younger leaves.



Figure 8. Progression of K (potassium) deficiency in Chardonnay from left to right. Symptoms: yellowing of leaf margins, followed by burning and sometimes downward curling of leaf margins. With increasing severity, the burning progresses inwards and appears in patches within the remainder of the leaf. Emerging leaves (leaves at the shoot tip) initially look normal. However, as these grow/expand they will be deformed, shiny and roll downwards.



Figure 9. Progression of Mg (magnesium) deficiency in Chardonnay from left to right. Symptoms: interveinal areas form yellow striations followed by necrotic lesions. The lesions first appear somewhat interior to the leaf margin and then progress inwards. This is different from K deficiency where burning is initiated on the leaf margin. Symptoms appear first in the older leaves.



Figure 10. Progression of Ca (calcium) deficiency in Chardonnay from left to right. Symptoms: burning at leaf margins which progressively moves inwards in distinct patches towards the centre of the leaf. Older leaves are affected first.



Figure 11. Progression of B (boron) toxicity in Chardonnay from left to right. Symptoms: small reddish-brown lesions begin at the leaf margins and then appear across the blade. Small lesions may join to form larger lesions and the entire margin may appear uniformly burnt.



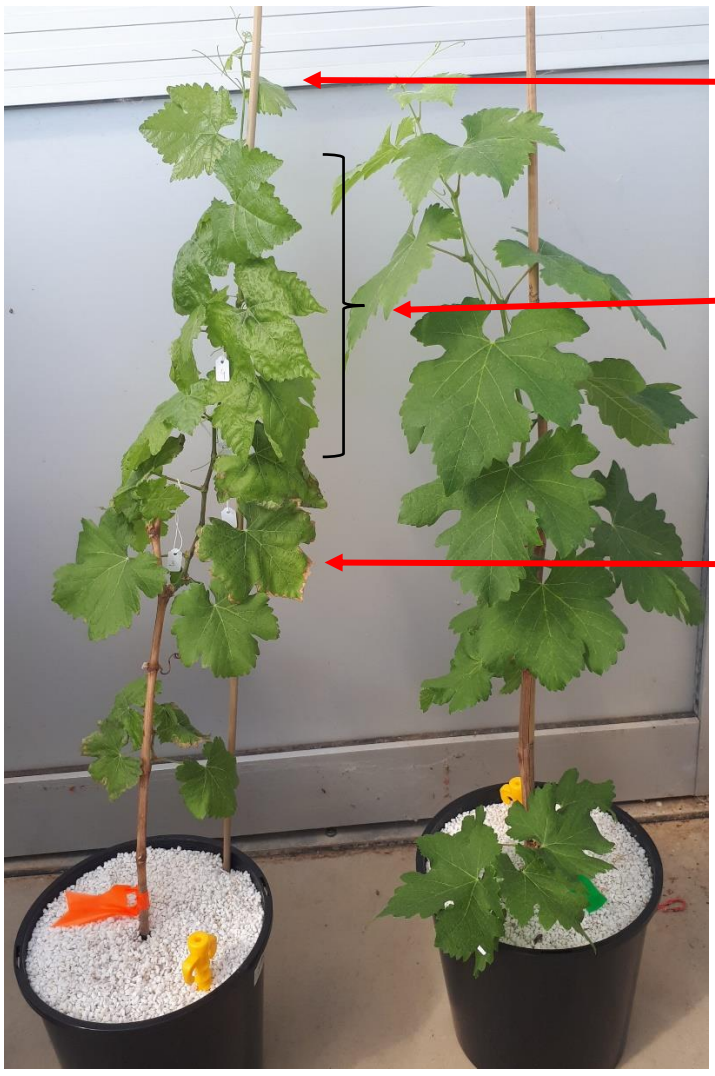
Shiraz Symptoms

Figure 12. Progression of N (nitrogen) deficiency in Shiraz from left to right. Symptoms: uniform loss of greenness and yellowing across the leaf blade. The veins do not remain bright green. Mature leaves are usually more yellow than younger leaves.



Figure 13. Progression of K (potassium) deficiency in Shiraz from left to right. Symptoms: yellowing of leaf margins, followed by burning and sometimes downward curling of leaf margins. With increasing severity the burning progresses towards the centre of the leaf. Emerging leaves (leaves at the shoot tip) initially look normal. However, as these grow/expand they will be deformed, shiny and roll downwards.





Emerging leaves look normal initially.

When potassium deficient young leaves grow/expand they will be deformed; shiny and rolled downwards.

Old leaf showing burnt margins

K deficient plant Normal plant

Figure 14. Progression of Mg (magnesium) deficiency in Shiraz from left to right. Symptoms: interveinal areas form yellow or reddish striations. The major veins retain a band of dark green. The minor veins do not become accented as in Fe deficiency. In severe cases, necrosis occurs in the interveinal area starting from near the leaf margin and extending inwards. Symptoms appears first in the older leaves.



Figure 15. Progression of Ca (calcium) deficiency in Shiraz from left to right. Symptoms: burning at leaf margins which progressively moves inwards in distinct patches towards the centre of the leaf. Older leaves are affected first.



Figure 16. Progression of Fe (iron) deficiency in Shiraz from left to right. Symptoms: younger leaves are affected first. These young leaves show interveinal chlorosis and very dark green veins- including the minor veins to give a very intricate lacy pattern. Necrosis is unusual. However, as the severity of the deficiency increases, chlorosis can begin in the older leaves.



Figure 17. Progression of B (boron) toxicity in Shiraz from left to right. Symptoms: small reddish-brown lesions begin at the leaf margins and then appear across the blade. Small lesions may join to form larger lesions and the entire margin may appear uniformly burnt. Cupping and deformation of young leaves. Whole vine growth and leaf size also reduced.





P (phosphorus) deficiency did not result in obvious visual leaf symptoms, however vines were severely stunted with both root and shoot growth affected.





Figure 18. Size difference between a P deficient (below) and control Chardonnay plant (left). Note no visual leaf symptoms on the P deficient vine.

Boron (B) deficiency also did not result in obvious leaf symptoms however plants were stunted and new growth on the shoot tips was severely compromised. Chardonnay plants were more sensitive to B deficiency than Shiraz plants and would not undergo budburst.

Figure 19. Developing shoot on control Shiraz plant with adequate nutrition (left) and on B deficient plant (right). Newly forming leaves are necrotic and curl downward.





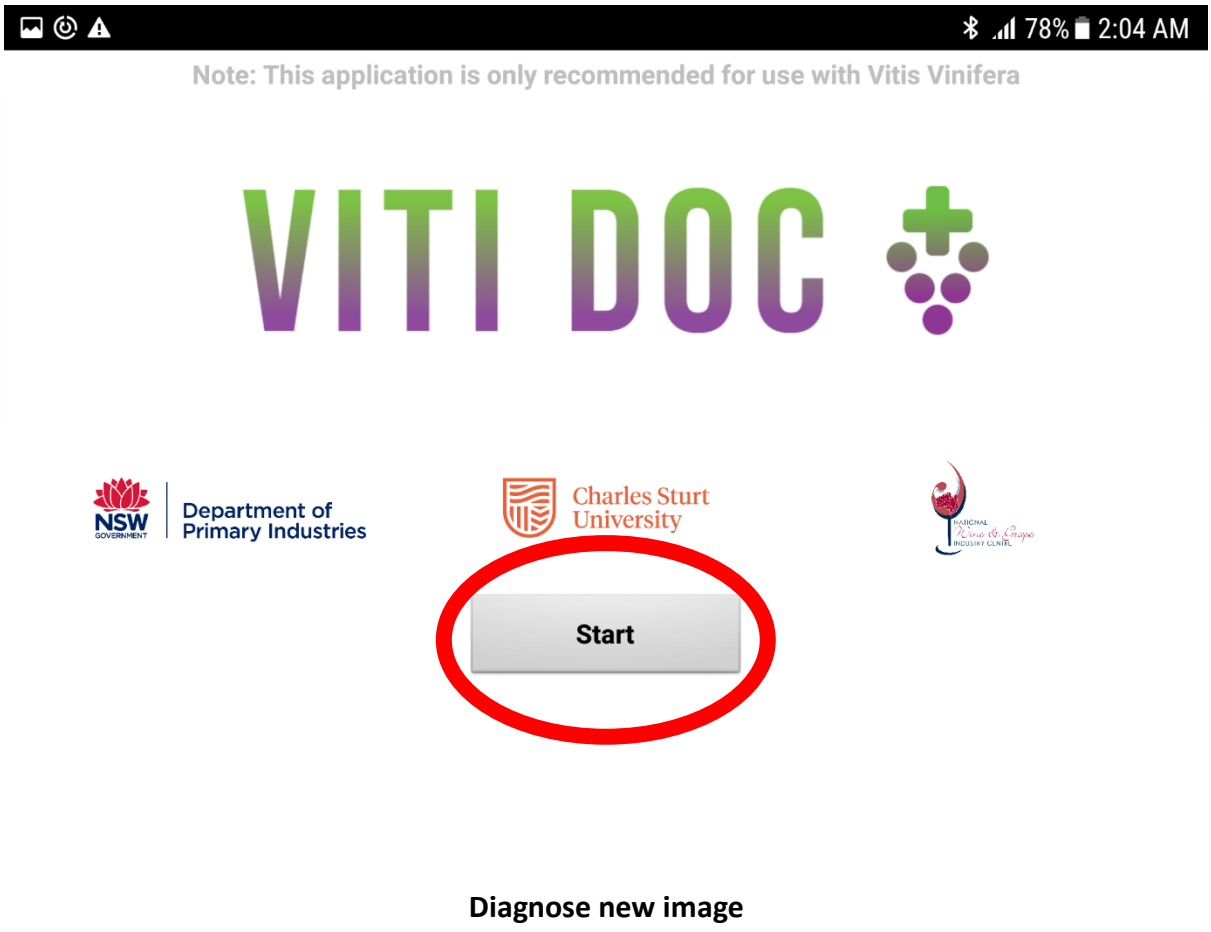
Table 1. Summary of nutrient disorder symptoms for well-watered Chardonnay and Shiraz vines grown in greenhouse conditions at 25°C.

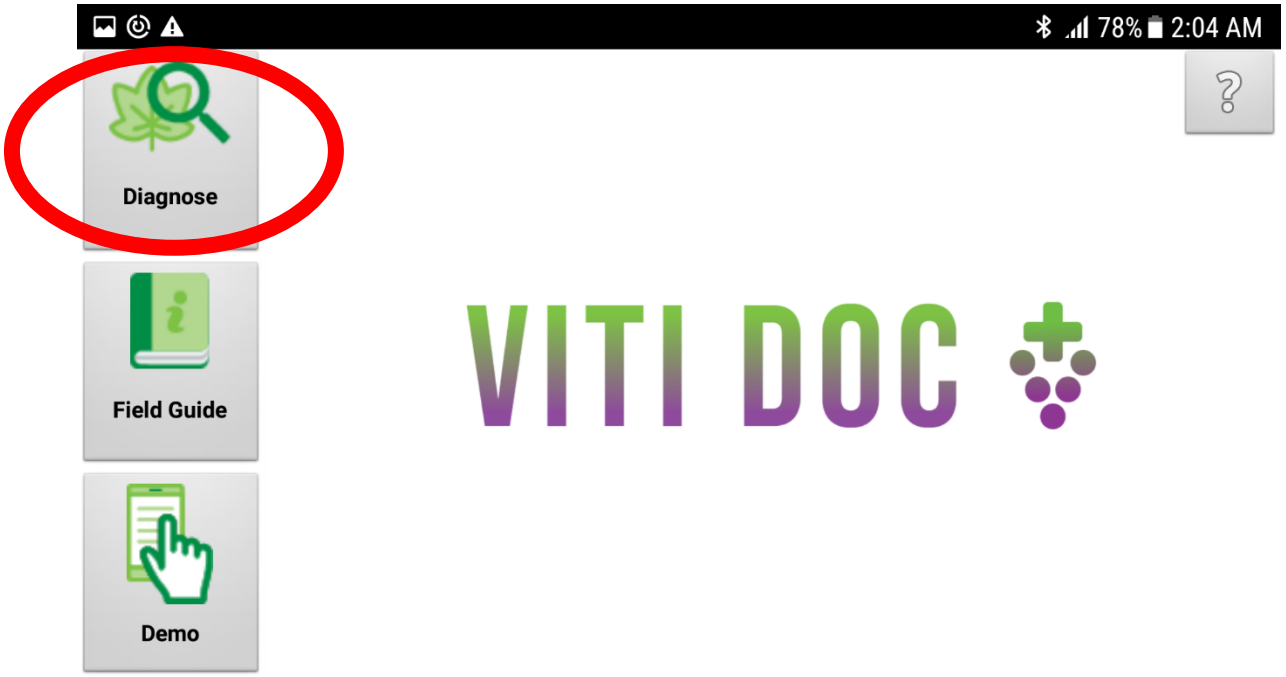
Nutrient disorder	First leaves to show symptoms	Necrotic leaf margins	Interveinal chlorosis	Distinct necrotic legions across blade	Leaf rolling	Vein coloration
N deficiency	Older	X	Even yellowing	X	X	Normal
P deficiency	Emerging leaves	X	X	X	Emerging leaves- downward rolling	Normal
K deficiency	Older	Yes	Striations	Yes	downward rolling of mature leaves	Normal
Mg deficiency	Older	X	Striations	Yes	X	Normal
Ca deficiency	Younger	Yes	X	Yes	X	Normal
Fe deficiency	Younger	X	Even interveinal chlorosis across the blade	X	X	Dark green major and minor veins giving intricate pattern
B deficiency	Shoot tips necrotic	X	X	X	Cupping of young emerging leaves	Normal
B toxicity	older	Yes	Yes	Yes	Cupping of emerging leaves	Normal

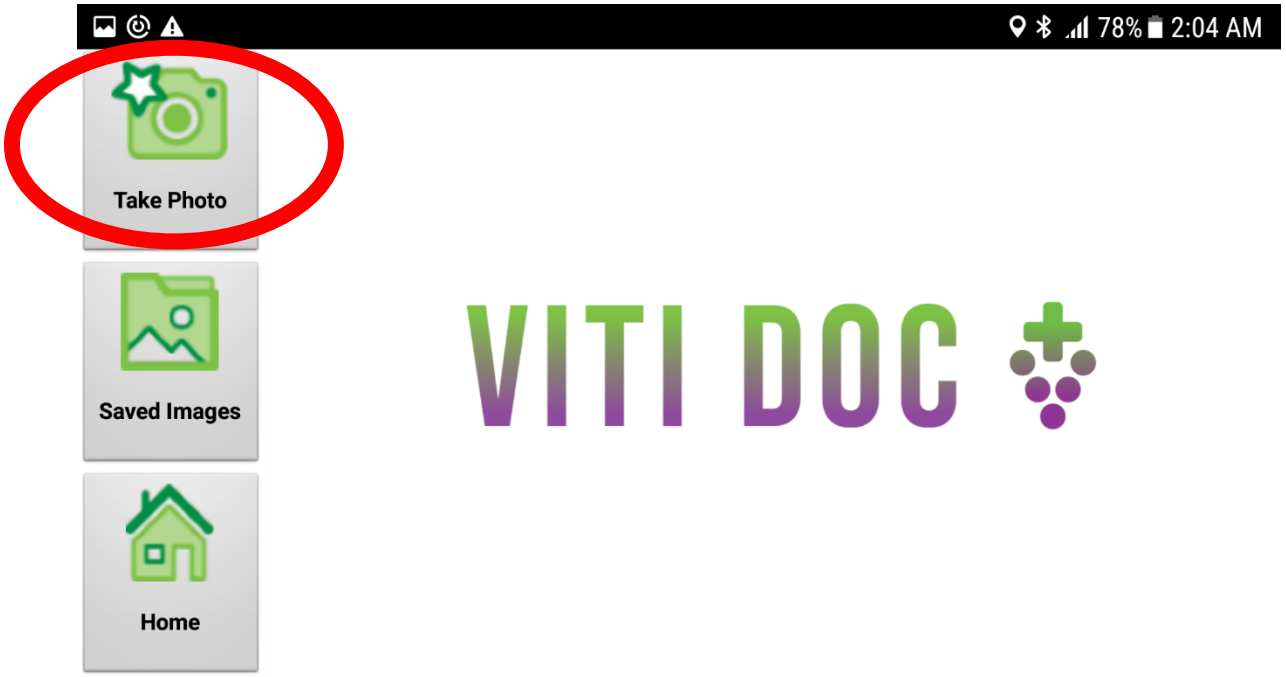
4. Algorithm development

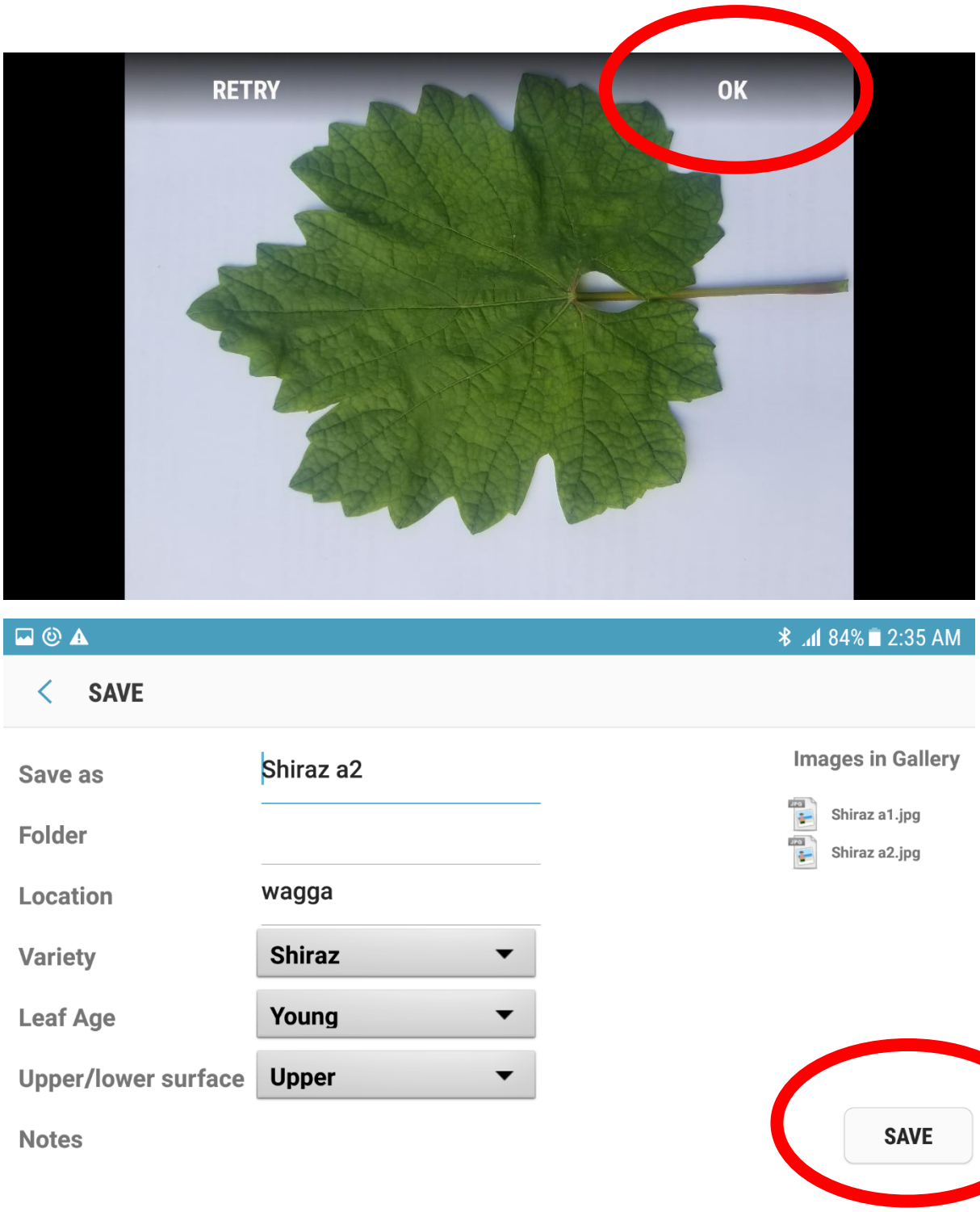
This section contains commercial-in-confidence information and is therefore not available for publication.

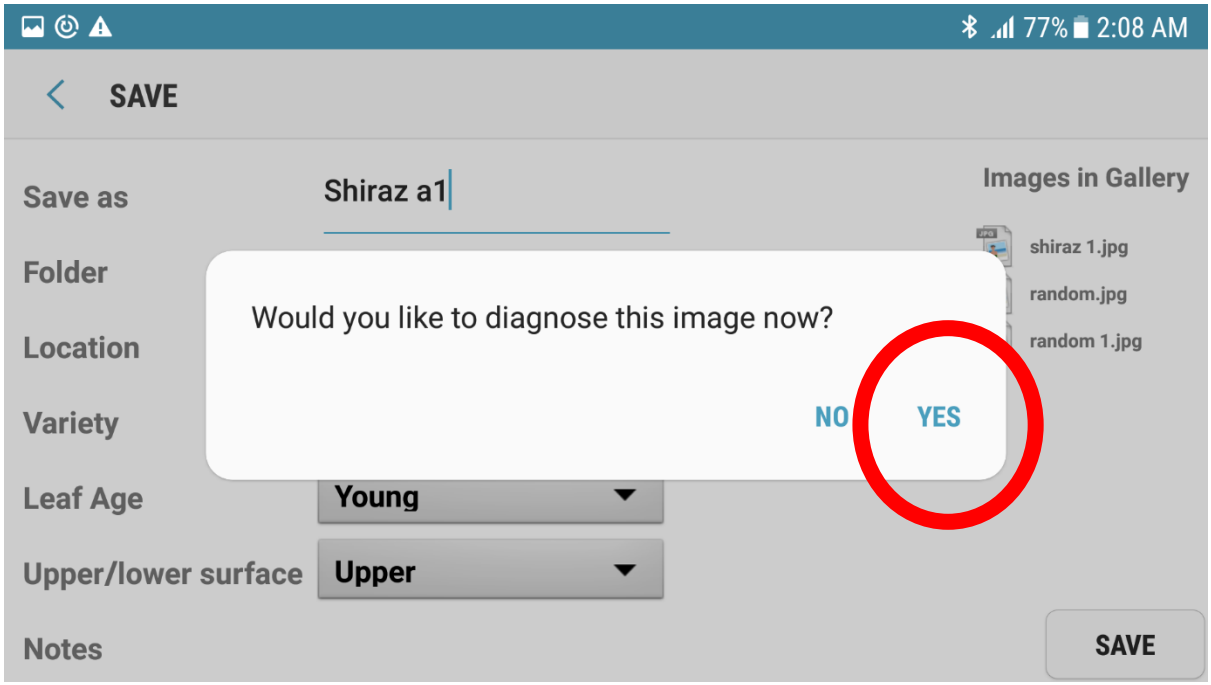
5. Prototyping and testing

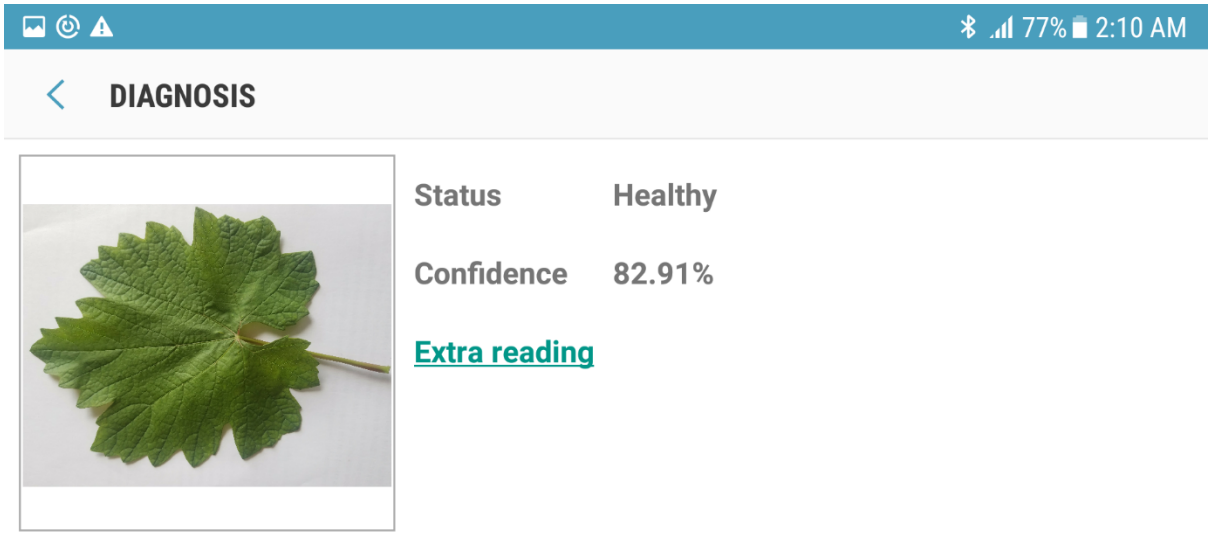



78% 2:04 AM
Diagnose
Field Guide
Demo
VITI DOC


78% 2:04 AM
Take Photo
Saved Images
Home
VITI DOC

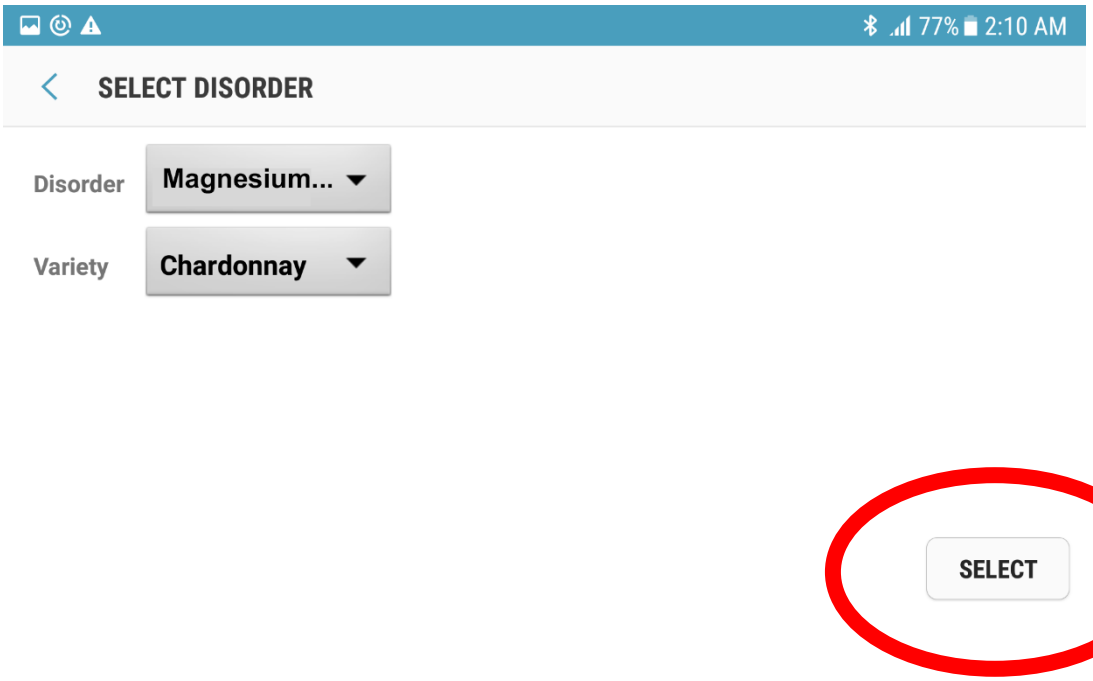

RETRY
OK
84% 2:35 AM
SAVE
Save as
Shiraz a2
Folder
Location
wagga
Variety
Shiraz
Leaf Age
Young
Upper/lower surface
Upper
Notes
Images in Gallery
Shiraz a1.jpg
Shiraz a2.jpg
SAVE

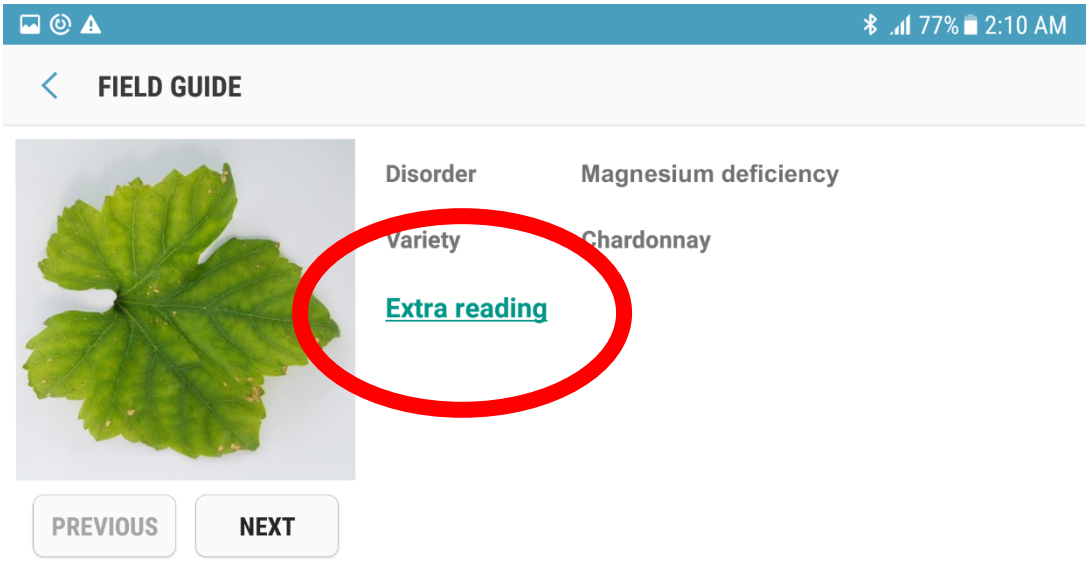

77% 2:08 AM
SAVE
Save as
Shiraz a1
Images in Gallery
shiraz 1.jpg
random.jpg
random 1.jpg
Folder
Location
Variety
Would you like to diagnose this image now?
NO
YES
Leaf Age
Young
Upper/lower surface
Upper
Notes
SAVE

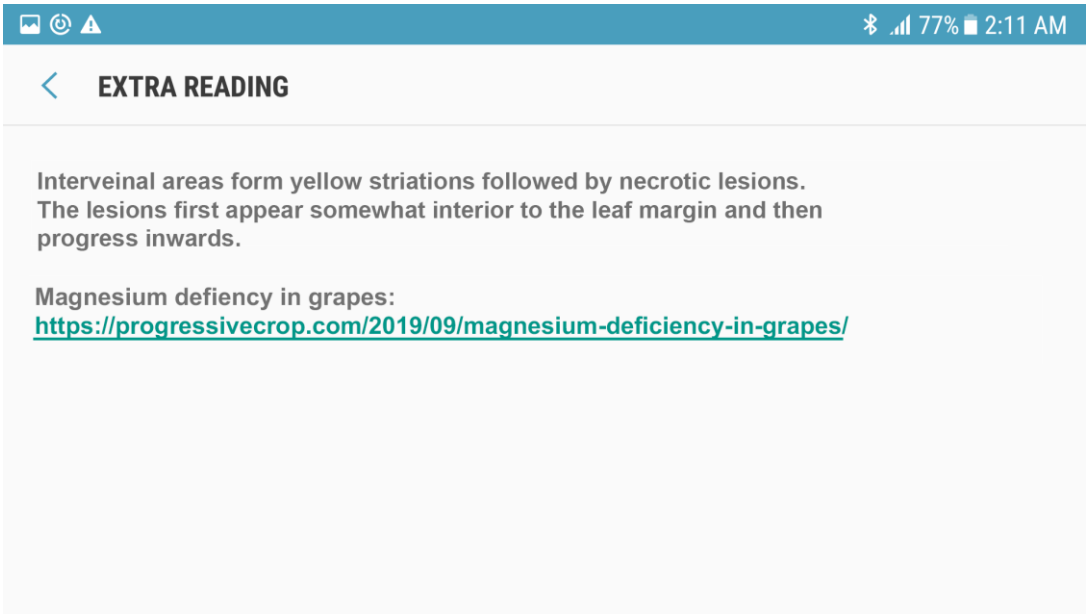

77% 2:10 AM
DIAGNOSIS
Status
Healthy
Confidence
82.91%
Extra reading

Field Guide

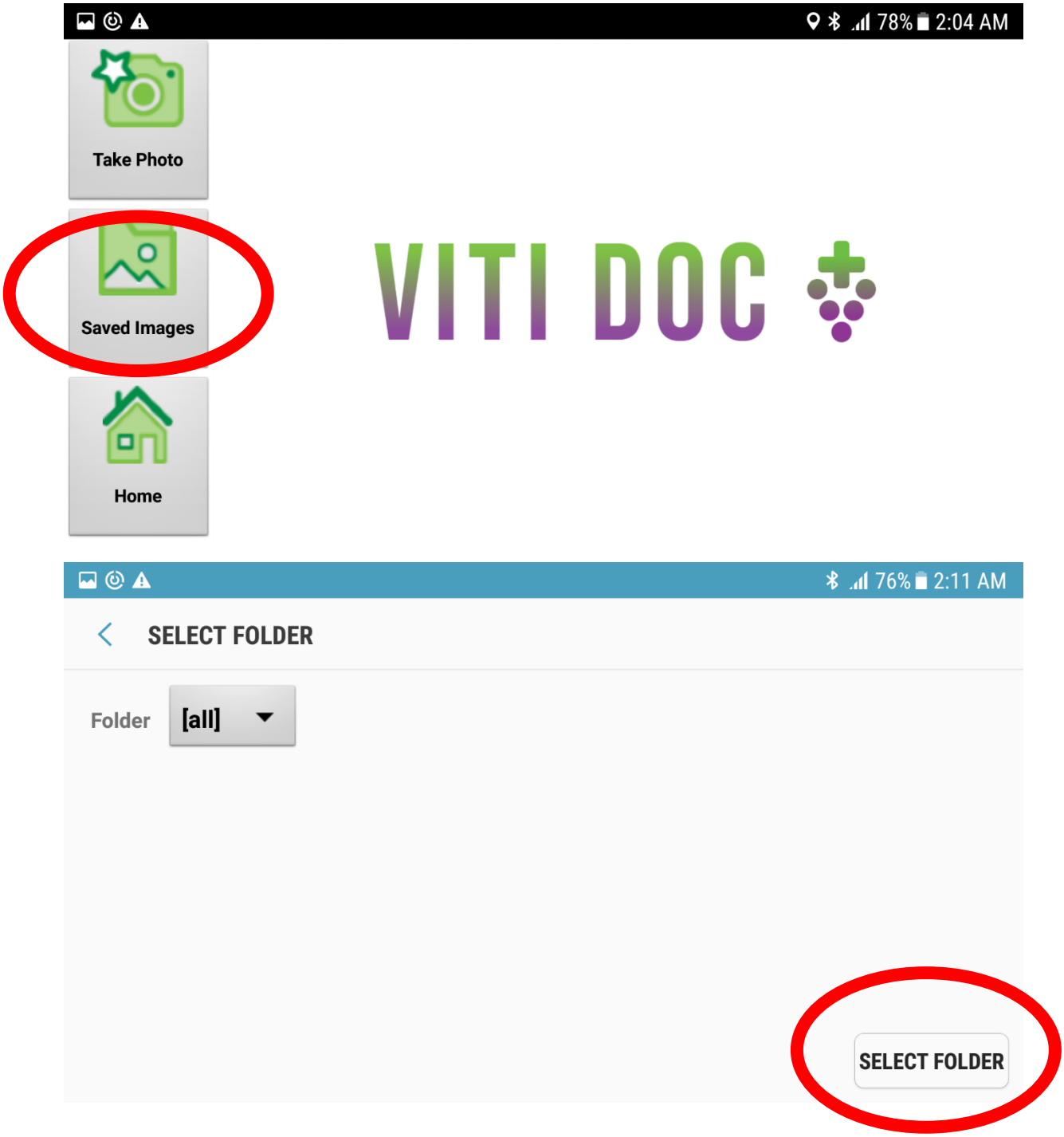

78% 2:04 AM
Diagnose
Field Guide
Demo
VITI DOC

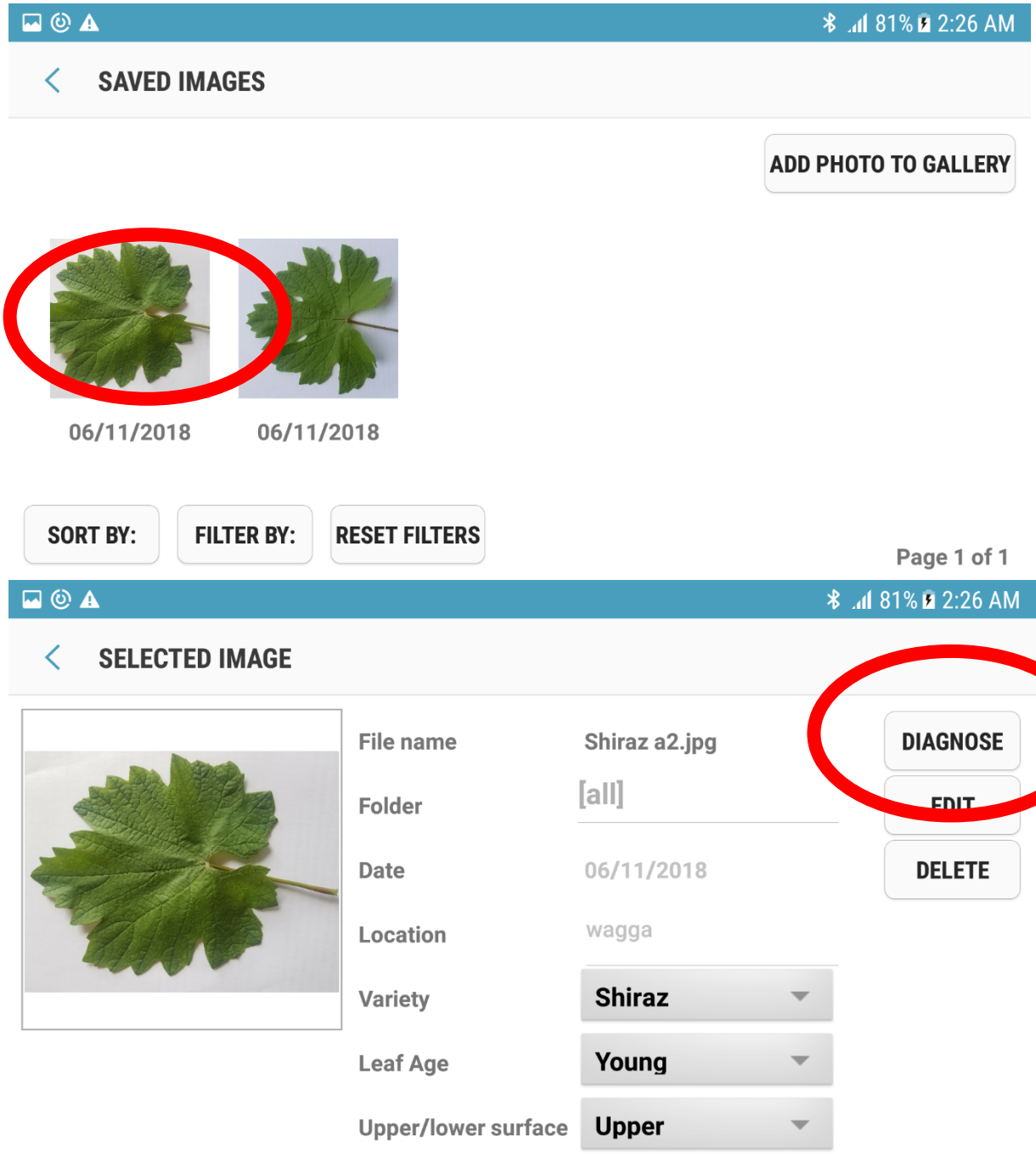

77% 2:10 AM
SELECT DISORDER
Disorder
Magnesium...
Variety
Chardonnay
SELECT

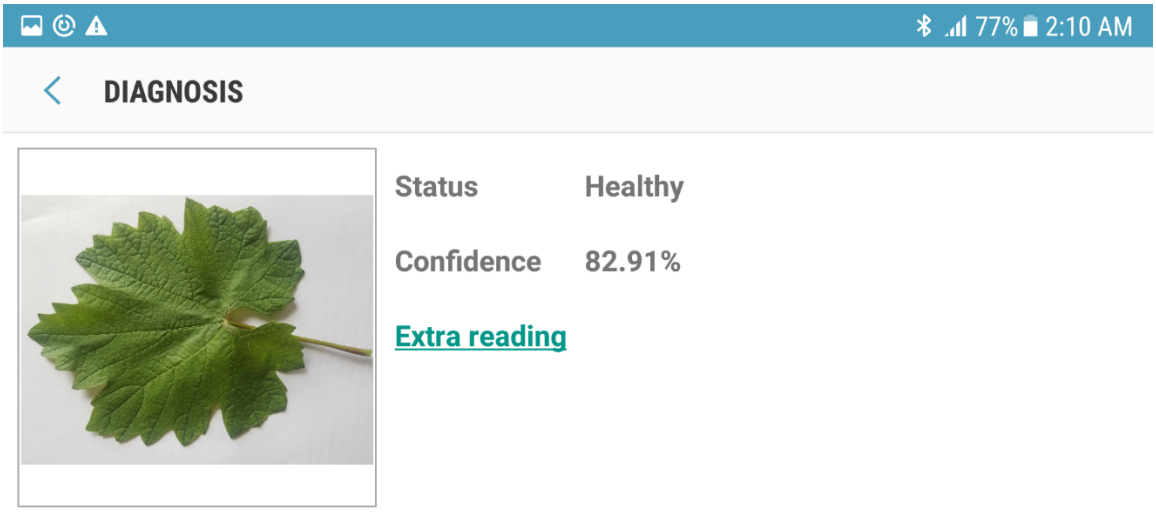

77% 2:10 AM
FIELD GUIDE
Disorder
Magnesium deficiency
Variety
Chardonnay
Extra reading
PREVIOUS
NEXT


77% 2:11 AM
EXTRA READING
Interveinal areas form yellow striations followed by necrotic lesions. The lesions first appear somewhat interior to the leaf margin and then progress inwards.
Magnesium defiency in grapes:
https://progressivecrop.com/2019/09/magnesium-deficiency-in-grapes/

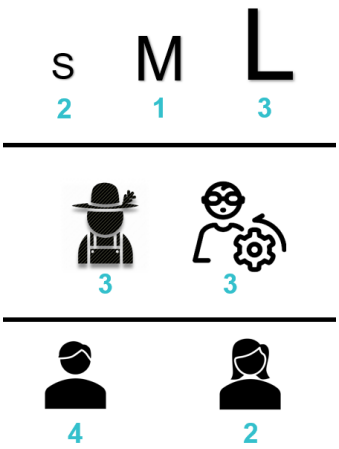
Diagnosing saved image in library




81% 2:26 AM
SAVED IMAGES
ADD PHOTO TO GALLERY
06/11/2018
06/11/2018
SORT BY:
FILTER BY:
RESET FILTERS
Page 1 of 1
81% 2:26 AM
SELECTED IMAGE
File name
Shiraz a2.jpg
Folder
[all]
Date
06/11/2018
Location
wagga
Variety
Shiraz
Leaf Age
Young
Upper/lower surface
Upper
DIAGNOSE
EDIT
DELETE


77% 2:10 AM
DIAGNOSIS
Status Healthy
Confidence 82.91%
Extra reading

Face-to-face user experience trials (6 in total) were conducted in vineyards in Orange, Griffith and Wagga (Dec 17-22/2020). We tested it with 6 users-2 were small growers, one from an intermediate sized company and three from large companies. 3 of these were technical managers.



The overall response was very positive. Following are some quotes from the testers:

- “it’s insane - it’s so quick"
- “Very easy to use”
- “I’ve been looking for something like this”
- “I’m not tech savvy but still found it easy to use”
- “Pretty straight forward!”
- “Saves carrying a book around- that would be handy”

Other feedback included:

- Spell out all elements rather than using abbreviation
- Zoom in ability for images in the gallery
- Make icons and font bigger for when entering all information (perhaps by switching the direction to portrait rather than landscape
- Drop down menus need to be larger font
- Add note that the app will not work on other species
- Give option to share the image with someone, or to share the diagnosis with someone
- Show GPS location on the diagnosis

These adjustments have been made.

Chapter 2- Hyperspectral Imaging of leaves to detect nutrient disorders

This chapter has been published in Sensors: https://arxiv.org/ftp/arxiv/papers/2007/2007.05197.pdf

Debnath S, Debnath T, Paul M, Rogiers SY, Baby T, Rahaman DM, Zheng L, Schmidtke L. 2020. Hyperspectral imaging to detect age, defects and individual nutrient deficiency in grapevine leaves. Sensors 20, 1-24: arXiv:2007.05197

Introduction

Over the ages, researchers in Computer Science and other disciplines have utilized various image based (including but not limited to hyperspectral (HS) image methods) experimental and analytical techniques for performing investigations with different fruits and vegetables. Diseases for pomegranate, betel vine and fungal diseases in plants were detected using image processing [1-3], and a spectral reflectance method was applied for early disease detection in wheat fields and to assess the effect of leaf age and psyllid damage of *Eucalyptus saligna* foliage [4, 5]. Additionally, head blight contamination in wheat kernels was detected by using multivariate imaging of Fusarium [6]. Detection of multi-tomato leaf diseases (late blight, target and bacterial spots) at different stages by using a spectral-based sensor was also reported [7]. Early blight and late blight diseases on tomato leaves, Fusarium head blight in wheat kernels, early detection of tomato spotted wilt virus and stress were detected using HS imaging [8-11].

HS imaging with high spectral and spatial resolutions is one of the most widely used techniques for studies in disease/defect detection in leaves. It collects both spatial and spectral information simultaneously from an object in a non-destructive and non-contact way between ultra violet (UV) and infrared (IR) regions. As a result, its high spectral resolution provides an extensive volume of information in recognizing, classifying and measuring objects [12, 13]. Changes in spectral reflectance of wheat and lettuce leaves have been studied in response to macronutrient deficiencies using HS data [14, 15]. In these literature wheat plants with different nutrient deficiency were compared with that grown in the controlled environment with the aid of HS data.

Grapes are one of the most widely grown berries in the world due to their nutrition values and importance in the multibillion dollar wine industry thereby related to thousands of jobs worldwide and hence are an active area of research [16]. Grapevine leaves are a source of biomolecules which have an influence on the quality and quantity of grapes. Photosynthetic performance of grapevine leaves is an important process for producing fruits both qualitatively and quantitatively [17]. The photosynthesis depends on the intensity of light, temperature as well as chlorophyll, carotenoids and other accessory molecules such as nitrogen, and protein [18-20]. The contents of chlorophyll as well as other molecules change during the life cycle of leaves. In the early stage of development contents of chlorophyll, nitrogen and protein are high in leaves, but after a period when leaves enter senescence phase, they gradually lose chlorophyll and protein. On the other hand, health of leaves also affects photosynthetic process as cellular structures of unhealthy leaves undergo changes thereby

influencing grape production [21-23]. Therefore, it is believed that an experimental study which is in the context of determining age and analysing various defects in grapevine leaves would be important and interesting to improve the general understanding in this research area. But very few research papers are available at present that demonstrate the analysis of grapevine leaves utilizing HS imaging. This work presents an extensive experimental study to detect age and defect of grapevine leaves with the aid of HS imaging. The primary objectives are:

- to predict age of grapevine leaves through experimental study of leaf surfaces,
- to determine effective wavelength region for age detection,
- to distinguish unhealthy leaves from healthy leaves in terms of both visually defective leaves and leaves with nutrient deficiencies,
- to determine appropriate wavelength region for detection of visually defective leaves,
- to introduce a new metric called the variation index that indicates the deviation of a leaf's brightness compared to a benchmark leaf as well as controlled leaf which was employed for both age and unhealthy leaves detection studies,
- to distinguish between controlled leaf and nutrient deficient leaves, and
- to distinguish nutrient deficient leaves individually.

This report is organized as follows: section 2 details the experimental setup, section 3 describes the experimental results and related in depth discussions and section 4 presents the conclusion of this work.

Method

A number of healthy and unhealthy grapevine leaves as presented in Figure 1(b) were collected from a vineyard located in central west NSW, Australia. For nutrient deficiency study grapevine leaves were collected from the NWGIC research centre, Charles Sturt University (CSU), NSW, Australia. They were scanned by us to generate HS data cubes on the same day of procurement by utilizing Resonon's benchtop hyperspectral imaging system available in the Computer Vision research laboratory at CSU. The HS imaging system is shown in Figure 1(a) and is comprised of a Pika XC2 high-precision HS camera, linear translation stage, mounting tower, lighting assembly, and software control system known as SpectrononPro. The imaging spectrometers are line-scan imagers, which means they collect data one line at a time. The Pika XC2 HS camera is Resonon's highest precision UV, Visible and Near-Infrared (VNIR) imager covering the ~380 - 1000 nm spectral range.

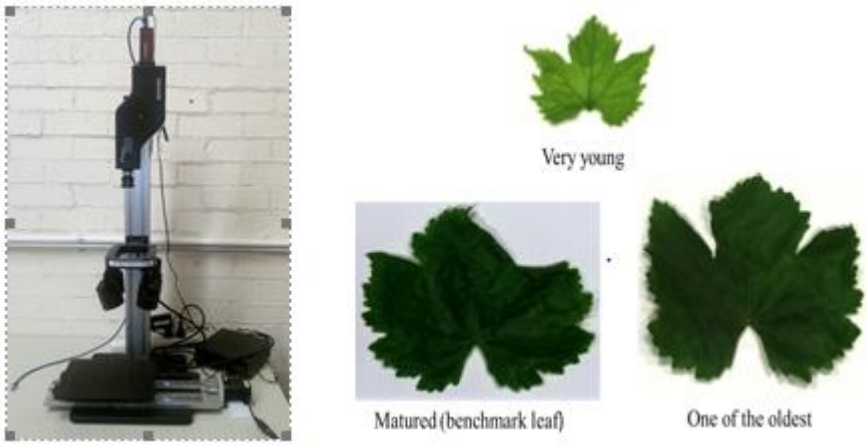


Figure 1(a). Hyperspectral camera

Figure 1(b). Samples of grapevine leaves according to age including the benchmark leaf

To assemble a complete two-dimensional image, multiple lines are scanned as the object is translated. The multiple line images are then assembled line by line to form a complete image. Two-dimensional images are constructed by translating the sample relative to the camera. This is typically accomplished by placing the sample leaves on a linear translation stage. For camera settings the frame rate and integration time were selected as 62.04244 Hz (default) and 244.01 ms respectively. The dark current has been acquired in absence of a light source. After collecting multiple dark frames SpectrononPro then uses these measurements to subtract the dark current noise from the measurements. Measuring absolute reflectance of an object requires calibration to account for illumination effects. To implement this a white reflectance reference was placed on the stage under light for a scan of the reference material. The collected data is then scaled in reflectance to the reference material, including flat-fielding to compensate for any spatial variations in lighting. Once the imager is calibrated for both dark current and reflectance reference, the imager will remain calibrated until the references are removed by the user. The speed unit and scanning speed were selected to be linear and 0.07938 cm/s (lowest). All samples were scanned for 10000 lines. The above-mentioned setting parameters were selected by trial and error method to obtain the best resolution and quality of the HS images of the experimental samples. Each scan of a leaf generated a HS image file with .bil extension with approximate size of 700 MB - 900 MB which were later processed by the SpectrononPro software.

For age detection studies the experiments were conducted on a number of grapevine leaves according to ascending order of their age i.e. the youngest to the oldest leaf of a vine. All leaves in this group were healthy by appearance. To study the features of healthy and unhealthy leaves, the experiment was done on visibly defective leaves. Nutrient deficiency study was conducted on a number of leaves which were grouped in controlled leaves and leaves with potassium (K), Magnesium (Mg) and Nitrogen (N) deficiency.

Results

Sections 3.1, 3.2.1 and 3.2.2 present experimental results and discussions related to age detection, distinction between healthy and unhealthy leaves and nutrient deficiency detection respectively. Spectra for each leaf were taken for ~380 nm to 1000 nm.

Age Detection

Figure 1(b) displays samples of grapevine leaves including benchmark leaf used for the age detection studies. In this experiment grapevine leaves in the wavelength between ~380 nm and 1000 nm have been studied. In the visible range of spectra, a characteristic high brightness peak within the green wavelength range has been obtained (Figure 2). This is because in the visible wavelength range the curve shape is governed by absorption effect from chlorophyll and other leaf pigments. It absorbs blue and red wavelengths more strongly than green. As a result, it reflects higher amount of green compared to blue and red and hence the characteristic high brightness [24-26]. It can also be observed that the magnitude of mean brightness of very young leaf is higher than those of youngest, benchmark and older leaves.

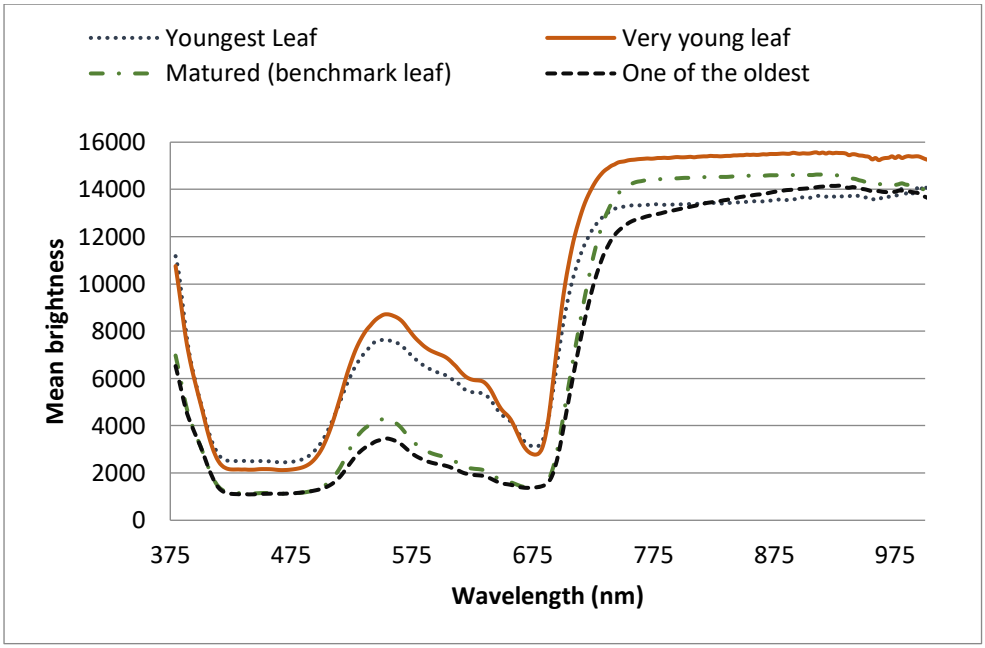


Figure 2: Mean brightness spectra of grapevine leaves of different age in the wavelength range of ~380-1000 nm.

Figure 2 also corroborates that at NIR wavelength range the mean brightness of grape vine leaves is higher than that of visible wavelength range. This is because a plant leaf has a low reflectance in the visible spectral region due to strong absorption by chlorophylls and carotenoids. On the other hand, a relatively high reflectance in the near-infrared is observed because of internal leaf scattering and no absorption.

Although mean brightness spectra from UV to NIR range provide characteristics curves the indication of age of leaves is not significantly observed. Therefore, for further age detection study the brightness of other leaves were compared with respect to the brightness of benchmark leaf at 554.3 nm. This wavelength was selected as a reference wavelength because it has been found from the spectral analysis that between UV and NIR range the brightness difference is higher for the consecutive leaves according to their age at ~ 554.3 nm. On the other hand, benchmark leaf has been selected as a reference leaf because by visual inspection this leaf (see Figure 1(b)) could be considered as a matured and healthy leaf. From Figure 3 it has been found that though the ratio of brightness of first few young

leaves increases, after that it decreases with the increasing age of leaves at 554.3 nm. The phenomenon of increasing brightness ratio for the first few very young leaves could be due to the effect of water content. Though the chlorophyll content of the younger leaves was lower than that of matured and older leaves [5], amount of water content was higher for younger leaves [28] compared to older leaves. It has been reported that a decrease in water content was found to increase reflectance [29]. Therefore, the level of water content has a dominant effect on the reflectance of young leaves of certain age. Hence reflectance of green wavelength as well as brightness is lowest for the youngest leaf. As leaves get older water content decreases thereby increasing brightness of young leaves up to certain ages. From Figure 3 it can be seen that few very young leaves have slightly lower brightness ratio than those of young leaves of certain ages. As leaves transit from young state to matured state the brightness ratio decreases sharply and for matured to oldest leaves transition the brightness ratio decreases gradually. From literature study it has been found that expanding leaves combine high greenness with low photosynthetic rate as well as the decrease in photosynthetic capacity is caused by effects such as leaf aging [30, 31]. Therefore, decreasing brightness ratio could be because of the low photosynthetic rate of leaves due to the ageing effect.



Figure 3. Ratio of brightness intensity of all grapevine leaves with benchmark leaf at 554.3 nm

To further study the age detection, mean 1st derivatives of the mean brightness data have been analysed. From the mean 1st derivative spectral analysis longer wavelength shifts of the 1st derivatives mean brightness peaks according to age with respect to wavelength has been observed. These shifts of the 1st derivative mean brightness peaks are clearly demonstrated in Figure 4 where it can be found that there is a correlation between these shifts and age of the leaves. For the ease of explanation leaves are presented here according to the ascending order of age. As the leaves get older the 1st derivative mean brightness peaks between 470 nm and 550 nm shift to the higher wavelength.

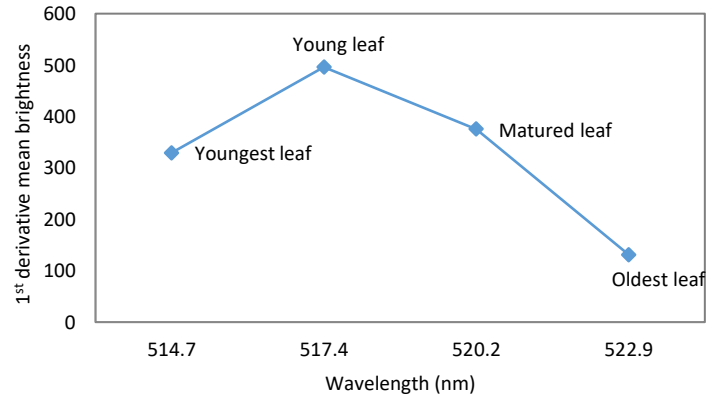


Figure 4. Maximum 1st derivative brightness peak as a function of wavelength in the 470 to 550 nm range

To clearly understand the effect of age of leaves in the red and near infrared region (675 nm - 775 nm) the mean 1st derivative brightness data have been considered. Figure 5 represents the mean 1st derivatives brightness of a number of grapevine leaves between 675 nm and 775 nm. From Figure 5 it could be stated that the brightness peak started gradually broadening when leaves transit from matured to old phase. This broadening could be due to the amount of chlorophyll content and ageing effect of leaves. As leaves going towards maturity the mean rate of change of brightness becomes slower. As in Figure 4, shifts of mean 1st derivatives brightness peak between 675 nm and 775 nm could be observed, but there is no significant shift based on age of leaves for this wavelength range.

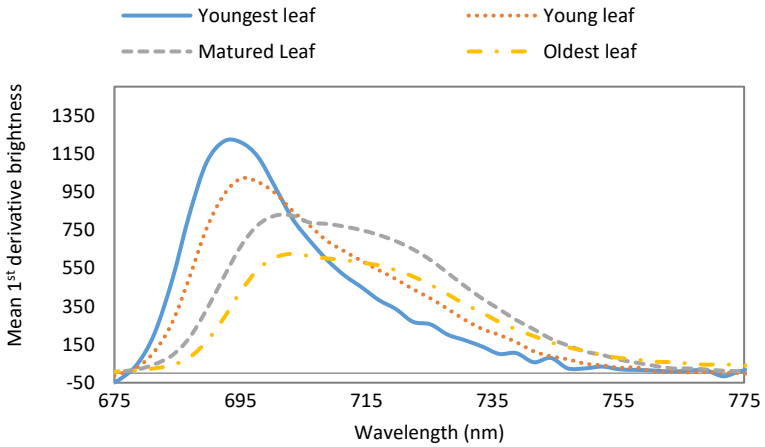


Figure 5. Mean 1st derivative of brightness of leaves in the 675 to 775 nm range

For further study of age detection of age, a variation index (v_i) has been defined from the standard deviation of brightness as:

$$v_i = \frac{(\sigma_{\text{benchmark leaf}} - \sigma_i) \times 100}{\sigma_{\text{benchmark leaf}}}\% \qquad \text{Equation 1}$$

where v_i is the variation index of i^{th} leaf, $\sigma_{\text{benchmark leaf}}$ and σ_i are the standard deviations of benchmark leaf and i^{th} leaf respectively. This index represents how much the brightness of a leaf deviates from that of a matured leaf. Figure 6 demonstrates that there is a correlation between age of leaves and v_i in both UV and NIR regions. It can be observed that v_i follows a specific trend according to the age of leaves in both UV and NIR regions. As the leaves continue to age, v_i starts increasing in the UV region but shows the opposite characteristics in the NIR region.

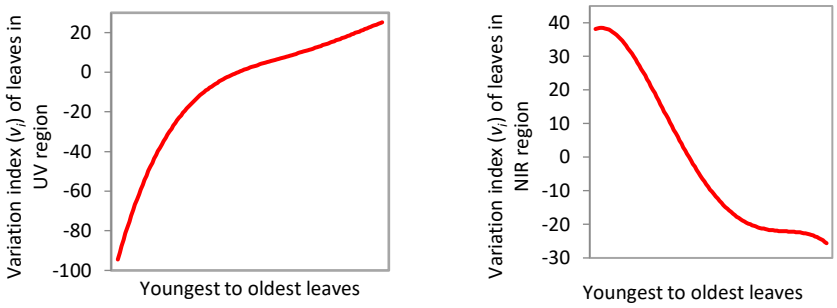
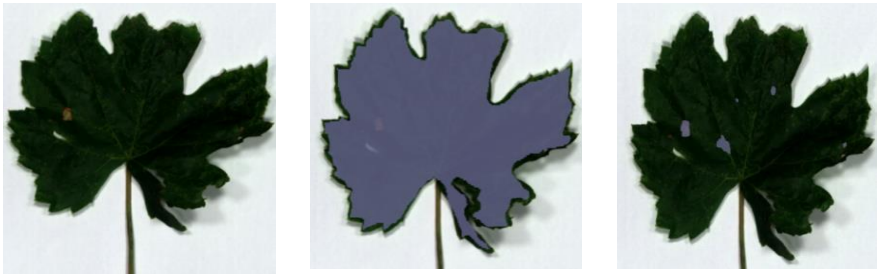


Figure 6. Variation index (v_i) of youngest to oldest leaves at different spectrum regions for determination of age of leaves

Detection of Healthy and Unhealthy leaves



(a) Unhealthy leaf with many small white spots and few small brown spots.

(b) Area (grey area) selected for unhealthy leaf

(c) Specific grey areas selected for unhealthy leaf

Figure 7. Unhealthy leaf with white spots and few brown spots and its selected areas for data cube accusation

In this section the characteristic features of healthy and unhealthy leaves have been studied. This section is further divided in to two subsections. Section 3.2.1 demonstrate the comparison of characteristic features of healthy and unhealthy leaves. Here healthy and unhealthy leaves have been defined by their appearances. On the other hand Section 3.2.2 presents the comparison of characteristic features of healthy and unhealthy leaves in terms of their nutrients content. In this study healthy leaves are represented by the controlled leaves and unhealthy by leaves with different nutrient deficiency.

1.1.1 Comparison of features of healthy and unhealthy leaves (considering appearance)

For the detection of the features of healthy and unhealthy leaves the data cubes have been obtained by selecting both whole area and as well as selective areas of leaves using Lasso tool of SpectrononPro software. Both whole and selective areas have been studied to obtain an optimum selection method

for distinguishing healthy and unhealthy leaves. The following paragraphs detail the experimental results and analysis for the 9 unhealthy leaves by appearance in terms of mean brightness and mean 1st derivatives brightness vs wavelength. The characteristics of these leaves were also compared with a healthy leaf from the age detection group i.e. the benchmark leaf (Figure 1(b)). This was selected as it appeared to be a matured leaf. As seen in Figure 7(a), this particular unhealthy leaf contains white spots along with few brown spots. Figure 7 (b and c) represent examples of the whole area and selective areas.

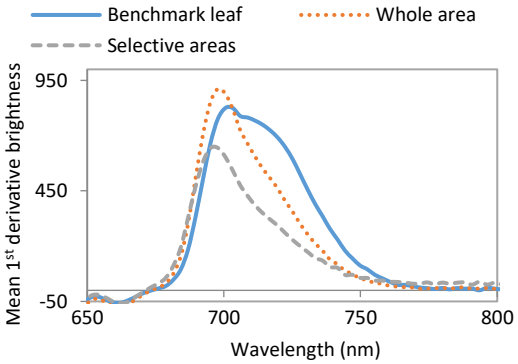


Figure 8. Demonstration of mean 1st derivatives of brightness of healthy (benchmark leaf) and unhealthy (whole and targeted necrotic areas) leaves to differentiate healthy and unhealthy leaves.

Figure 8 demonstrates that mean 1st derivative brightness in the NIR wavelength range is higher for unhealthy leaf of whole area case compared to benchmark leaf. Narrowing of brightness curves for unhealthy leaf is also observed for whole area case compared to benchmark leaf. A whole area case shorter wavelength shift of mean 1st derivative brightness peak is also observed for unhealthy leaf compared to benchmark leaf. From the literature study it has been found that reflectance in NIR is insensitive to change in chlorophyll content but sensitive to internal leaf structure, water content, structural compound and changing of internal mesophyll structure [32]. Therefore, the deviation of mean 1st derivative brightness curves of unhealthy leaf with respect to benchmark leaf could be due to the difference in internal leaf structures of unhealthy and healthy leaves. From Figure 8 it can be observed that though selective areas case exhibits similar features as whole area the magnitude of mean 1st derivatives brightness is lower compared to whole area case. For selective areas case, areas have been selected based on the visible spots or defective areas. Therefore, characteristic features of only visibly defective areas have been obtained. On the other hand, for whole area case, whole area of a leaf has been selected regardless of visible defects. As a result, the features of both visible and nonvisible defective areas have been acquired with the aid of hyperspectral imaging in the NIR region. Therefore, whole area case probes significant features compared to selective areas' case.



Unhealthy leaf with brown areas and many small brown spots



Unhealthy leaf with several big brown spots



Unhealthy leaf with few brown spots



Unhealthy leaf with some brownish areas



Unhealthy leaf with few brown spots and some holes surrounded with brown regions



Unhealthy leaf with brown and yellowish regions



Unhealthy leaf with many large brown regions



Unhealthy leaf with few brownish areas and holes surrounded by brownish areas

Figure 9. Sample of unhealthy leaves with visible defects.

Sample of unhealthy leaves with visible defects are presented in Figure 9. For most of the unhealthy leaves similar features to Figure 8 such as narrowing and shorter wavelength shift of the curves have also been observed. It has been found that a sharp transition from low to high reflectance usually occurs in the wavelengths between the visible and the NIR regions, and this transition usually shifts to shorter wavelengths in diseased crops [34]. The wavelength where this transition occurs can be observed in the 1st derivative brightness curves. Hence, this deviation of 1st derivative brightness curve

shapes of leaves with respect to benchmark leaf could be due to the brown spots of the leaf. Mean 1st derivative brightness curves were able to significantly distinguish the healthy and most (though not all) unhealthy leaves in the NIR region. Therefore, mean spectral ratios analysis has been employed.

Mean Spectral Ratios.

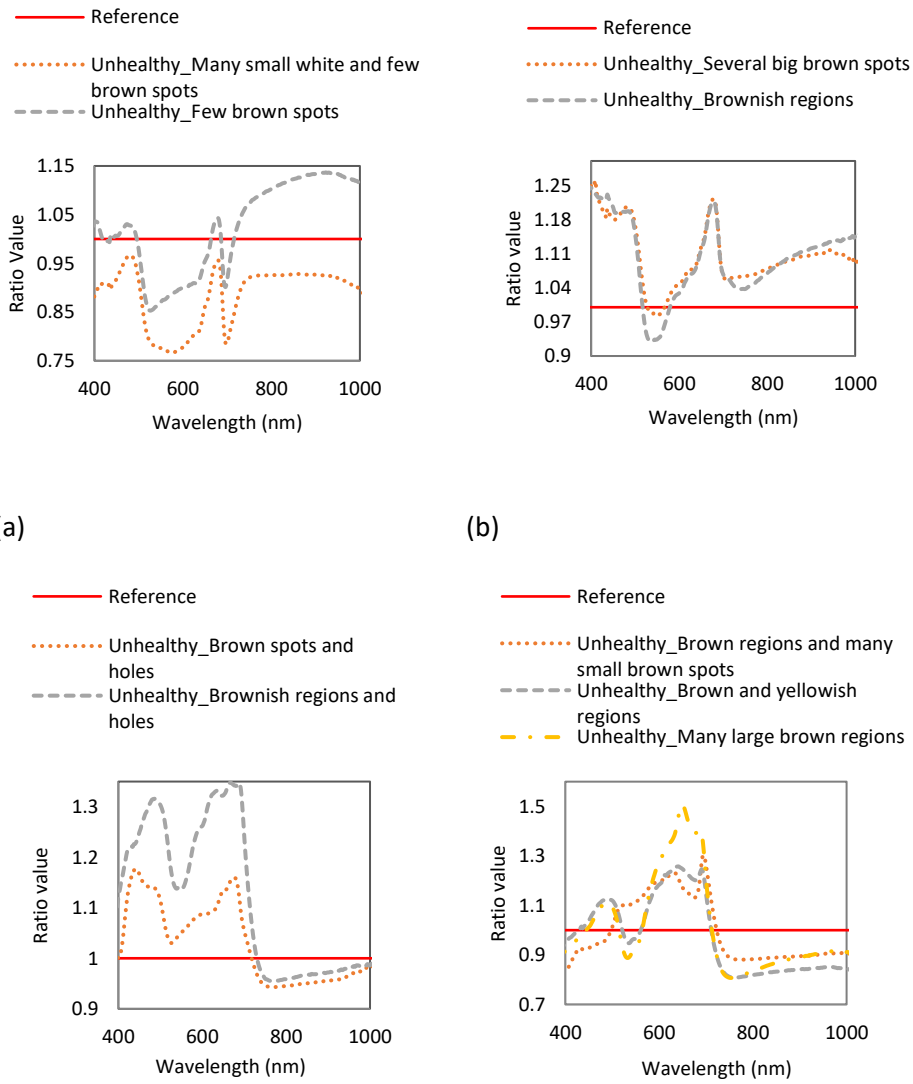


Figure 10. Mean spectral ratios of different unhealthy leaves (whole area) to benchmark leaf.

To highlight the difference between healthy and unhealthy leaves, the mean brightness spectra for the unhealthy leaves were each divided by the mean brightness spectrum of the representative healthy leaf *i.e.* benchmark leaf for both whole and selective areas of unhealthy leaves.

Unhealthy leaf with many small white and few brown spots and unhealthy leaf with few brown spots exhibit almost similar ratio curve trends from ~ 400 nm to 1000 nm as per Figure 10(a). In this wavelength range the brightness ratio is higher for unhealthy leaf with few brown spots than that of unhealthy leaf with many small white and few brown spots. From Figure 10(b) it can be surmised that unhealthy leaf with several big brown spots and unhealthy leaf with brownish regions have almost

similar ratio curves. The brightness ratio of unhealthy leaf with several big brown spots is greater than unhealthy leaf with brownish regions between the wavelength range ~ 491 nm and ~ 825 nm. After 825 nm the brightness ratio is higher for unhealthy leaf with brownish regions than unhealthy leaf with several big brown spots. Figure 10(c) presents that unhealthy leaf with brown spots and holes and unhealthy leaf with brownish regions and holes have similar shaped ratio curves. The brightness ratio of unhealthy leaf with brownish regions and holes is greater than unhealthy leaf with brown spots and holes between the wavelength range ~ 400 nm and 1000 nm. Also from Figure 10(d) it can be found that for whole area cases unhealthy leaves with brown and yellowish regions and unhealthy leaf with many large brown regions have similar ratio curves with higher ratio value for unhealthy leaf with many large brown regions between ~ 570 nm to 1000 nm compared to unhealthy leaves with brown and yellowish regions. Between ~ 400 nm and ~ 570 nm the ratio value is greater for unhealthy leaves with brown and yellowish regions than that of unhealthy leaf with many large brown regions. On the other hand for unhealthy leaf with brown regions and many small brown spots the ratio curve is similar shaped to unhealthy leaves with brown and yellowish regions and unhealthy leaf with many large brown regions between ~ 603 nm and 1000 nm. From ~ 400 nm to ~ 603 nm the unhealthy leaf with brown regions and many small brown spots ratio curve is different to unhealthy leaves with brown and yellowish regions and unhealthy leaf with many large brown regions as well as curves of other unhealthy leaves.

Variation Index.

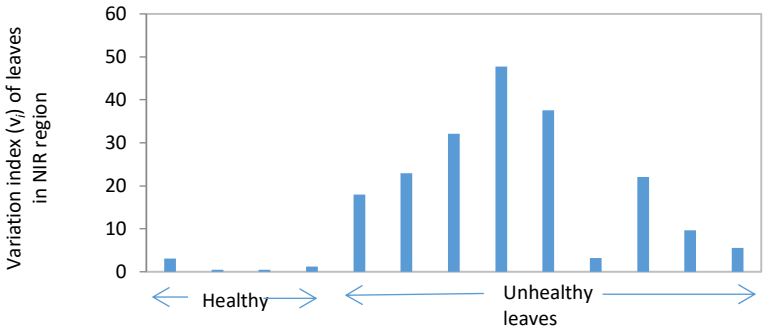


Figure 11. Variation index (v_i) of healthy and unhealthy leaves in NIR region for distinguishing healthy and unhealthy leaves

To obtain a correlation between healthy and unhealthy leaves, variation index v_i index (Equation 1) has also been applied. In this case σ_i represents the standard deviations of i^{th} unhealthy leaf. Figure 11 demonstrates that for wavelengths in the NIR region healthy leaves have v_i index closer to benchmark leaf, i.e. unhealthy leaves have higher value of v_i index compared to healthy leaves. There is no such pattern that has been observed for unhealthy and healthy leaves for wavelengths in the UV region.

1.1.2 Comparison of leaf features afflicted with specific nutrient deficiencies

To compare the features of healthy and unhealthy leaves a number of controlled leaves and leaves with nutrients deficiency such as K, Mg and N have been studied using Hyperspectral imaging. In this

study the data cubes have been obtained by selecting whole area with nutrient deficiency leaves using Lasso tool of SpectrononPro software. The obtained data of both controlled leaves and data of leaves with corresponding nutrient deficiency were then averaged.

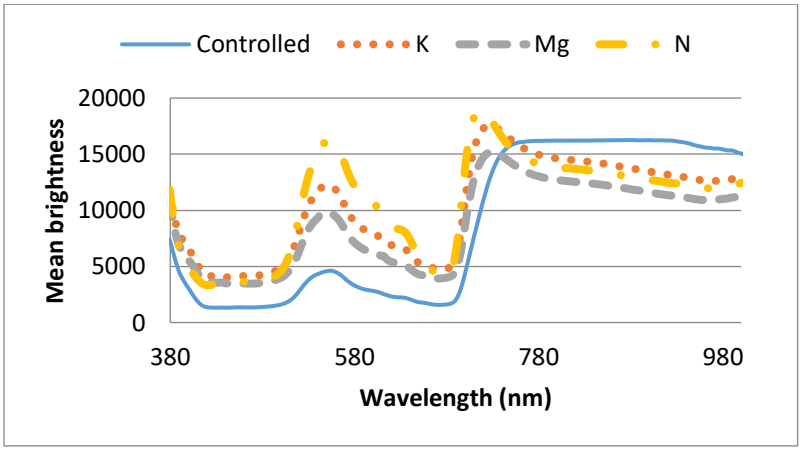


Figure 12: Mean brightness spectra of controlled and different nutrient deficiency leaves between ~380 nm – 1000 nm

Figure 12 shows the mean brightness spectra of wavelength range from ~380 nm to 1000 nm of controlled and nutrients deficiency leaves. From this figure it can be observed that in the VIS wavelength (400 nm- 700nm) the brightness of leaves with nutrients deficiency are higher than the controlled leaf. All nutrient deficiencies affected chlorophyll content and generally increased brightness in the VIS wavelength. The brightness peak normally centered at about 550 nm, then broadens towards the red as absorption of incident light by chlorophyll decreases [14]. It can also be seen from Figure 12 that N deficiency leaf has higher brightness compared to controlled, K and Mg deficiency leaves at ~550 nm. Nitrogen is needed for chlorophyll production [35]. The higher brightness at about 550 nm for N deficiency may be due to the lower content of chlorophyll in this leaf relative to control leaves as well as leaves with other deficiencies.

From Figure 12 it can be shown that the brightness peak of nutrient deficiency leaves appeared at the shorter wavelength (red shift) compared to the controlled leaf in the wavelength range between ~ 680 nm and 1000 nm. The slope of the red shift was steeper for nutrients deficient leaves than that of the controlled leaf. It has been reported that when plants are under stress, such as nutrient deficiency, there is a loss of chlorophyll, which causes a shift on the red edge position to shorter wavelengths occurring between the areas of red and near infrared [14, 15]. From this figure it can also be observed that N deficiency leaf shifted more to the shorter wavelength compared to the Mg and K deficiency leaves. On the contrary it can be seen that brightness of nutrients deficiency leaves are lower compared to the controlled leaf in the wavelength region between ~750 nm to 1000 nm. In this region Mg has the lowest brightness compared to the other leaves. From the literature review it has been found that in stressed vegetation chlorophyll absorption decreases and IR reflectance decreases due to structural changes in the plant [15].

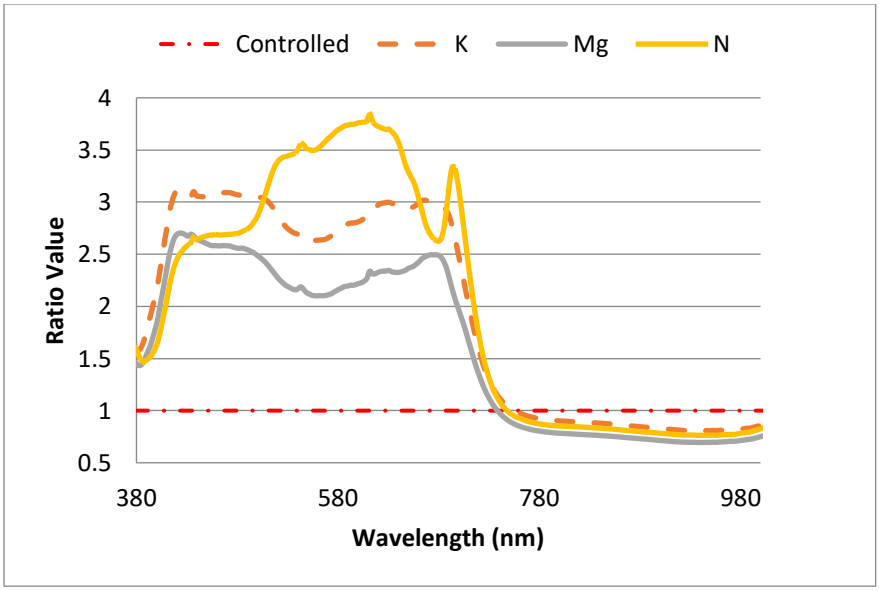


Figure 13: Mean spectral ratios of different nutrient deficiency leaves to controlled leaf for distinguishing controlled and different nutrient deficiency leaves.

To compare the brightness of nutrient deficient leaves with that of controlled leaf the ratio between brightness of nutrients deficiency leaves and controlled leaf have been plotted in Figure 13. It can be observed from this figure that the curve shapes for K and Mg deficiency leaves are similar but the magnitude of Mg deficiency leaf is lower than that of K deficiency leaf. On the other hand, the curve shape of N deficiency leaf is quite different from those of K and Mg deficiency leaves. Furthermore, it can be seen that there are peaks between ~650 nm and ~ 750 nm for N, Mg and K deficiency leaves. In this wavelength region peaks at ~693 nm, ~680 nm and ~663 nm have been found for N, Mg and K deficiency leaves respectively. It can also be found that magnitude of these peaks at above mentioned wavelengths is ~3.3, ~2.5 and ~3 times higher for N, Mg and K deficiency leaves compared to controlled leaf. It has been reported that all mineral deficiency caused modifications brightness of leaves relative to the controlled [14].

To distinguish features of controlled and nutrient deficiency leaves normalized difference vegetation index (NDVI) has been applied [36-39]. This index quantifies vegetation by measuring the difference between near-infrared (which vegetation strongly reflects) and red light (which vegetation absorbs). NDVI always ranges from -1 to +1 where positive values indicate vegetated areas and negative values signify non-vegetated surface features such as water, barren, clouds, and snow. Higher positive value of NDVI refers to healthy and dense vegetation [37] The NDVI is associated with the reflectance of photosynthetic tissues that is calculated for individual images by the following equation [37] where RED and NIR stand for the spectral reflectance measurements acquired in the red (visible) and near-infrared regions, respectively.

$$NDVI = \frac{NIR-\mathrm{RED}}{\mathrm{NIR+RED}}$$ Equation 2

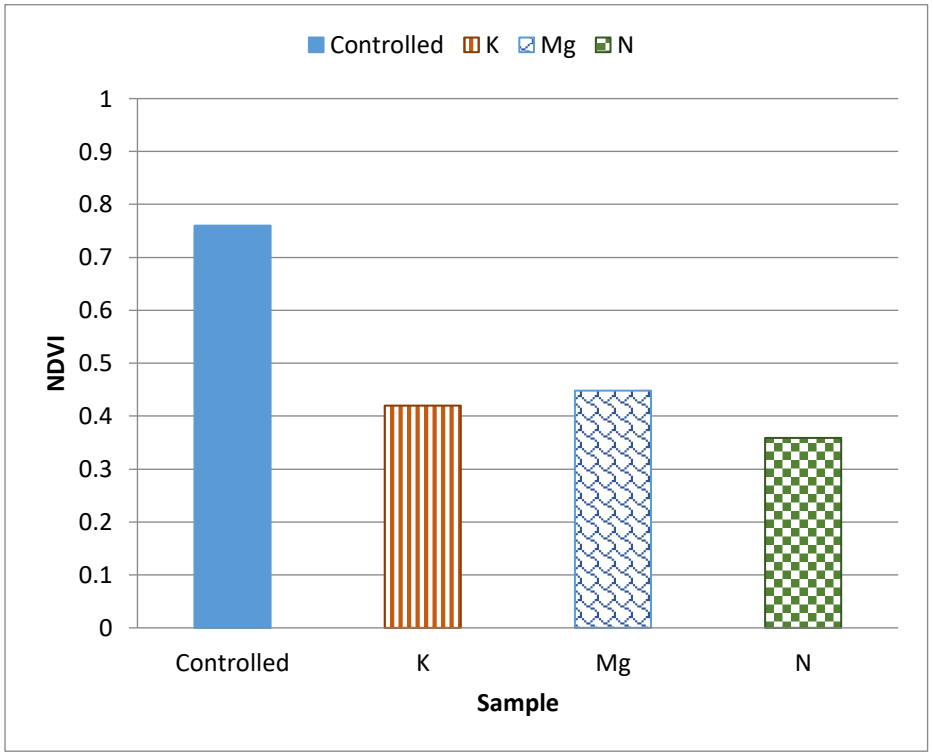


Figure 14: NDVI for control and different nutrient deficiency leaves s.

From the NDVI value of Figure 14 it can be observed that it is significantly higher for controlled leaf than those of nutrient deficiency leaves. This value indicates that the control leaf is healthier compared to leaves with N, K and Mg deficiency. It can also be observed that the NDVI value for leaves with N, K and Mg deficiency are not significantly different to each other.

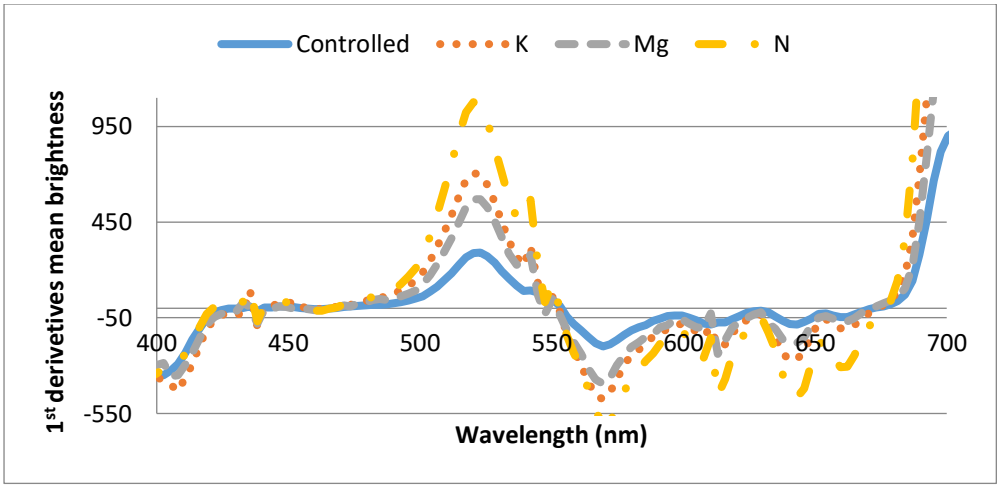


Figure 15: 1st derivative mean brightness spectra of control leaves and leaves with different nutrient deficiencies within the VIS wavelength range.

The 1st derivatives spectra have also been used to define and analyse the location and properties of the red edge as it provides more sensitive measures of stress than broadband methods [15]. Figure 15 shows the 1st derivatives spectra of controlled and nutrients deficiency leaves between VIS wavelength. From this figure it can be found that between ~460 nm and ~540 nm peak magnitude of 1st derivatives of mean brightness is higher for nutrients deficiency leaves compare to that of controlled leaf. In this wavelength region the 1st derivatives brightness magnitude is ~36%, ~19% and ~24% higher for N, Mg and K deficiency leaves compared to controlled leaf. [15]

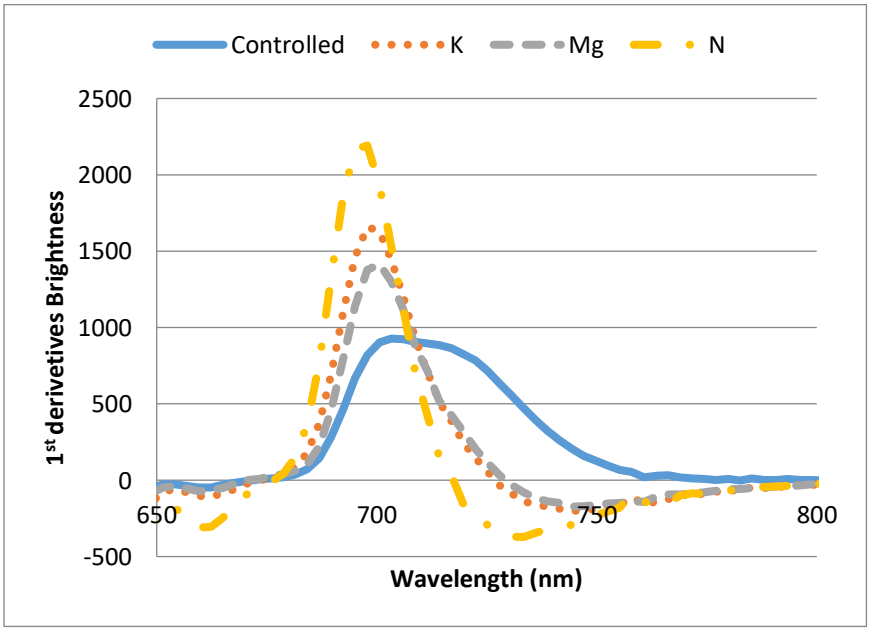


Figure 16 1st derivative spectra of control and nutrient deficiency leaves between 650 nm and 800 nm.

Furthermore considering Figure 16 it can be observed that the ~ 700 nm derivative peaks are dominant in leaves with nutrient deficiency. Similar results have found from literature study [40, 41]. On the other hand narrowing of 1st derivative brightness peak can be also found for the nutrient deficient leaves compared to controlled leaf. The midpoint of this broad peak for the controlled leaf has been found to be at ~ 708 nm. This broadening and narrowing of 1st derivative peaks of controlled and nutrient deficiency leaves respectively could be due to the amount of chlorophyll content in the leaves. In this region the 1st derivative peak magnitude was ~ 15%, ~ 9% and 7% higher for N, K and Mg deficiency leaves with respect to controlled leaves. Form Figure 15 it can also be found that in this wavelength range 1st derivative peak of nutrient deficient leaves shifted to the shorter wavelength (red shift) compared to the controlled leaf. From the literature it has been found that this shift occurs if vegetation is exposed to low nutrients or environmental stress [40].

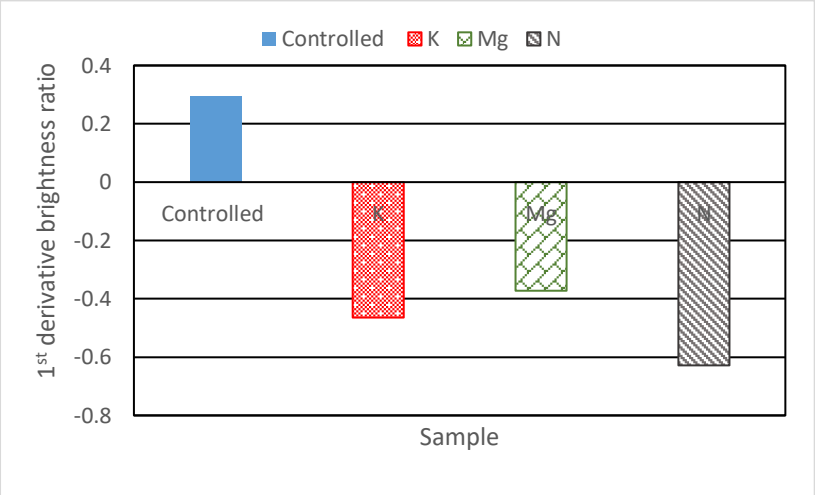


Figure 17: A plot of 1st derivative mean brightness ratio of control and different nutrient deficiency leaves.

This 1st derivative mean brightness shift can further be studied by using the hyperspectral derivative ratio in the boundary between the region of strong absorption of red light by chlorophyll (~ 680 nm) and the region of high multiple scattering of radiation (~750 nm) [40]. From the 1st derivative ratio plot of Figure 17 it can be seen that this 1st derivative ratio is positive for controlled leaf and negative for nutrient deficient leaves. Furthermore, this ratio value has been found to be ~ 62%, ~47% and ~37% for N, K and Mg in the negative direction respectively.

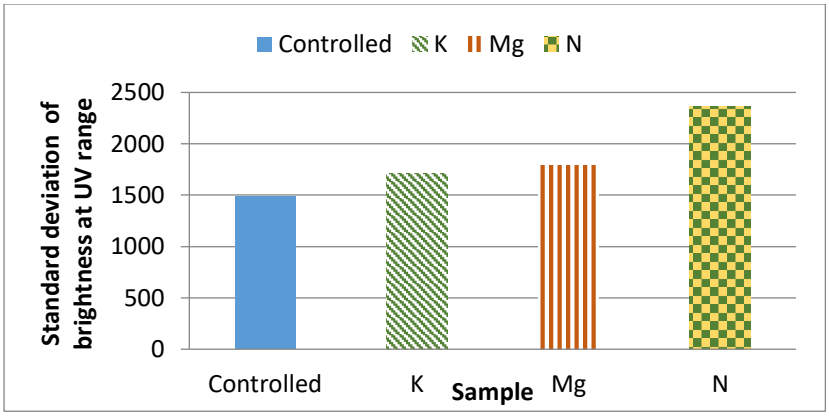


Figure 18: A plot of standard deviation of controlled and different nutrient deficiency leaves in UV region.

To distinguish features of controlled and nutrient deficient leaves standard deviation has also been studied for UV, VIS and NIR regions of wavelength. It can be found from Figure 18 that the standard deviation of controlled leaf in UV range has lowest value compared to those of nutrient deficient leaves. This value has been found to be highest for N deficient leaves with respect to controlled, K and Mg deficient leaves. But the difference of this standard deviation value between K and Mg deficiency leaves is ~ 100.

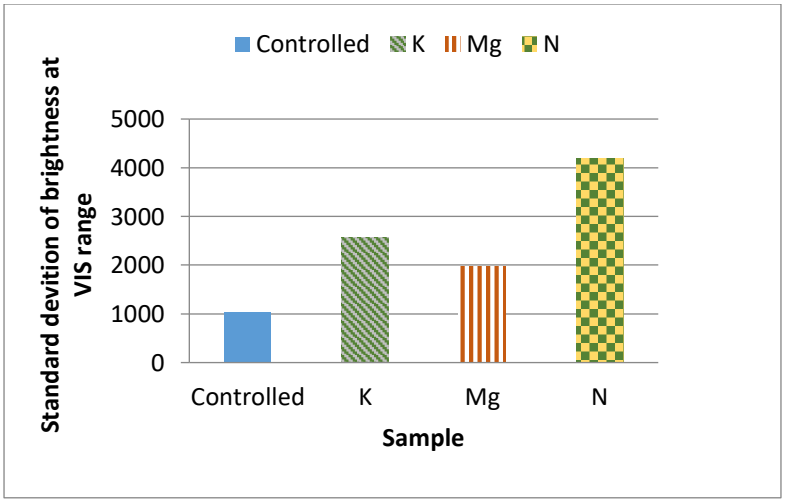


Figure 19: A plot of standard deviation of controlled and different nutrient deficiency leaves in VIS region.

Figure 19 shows the standard deviation of controlled and N, Mg and K deficiency leaves in the visible region of wavelength. It can be found that similar to UV region (Figure 19), here controlled leaf has lowest standard deviation value compared to different nutrient deficiency leaves. Again N deficient leaves have highest value among these leaves. On the other hand the difference between standard deviation of K and Mg is 600 in Vis region. This difference value is higher in visible region compared to UV (Figure 19).

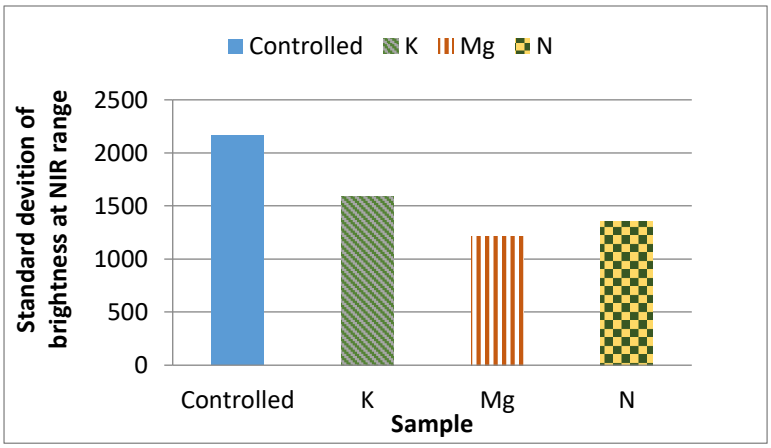


Figure 20: A plot of standard deviation of controlled and different nutrient deficiency leaves in NIR region.

Opposite to UV (Figure 18) and VIS (Figure 19) region the standard deviation value has been found to be highest for controlled leaves than those of nutrient deficient leaves in NIR region (Figure 20). In this region this value has been found to be highest for N deficiency leaves compared to K and Mg deficiency leaves. But in this case the standard deviation values of N, Mg and K are close to each other. The difference of standard deviation value between N and Mg, N and K, and K and Mg have been found to be 100, 300 and 400.

To distinguish between healthy and unhealthy leaves in terms of nutrient content, variation index v_i index has also been studied. In this case $\sigma_{benchmark\ leaf}$ and σ_i represents the standard deviations of controlled leaf and leaves with different nutrient deficiency respectively. This index represents how much the brightness of a leaves with nutrient deficiency deviates from that of a controlled leaf. This study has been conducted for UV, VIS and NIR wavelengths. In this study the value of v_i indicates how much the nutrient deficiency leaves differ from the controlled leaf in different wavelength regions.

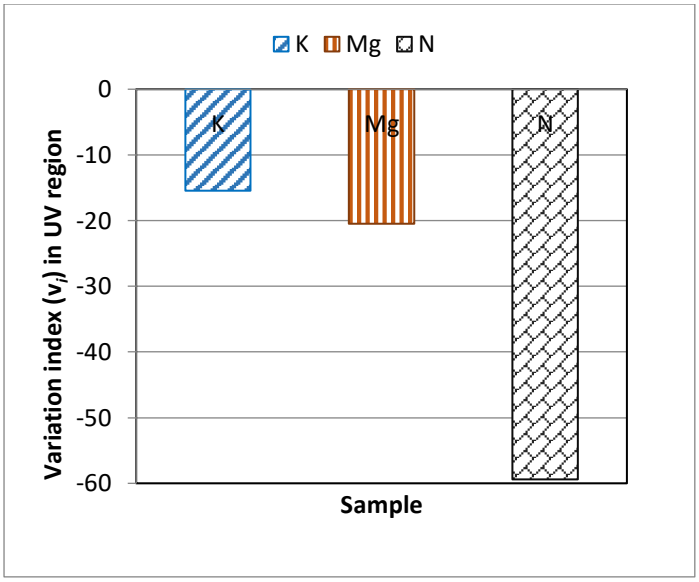


Figure 21: Variation index (v_i) of leaves in UV region for distinguishing controlled and different nutrient deficiency leaves.

Form Figure 21 it can be seen that v_i is ~60%, ~21% and ~16% higher for leaves with N, Mg and K deficiency respectively in negative direction in the UV region. This indicates that the standard deviation of leaves with nutrient deficiency is higher than that of controlled leaf.

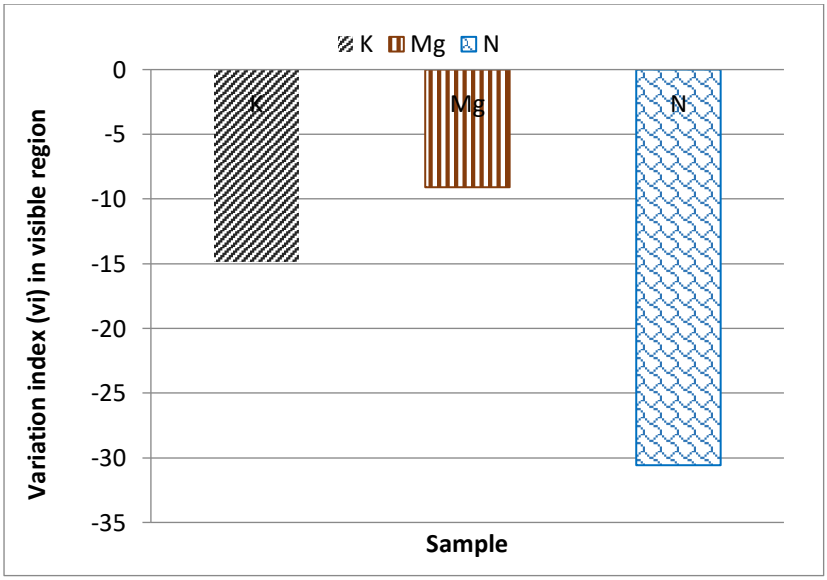


Figure 22: Variation index (v_i) of leaves in VIS region for distinguishing controlled and different nutrient deficiency leaves.

In the case of VIS region (Figure 22) it can be observed that v_i values deviate ~31%, ~ 8% and ~15% for leaves with N, Mg and K deficiency respectively in negative direction indicating in VIS region standard deviation of leaves with nutrient deficiency is higher than that of controlled leaf. Furthermore it can be obtained from Figure 23 that in NIR region v_i values deviate ~38%, ~ 44% and ~27% for leaves with N, Mg and K deficiency respectively in positive direction indicating in NIR region standard deviation of leaves with nutrient deficiency is lower than that of controlled leaf. Table 1 summarizes different features to differentiate controlled leaf and leaves with nutrient deficiency.

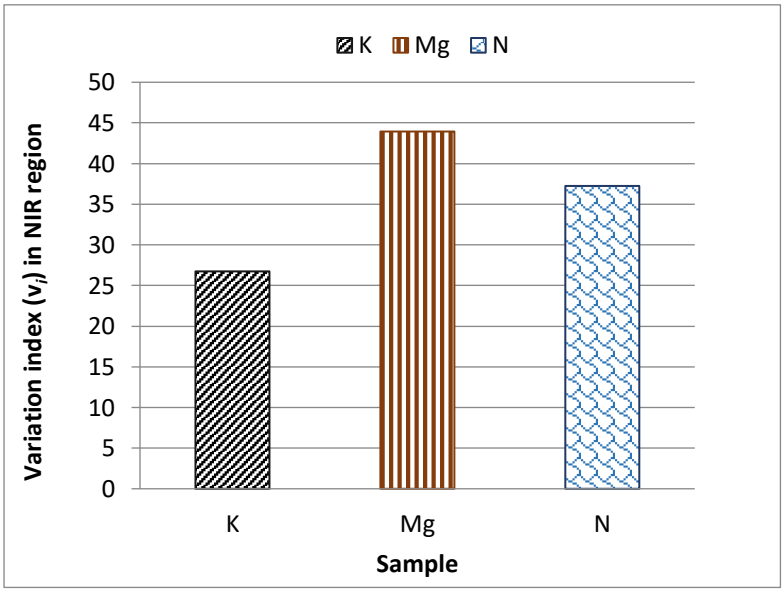


Figure 23: Variation index (v_i) of leaves in NIR region for distinguishing controlled and different nutrient deficiency leaves.

Table 1: Different important features, corresponding values and significance for classification ability in terms of remarks to distinguish healthy and nutrient deficiency leaves.

Features	**Control**	N	Mg	K	Remark
NDVI	High (0.75)	Lowest (0.35)	Lower (0.45)	Lower (0.42)	Can be a good feature to distinguish from control leaves but individual nutrient deficiencies may not be uniquely identified

Variation index (v_i) in UV region		High (59)	Lower (21)	Lowest (15)	Can be used as a feature to distinguish N deficiency from K and Mg deficiency but K and Mg may not be uniquely identified.
Variation index (v_i) in VIS region	-	High (31)	Low (9)	Moderate (14.5)	Can be used as a feature to distinguish N deficiency from K and Mg deficiency but K and Mg deficiency may not be uniquely identified
Variation index (v_i) in NIR region	-	Moderate (37)	High (44)	Low (27)	Can be used as a feature to distinguish K deficiency from N and Mg deficiency but N and Mg deficiency may not be uniquely identified
Brightness at 550 nm	Lowest (~4614)	Highest (~16000)	Lower (~9707)	Lower (~12126)	Can be used as a feature to distinguish from controlled and also N nutrient deficiency but K and Mg may not be uniquely identified.
Brightness at 800 nm	Highest (~16210)	Lower (13820)	Lowest (12700)	Lower (14616)	Can be a good feature to distinguish from controlled but not individual nutrient deficiency may not be uniquely identified.
Ratio (Controlled /Nutrients Deficiency)	-	Highest at ~ 617 nm (3.7015)	Low at ~617 nm (2.16636)	Moderate at ~617 nm (2.743)	Can be used as a feature to distinguish from controlled and also individual nutrients deficiency.
Standard Deviation in UV region	Lowest (~1500)	High (~2300)	Lower (~1800)	Lower (~1700)	Can be used as a feature to distinguish from controlled and also N deficiency leaves.
Standard Deviation in VIS region	Lowest (~1000)	High (~4100)	Lower (~2000)	Lower (~2600)	Can be used as a feature to distinguish from controlled and also

					individual nutrients deficiency.
Standard Deviation in NIR region	Highest (~2200)	Lower (~1300)	Low (~1200)	High (~1600)	Can be used as a feature to distinguish from controlled leaves and individual nutrient deficiencies.
1st derivative ratio between 680nm and 750 nm	~ 30% Positive direction	~ 62% Negative direction	~ 37% Negative direction	~47% Negative direction	Can be used as a feature to distinguish from controlled and also individual nutrients deficiency.

Discussion

This paper demonstrated the study of age detection and distinguishes between healthy and unhealthy grapevine leaves with the aid of hyperspectral imaging in the range between ~380 nm and 1000 nm. For age detection leaves aged very young to old have been studied. From the analysis it was found that the magnitude of mean brightness of leaves has strong correlation with aging. This variation was found to be more prominent at ~ 554.3 nm. Mean 1st derivative brightness study demonstrated that mean 1st derivatives brightness peaks in visible wavelengths shifted to the longer wavelengths as the leaves age. Mean 1st derivatives brightness curves in the range between ~ 675 nm and ~ 775 nm revealed that the rate of change of mean brightness decreased with gradual aging of leaves. Variation index, a new metric introduced in this manuscript, also indicated to be correlated with age of leaves.

To distinguish between healthy and unhealthy grapevine leaves the unhealthy leaf samples were divided into two groups. The 1st group contained leaves that were visibly unhealthy and features of these leaves were compared with those of visibly health leaf (i.e. benchmark leaf). In this case both whole area and selective areas containing defects on the leaves were investigated. From these studies it was found that mean 1st derivatives brightness in the NIR region disclosed distinguishable curves for both whole area and selective areas' leaves compared to a healthy leaf. But the variation of curve shapes was more significant for whole areas' leaves compared to selective areas' leaves. Furthermore, ratio analysis study established that more distinguishable curves could be obtained from the whole leaves' study. Experimental results suggest that variation index could be employed to detect defective leaves.

On the other hand, the 2nd group contained leaves that have N, K and Mg deficiency. The features of these leaves were studied with respect to those of controlled leaf as well as compared features of nutrient deficiency leaves with respect to each other. In this case it has been found that the brightness feature between VIS range can be used to distinguish between controlled and nutrient deficiency leaves as the brightness of leaves with nutrients deficiency are higher than the controlled leaf. This feature can also be employed to identify controlled and N deficiency leaves due to the highest brightness peak of N deficiency leaves compared to controlled, K and Mg deficiency leaves at ~550 nm. The feature such as the brightness peak of nutrient deficiency leaves appeared at the shorter wavelength (red shift) compared to the controlled leaf in the wavelength range between ~ 680 nm and 1000 nm can be used to identify controlled and nutrient deficiency leaves. Again the curve shape and magnitude of brightness ratio plot can be employed as a feature to distinguish between N, K and

Mg deficiency leaves. Furthermore, in this study NDVI value could significantly differentiate controlled and unhealthy leaves, though N, K and Mg deficiency could not be identified uniquely. The features of nutrient deficiency leaves between ~650 nm – 800 nm of 1st derivative peaks such as dominant peak at ~700 nm, narrowing of 1st derivative brightness peaks, and 1st derivative peaks shifted to the shorter wavelength (red shift) compared to the controlled leaf can be useful features to distinguish between controlled and nutrient deficiency leaves. Also from the 1st derivative ratio between 680 nm and 750 nm plot could be employed to distinguish between controlled and nutrient deficiency leaves as this 1st derivative ratio has been found to be positive for controlled leaf and negative for nutrient deficient leaves. Furthermore the magnitude of this ratio of different nutrient deficiency leaves could be utilized to distinguish between leaves with N, K and Mg deficiency. Again from the study of standard deviation it can be stated that in VIS wavelength this feature could be used to distinguish from controlled and also individual nutrients deficiency leaves. The study reveals that N and K deficiency could be identified from the variation index study in UV and NIR wavelength respectively. Further in depth analysis could indicate more specifically age and detection of healthy and unhealthy grapevine leaves as well as help to identify or classify the differences between leaves with various visible defects as well as nutrient deficiency uniquely.

Chapter 3- Grapevine Tissue Sampling for Nutrient Analysis

The text presented here has been published in the Australian Journal of Grape and Wine Research (https://onlinelibrary.wiley.com/doi/abs/10.1111/ajgw.12496)

Baby T, Moroni FJ, Gascon-Aldana P, Moroni NC, Holzapfel BP, Schmidtke LM, Walker RR, Rogiers SY. 2021. Characterising leaf petiole, blade and bunchstem nutrient concentration across three cultivars. Australian Journal of Grape and Wine Research 27 https://doi.org/10.1111/ajgw.12496

Introduction

The growth and physiological functions driving yield and fruit quality of grapevines are influenced by key macro and micronutrients. Macronutrients include nitrogen, potassium, calcium, magnesium, phosphorus and sulphur, which are present at relatively large amounts and are often expressed as % of dry matter. The key micronutrients include boron, iron, manganese, zinc, copper and molybdenum, which occur at relatively lower concentrations and are often expressed as ppm of the dry matter. The physiological roles of each nutrient have been extensively reviewed by a number of researchers (Amiri and Fallahi 2007, Rogiers et al. 2017, Guo et al. 2016, Uchida 2000, Robinson 1988, Treeby 2004).

Accurate assessment of the nutrient status of grapevines is crucial for optimising fertilizer applications to avoid any nutrient imbalances, which can otherwise impact yield, berry composition and wine style. Analysis of plant tissues, most commonly leaf laminae (blades) and petioles (leaf stems), are widely used to assess the nutritional status of grapevines (Brunetto et al. 2007, Benito et al. 2013). As per the current Australian protocols, petiole samples are collected from opposite the basal bunch at 80% flowering and leaf blades at veraison. The results of the tissue analysis are compared with previously established standards of adequate ranges for each nutrient (AWRI 2010). Current Australian standards for petiole samples at flowering are based on Californian data, after modifications in response to a number of Australian field trials (Robinson et al. 1997).

In spite of a considerable effort to establish the most appropriate tissue type, sampling time, and adequate range for each nutrient, the current grapevine nutrient standards used in Australia are neither a perfect fit for all growing conditions nor cultivar specific. Plant mineral composition can vary greatly with internal factors such as cultivar and rootstock, tissue type, nodal position and age of tissues sampled, as well as external factors such as soil characteristics, climate and agronomic practices (Stellacci et al. 2010). The optimal nutritional requirements may also vary based on the yield expectations of specific vineyards and the required fruit quality for particular wine styles. Due to this variability, a number of researchers have tried to establish standards for local growing conditions, important commercial cultivars, and even for specific rootstock- scion combinations (Porro et al. 2001, Davenport et al. 2012, García-Escudero et al. 2013, Fallahi et al. 2005, Lehoczky and Kocsis 1998).

Findings on the reliability of specific tissue type and/or sampling time for assessing the vine nutrient status are inconsistent. While petioles are commonly recommended for tissue analysis (Robinson et al. 1978, Christensen 1984, Tandonnet et al. 2008, AWRI 2010), many studies suggest that the blade is superior to the petiole for nutrient diagnosis (Dominguez et

al. 2015, Schreiner and Scagel 2017). Some studies suggest that the tissue type and the sampling time should be determined based on the nutrient to be analysed (Benito et al. 2013, Laibarra et al. 2014). Choice of tissue type is based on factors such as: ease of sampling and processing of large sample numbers, ability to analyse all of the important nutrients in the same tissue, tendency to accumulate more nutrients compared to other plant parts (Christensen 1969, Christensen and Kearney 2000), and repeatability and stability of the nutrient concentrations within the tissue over a period within a phenological phase (Conradie 1981, Benito et al. 2013). A recent study comparing leaf blade and petiole nutrient concentrations in association with vine growth, yield, and must nutrient responses of 'Pinot Noir' grapevines recommended the use of leaf blades as opposed to petioles for diagnosing the N, P, and K status (Schreiner and Scagel 2017).

Leaf nutrient concentration varies with age and its relative position on the shoot (Christensen 1969, Garcia et al. 2001, Schaller 2006, Romero et al. 2010). The node position on which the most basal bunch is located is most commonly recommended for the sampling of leaves, for analysis of either petioles or blades, at both flowering and veraison (Kliewer 1991). However, based on a more recent study on Tempranillo (*Vitis vinifera* L.), Romero et al. (2010) proposed that sampling of leaves after veraison should occur from the node located one node distal (younger) to the most basal bunch (the second most basal bunch), considering the tendency of this cultivar to senesce prematurely. Fluctuations in the concentration of each nutrient in different tissue types are due to the dynamic nature of nutrient uptake, accumulation and remobilisation of nutrients into different tissues over the entire growth cycle (Holzapfel et al. 2019). Root pressure and leaf transpiration drive the uptake and translocation of mineral elements, with vine vigour also playing an important role (Keller 2005). Soil moisture and temperature have a large impact on the timing and extent of nutrient uptake and thus environmental and irrigation factors cause further fluctuations in vine nutrient content (Keller 2005, Clarke et al. 2015). Even though flowering and veraison are the most common sampling times in grapevines, either petioles or leaf blades are used inconsistently at different sampling times in various countries (Benito et al. 2013). Furthermore, some studies suggest that petioles should be collected during the month following bloom because during this time petioles showed reasonably stable nutrient levels (Conradie 1981).

The objective of this work was to assess the comparative value of tissue type and node location for determining tissue nutrient concentration of three main Australian wine grape cultivars Cabernet Sauvignon, Shiraz and Chardonnay grown in a warm-hot viticulture region of Australia under well-watered conditions. A secondary objective was to assess the extent of cultivar variation in tissue nutrient concentrations under the same growing conditions.

Methods

The trial was conducted in a replicated cultivar block at Charles Sturt University, Wagga Wagga, NSW (latitude: –35.1583S, longitude: 147.4573E, elevation: 212 m). This study included 15-year-old vines of cvs. Cabernet Sauvignon, Shiraz and Chardonnay vines on their own roots. For each cultivar there were six replicate panels of three vines per panel. The six panels of each cultivar were randomised throughout the block. Vines were planted in 2005 at a spacing of 3 m x 1.5 m in E-W row orientation (2,222 vines/ha). Vines were spur pruned to 40 buds per vine, and the single bilateral cordons were trained along a single horizontal wire. Vines were drip irrigated 1-3 times per week depending on the time in the growing season from late September to early May, the total amount of irrigation water applied was

4.3 ML for the growing season (2019/20). The vines received a fertiliser application (Pivot 400) in early December 2019, being 29.2 kg N/ha, 6.3 kg P/ha, 10.1 kg K/ha and 12.1 kg S/ha. The same amount was applied in the post-harvest period in the previous season (late April). The soil across the block was a well-drained sandy loam (Kandosol), with the inter-row area consisting of volunteer grass and broad leaf species that were regularly slashed, the undervine weeds were controlled by herbicides. Three replicate soil core samples were collected from the vine rows across the block at the end of the season. They were air dried, then analysed, and the soil properties are presented in Supplementary Table 1.

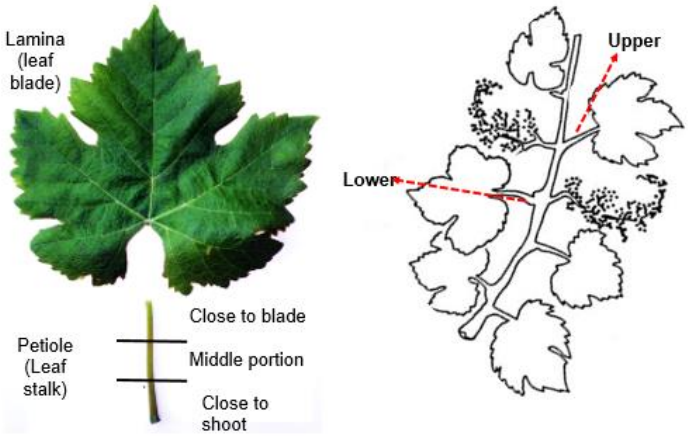
Supplementary Table 1. Soil properties in 0 - 30 cm layer

Soil properties	
pH Soil: Water, 1:5	7.0 ± 0.03
EC Soil:Water, 1:5 (dS/m)	87.1 ± 2.32
Effective Cation Exchange Capacity (ECEC)	9.6 ± 2.34
Exchangeable Bases *	
K (cmol (+) kg^{-1})	0.9 ± 0.06
Ca (cmol (+) kg^{-1})	5.1 ± 1.28
Mg (cmol (+) kg^{-1})	3.1 ± 1.17
Na (cmol (+) kg^{-1})	0.5 ± 0.07
Base saturation percentages	
K %	10.4 ±2.50
Ca %	52.6 ±1.68
Mg %	31.1 ±3.72
Na %	5.9 ±1.81

*Cations were extracted in 1 M ammonium chloride at pH 7.0, Values are averages of three replicates ± SE. n = 3.

Plant tissue sampling

Leaves were sampled at flowering (80% cap fall) and veraison (50 % berries soft) opposite inflorescences/bunches from two shoots per vine at two separate node positions: one opposite to the basal bunch (lower position) and the other at the subsequent more distal position (upper position). There was always an inflorescence/bunch opposite to the sampled leaves and those inflorescences/bunches were also sampled. Each leaf was separated into petiole and blade, and each petiole was further divided into three equal lengths (segment near blade, middle segment and segment near shoot). The peduncle of the inflorescence/bunch (bunchstem) was excised between the shoot junction and the first lateral of the rachis.



Nutrient analysis

For better accuracy, each sample from each plant (12 petiole segments, four leaf blades and four bunchstems) was analysed for nutrient concentration individually. Petiole sections, blades and bunchstems were dried at 60°C for 1 week and ground individually using a tissue lyser (TissueLyser II, Qiagen, Chadstone, Victoria). 100 mg of ground tissue was analysed for calcium (Ca), magnesium (Mg), potassium (K), phosphorous (P), iron (Fe), manganese (Mn), boron (B), copper (Cu), zinc (Zn), sulfur (S), and sodium (Na) by inductively coupled plasma atomic emission spectroscopy (ICP-AES) at the Environmental and Analytical Laboratories at Charles Sturt University, Wagga Wagga. Total nitrogen (N) was analysed on a 50 mg sample with a VarioMAX combustion analyser (Elementar, Hanau, Germany). Those samples collected at flowering were assessed for Ca, Mg, K, S, P, Fe, Zn, Mn, Mo and B in all three cultivars. The same elements were assessed for the samples collected at veraison but only for Cabernet Sauvignon and Chardonnay while the Shiraz samples were used for N analysis as not enough sample was available for both types of analyses.

Statistical analysis and data presentation

For multivariate analysis each data set (flowering and veraison) were considered separately. Data were analysed using the AComDim (Bouveresse, et al. 2011) approach which is appropriate for designed experiments with unbalanced and nested factors (Guisset, et al. 2019). For each data set the variances were partitioned according to a four factor ANOVA model with two and three way interactions with the following explanatory factors (EF) and levels- Veraison: Cultivar (Cabernet Sauvignon, Chardonnay [fixed]), Panel Replicate (R1 to R6 [random]), Node (upper, lower [fixed]), Tissue (bunchstem, blade end of petiole, blade, middle segment of petiole, shoot end of petiole [fixed]). The flowering data set was structured similarly with an additional level for Cultivar (Cabernet Sauvignon, Chardonnay, Shiraz [fixed]). Data variances were partitioned according to the general linear model for mixed model unbalanced ANOVA experiments (Thiel, et al. 2017). AComDim sequentially partitions data variance according to the experimental EF design and levels. The data matrix is sequentially deflated according to the ANOVA model until a residual data block remains thereby creating effects matrices for each EF and iterations. Each effects matrix is then augmented by addition of the residual data block, prior to a multiblock decomposition based upon extraction of orthogonal common components and determination of EF block contributions (saliences) indicative of the total variance associated with that common component (CC). Thus all data matrices have a common structure (the residuals) which is associated with the first CC, enabling subsequent CCs to be compared with the residuals to ascertain the overall EF levels

effects for a specific CC. Two approaches in determining the significance of CCs associated with specific EF can be used. Firstly an F-test ratio based upon the ratio of the salience of the CC of interest with the salience of the residual block in the first CC. Secondly, inspection of sample scores of the interesting CC versus the sample scores associated with the first common component, with confidence intervals determined using Hotelling T2 metrics, enables visualisation of overlapping or distinct confidence interval boundaries for EF levels. Associated variable loadings provides insight to the explanatory factors within the overall experimental design.

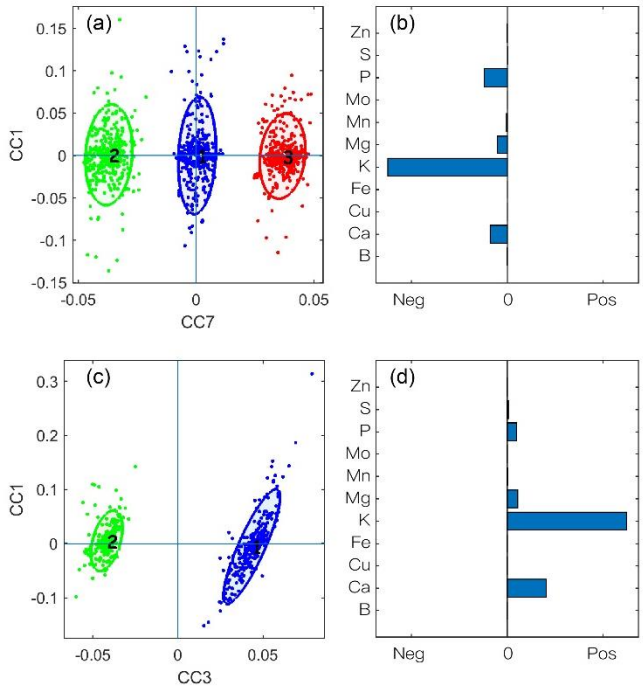
Significant differences between tissues: bunchstem, petiole, laminae as well as between petiole segments: segment near blade, middle segment, segment near shoot were determined by performing a one way ANOVA (with matching of data from each replicate), followed by Tukey's test. Significant difference between node positions for each tissue type was determined by Paired t-test. A P value <0.05 was considered significant. Petiole concentrations were calculated by dividing the total nutrient content in the three segments by total dry mass of the three segments. For the comparison between different tissue types and between different petiole segments data from upper and lower nodes were averaged for each cultivar. These analyses were performed using GraphPad Prism 8 (GraphPad Software, San Diego, California, USA). Correlation analyses were performed between node positions, between tissue types (blade, petiole and bunchstem), and between petiole segments for each nutrient using IBM SPSS Statistics Data Editor (IBM SPSS Statistics 26, New York, USA).

Results

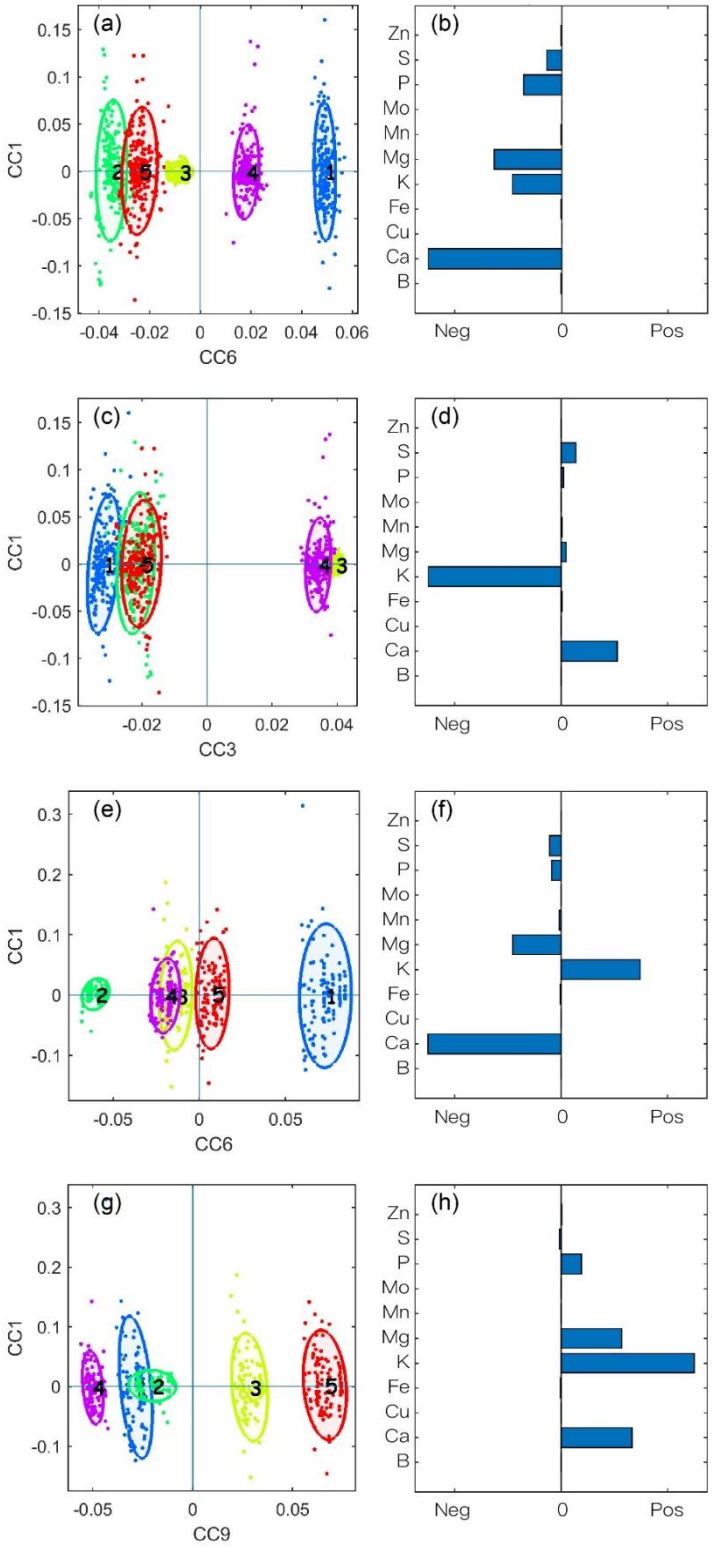
Preliminary data analysis using AComDim

A clear clustering of samples along the CCs for cultivar (Supplementary Figure 1a,c) and tissue type (Supplementary Figure 2a,c,e,g) were apparent at both the flowering and veraison sampling times. For cultivar, the clustering of samples was primarily driven by K, but Ca, P and Mg also contributed (Supplementary Figure 1b,d). For tissue type differences, these four elements were again important drivers, including S depending on the model (Supplementary Figure 2b,d,f,h). The subsequent results are thus focussed on these macronutrients.

Supplementary Figure 1. Sample groupings (left panels) and salience plots (right panels) from the AComDim analysis depicting cultivar differences at (a,b) flowering and (c,d) veraison. Cultivar scores plot with each ellipse represent 95% confidence intervals. Group centroids indicated with numerals: 1=Cabernet Sauvignon, 2=Chardonnay, 3=Shiraz. Variable loading values for each nutrient indicate the relative contribution of that nutrient to sample clusters in the model.



Supplementary Figure 2. Sample groupings (left panels) and salience plots (right panels) from the AComDim analysis depicting tissue differences at (a-d) flowering and (e-h) veraison. Cultivar scores plot with each ellipse represent 95% confidence intervals. Group centroids inidcated with numerals: 1=Bunchstem; 2=Blade; 3=Petiole segment near blade; 4=Middle segment of petiole; 5= Petiole segment near shoot. Variable loading values for each nutrient indicate the relative contribution of that nutrient to sample clusters in the model.



Petiole, leaf blade and bunchstem comparisons

Significant differences in nutrient concentrations were observed between the tissues in the three cultivars (Table 1). K was lower in the blades than the petiole or bunchstem in all three cultivars at flowering and veraison, whereas for Chardonnay at veraison, there was no difference in K concentration between the tissues. Ca, Mg , P and S, were lowest in bunchstems in each of the cultivars at flowering and veraison, with the exception of Chardonnay for P at veraison. Ca was higher in the blades relative to the other tissues in all

three cultivars at flowering. At veraison, the blades contained the highest concentrations of Ca in Chardonnay, while in in Cabernet Sauvignon both petioles and blades had significantly higher concentrations than the bunchstem. While Mg was highest in the petioles of all three cultivars at flowering, at veraison Cabernet Sauvignon showed the same trend, however there was no significant difference in Chardonnay between Mg concentrations in petioles and leaf blades. As assessed in Shiraz at veraison, N was higher in the blade relative to the other tissues (Figure 1).

Figure 1. The N concentrations in different tissue types (bunchstem, blade, three different segments of petiole) in Shiraz at veraison. Values for each tissue type are averages of the upper and lower node. Each bar represents mean + SE (n= 36 replicates). Petiole segment near shoot (orange), middle petiole segment (purple), petiole segment near blade (red), bunchstem (blue), and blade (green). Significant differences in nutrient concentrations between different tissue types were determined by performing one way ANOVA (with matching of data from each replicate), followed by comparison of replicate means by Tukey's test ($P<0.05$). Different superscripts show significant difference.

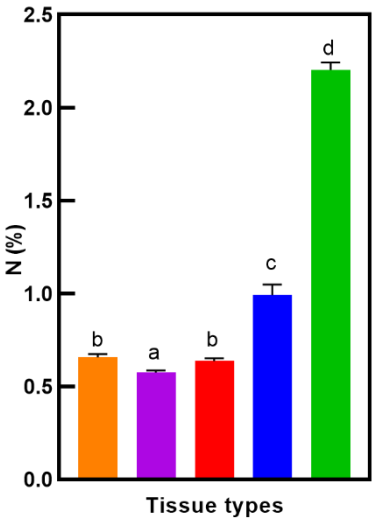


Table 1. Nutrient concentrations in three different tissue types (petioles, blade, bunchstem) in three cultivars (Cabernet Sauvignon, Chardonnay and Shiraz at flowering, and Cabernet Sauvignon and Chardonnay at veraison).

		Cabernet Sauvignon				Chardonnay				Shiraz			
		Petiole	**B.stem**	**Blade**	**Sig [1]**	**Petiole**	**B.stem**	**Blade**	**Sig [1]**	**Petiole**	**B.stem**	**Blade**	**Sig [1]**
Macronutrients (g/kg)													
P	Flowering	3.5^{c}	1.3^{a}	2.5^{b}	** **	4.0^{c}	1.7^{a}	2.5^{b}	** **	2.6^{b}	1.2^{a}	2.2^{b}	** **
	Veraison	4.2^{b}	2.2^{a}	3.2^{b}	** *	2.8^{b}	1.5^{a}	1.0^{a}	*				
K	Flowering	14.5^{b}	14.3^{b}	8.9^{a}	** **	17.9^{b}	18.4^{b}	9.5^{a}	** **	10.3^{a}	14.0^{b}	8.1^{a}	** **
	Veraison	25.0^{b}	27.2^{b}	7.1^{a}	** **	7.9	8.8	6.0	**ns**				
Ca	Flowering	9.4^{b}	2.8^{a}	11.6^{c}	** **	9.2^{b}	3.5^{a}	11.3^{c}	** **	8.0^{b}	2.8^{a}	11.1^{c}	** **
	Veraison	16.4^{b}	4.7^{a}	16.0^{b}	** **	6.7^{b}	2.0^{a}	15.6^{c}	** **				
Mg	Flowering	3.9^{c}	0.7^{a}	2.9^{b}	** **	4.7^{c}	0.8^{a}	3.3^{b}	** **	4.0^{c}	1.1^{a}	2.5^{b}	** **
	Veraison	7.1^{c}	0.5^{a}	4.5^{b}	** **	4.5^{b}	0.3^{a}	3.3^{b}	**				
S	Flowering	0.9^{b}	0.5^{a}	2.1^{c}	** **	1.0^{b}	0.4^{a}	2.0^{c}	** **	1.0^{b}	0.5^{a}	2.1^{c}	** **
	Veraison	1.0^{b}	0.5^{a}	2.2^{c}	** **	1.0^{b}	0.3^{a}	0.9^{b}	**				
Micronutrients (mg/kg)													
B	Flowering	15.6^{b}	11.6^{a}	30.4^{c}	** **	19.8^{b}	11.6^{a}	17.4^{ab}	*	14.1^{b}	6.7^{a}	27.4^{c}	** **
	Veraison	39.0^{b}	18.9^{a}	80.6^{c}	** **	43.9^{b}	18.3^{a}	27.4^{b}	*				
Cu	Flowering	3.5^{a}	6.0^{b}	7.7^{c}	** **	2.8^{a}	6.2^{b}	5.8^{b}	** **	8.3^{ab}	8.0^{a}	11.8^{b}	**
	Veraison	3.7^{a}	11.1^{b}	3.2^{a}	** **	0.7^{a}	1.9^{b}	7.5^{c}	** **				
Fe	Flowering	12.2^{a}	16.1^{b}	113.8^{c}	** **	19.8^{a}	17.9^{a}	96.7^{b}	** **	16.7^{a}	13.1^{a}	100.1^{b}	** **
	Veraison	46.3^{a}	29.2^{a}	161.5^{b}	** **	28.8^{b}	14.0^{a}	142.7^{c}	** **				
Mn	Flowering	79.3^{b}	19.6^{a}	114.5^{c}	** **	93.0^{b}	24.9^{a}	118.6^{c}	** **	65.9^{b}	16.5^{a}	97.5^{c}	** **
	Veraison	206.2^{b}	34.1^{a}	179.3^{b}	** **	114.3^{b}	13.6^{a}	149.1^{b}	** **				
Mo	Flowering	0.8	2.2	0.0	**ns**	0.0	0.0	0.0	**ns**	0.2	0.6	0.0	**ns**
	Veraison	45.4^{b}	12.4^{a}	1.3^{a}	** **	30.0^{c}	11.4^{b}	1.4^{a}	** **				
Zn	Flowering	25.2^{c}	9.2^{a}	15.1^{b}	** **	44.6^{c}	11.3^{a}	16.4^{b}	** **	24.6^{c}	11.2^{a}	15.4^{b}	** *
	Veraison	33.9^{b}	7.6^{a}	27.9^{b}	** **	43.2^{c}	5.0^{a}	12.3^{b}	** *				

**** P value <0.0001, *** P value <0.001, ** P value <0.01, * P value <0.05, **Sig[1]** Level of significance. Petiole nutrient concentrations are calculated from total nutrient content in the three segments divided by total dry mass of the three segments, and expressed as g/kg (macronutrients) and mg/kg (micronutrients). Each value represents mean of averaged data from upper and lower node positions (n= 36 replicates). Different superscripts show significant difference. ns = not significant.

The phenological stage of the sampling had a significant effect on the nutrient concentrations and this was further influenced by cultivar (Table 1). In Cabernet Sauvignon, most of the nutrients were generally higher at veraison than at flowering in all tissue types, with a few exceptions. In contrast, for Chardonnay, only a few nutrients were higher at veraison than at flowering.

The nutrient concentrations of the bunchstem were generally more closely correlated to that of the petiole than the leaf blade in all three cultivars. Sampling time and cultivar had an influence on the strength of the relationship between the nutrient concentrations of the different tissues (Table 2). For example, K levels in Cabernet Sauvignon and Chardonnay petioles were strongly correlated with bunchstem levels at flowering and veraison. However, no such correlation was evident between petioles and leaf blades at flowering in these two cultivars. Then again, for K at veraison, there was a strong correlation between petioles and leaf blades in Cabernet Sauvignon but not Chardonnay. In Cabernet Sauvignon, positive correlations were evident between the petiole and bunchstem for P, K, Ca, Mg and S at flowering and for K and S at veraison. Leaf blade and petiole K, Ca and Mg were also correlated at veraison. In Chardonnay, bunchstem and petiole K and S at flowering and P, K, Ca and Mg at veraison showed a positive relationship. Leaf blade and petiole P and Ca were also correlated at flowering in this cultivar. In Shiraz at flowering, positive correlations were evident between petiole and bunchstem P, K, Ca, Mg and S (Table 2). In Shiraz at veraison, total N levels of the petioles were not correlated with those of the leaf blades. In contrast, significant positive correlations for N were present between blades and bunchstems as well as petioles and bunchstems (Supplementary Table 2).

Table 2. The Pearson correlation coefficients (r) of nutrient concentrations between different tissues (leaf blade, bunchstem and petiole) at flowering and veraison in three cultivars.

	Cabernet Sauvignon						**Chardonnay**						**Shiraz**		
	B.stem vs Petiole		**Blade vs Petiole**		**Blade vs B.stem**		**B.stem vs Petiole**		**Blade vs Petiole**		**Blade vs B.stem**		**B.stem vs Petiole**	**Blade vs Petiole**	**Blade vs B.stem**
	Flow	**Verai**	**Flow**	**Verai**	**Flow**	**Verai**	**Flow**	**Verai**	**Flow**	**Verai**	**Flow**	**Verai**	**Flow**	**Flow**	**Flow**
P	.745**	.372*	.373**	ns	Ns	ns	.395*	.803**	.590**	ns	ns	ns	.695**	.509**	ns
K	.876**	.757**	ns	.580*	Ns	ns	.719**	.860**	ns	ns	ns	ns	.855**	.346*	ns
Ca	.605**	ns	.345*	ns	Ns	ns	.428**	.870**	.604**	ns	ns	ns	.629**	.347*	ns
Mg	.512**	.364*	ns	ns	Ns	ns	ns	.832**	.441**	ns	ns	ns	.534**	.396*	ns
S	.833**	.751**	.416**	ns	.441**	.706**	.719**	.810**	.417*	.389*	ns	.593**	.716**	ns	ns
B	.819**	.930**	ns	ns	Ns	ns	.903**	.758**	ns	.555**	ns	.575**	.818**	ns	ns
Cu	.460*	ns	.422*	ns	.408*	ns	.593**	-.458**	ns	ns	ns	ns	ns	ns	ns
Fe	.657**	.537**	.341*	ns	.366*	ns	ns	.827**	.363*	ns	.714**	-.420*	ns	ns	ns
Mn	.668**	ns	.704**	.599*	Ns	ns	.508**	.812**	.785**	ns	ns	ns	.602**	.869**	.341*
Mo	.571**	.921**	ns	ns	Ns	ns	ns	.933**	ns	ns	ns	ns	ns	ns	ns
Zn	ns	.705**	.363*	ns	Ns	ns	ns	.857**	.502**	ns	ns	ns	.390*	ns	ns

** Correlation is significant at the 0.01 level, * Correlation is significant at the 0.05 level. Petiole nutrient concentrations are calculated from total nutrient content in the three segments divided by total dry mass of the three segments. In each regression, each data point includes the mean value of upper and lower node positions (n=36 replicates). B.stem = bunchstem; ns = not significant.

Supplementary Table 2. The Pearson correlation coefficients (r) of nitrogen (N) concentrations between different tissues (blade, bunch stem and petiole), between different petiole segments (middle segment (M), segment near blade (L) and segment near shoot (S)), and between two node positions (opposite to basal bunch (lower) and the next upper node (upper)) in Shiraz at veraison.

	Tissues		
	B.stem vs petiole	**Blade vs Petiole**	**Blade vs B.stem**
N	.538**	ns	.468**

** Correlation is significant at the 0.01 level, * Correlation is significant at the 0.05 level. In the regressions of tissues, and petiole segments each data point includes the mean value of upper and lower node positions. In the regressions of tissues the petiole values used were calculated from total nutrient content in the three segments divided by total dry mass of the three segments (n=36 replicates). B.stem = bunchstem; ns = not significant.

Node position

Node position had a significant impact on K, Ca and Mg in all tissue types for all the cultivars at flowering, with the exception of petiole K in Cabernet Sauvignon (Tables 3 and 4). At veraison, there were fewer effects of node position. Ca and Mg concentrations were higher in the blades and petioles collected from the more basal position on the shoot, whereas in the bunchstems these nutrients were higher in the more distal node position. This effect was significant at flowering time in all cultivars but at veraison a similar trend was observed only in the blades of Chardonnay. At veraison, Ca and Mg in Chardonnay blades were higher in the more basal node position but not so in Cabernet Sauvignon. Interestingly, in all cultivars, K levels were significantly higher in the more distal (younger) node position at flowering, while at veraison, this was not apparent in either Cabernet Sauvignon or Chardonnay (Table 3). At veraison, in Shiraz, N was found to be significantly higher in the basal node than the distal node for the bunchstem and blade (Table 3).

For petioles and blades, there was a significant positive correlation between the node positions in most nutrients in all the cultivars (Supplementary Table 3). For the bunchstem a weaker correlation was observed for most nutrients especially for Cabernet Sauvignon at veraison and Chardonnay at flowering (Supplementary Table 3). In Shiraz, for N at veraison there was a significant correlation between the node positions for each tissue type (Supplementary Table 2).

Table 3. Macronutrient concentrations in three different tissue types at two node positions in three cultivars: Cabernet Sauvignon, Chardonnay and Shiraz.

Nutrients (g/kg)	Tissue	Cabernet Sauvignon			Chardonnay			Shiraz		
		Lower	Upper	Sig[1]	Lower	Upper	Sig[1]	Lower	Upper	Sig[1]
Flowering										
	B. stem	1.1	1.5	**	1.5	1.9	*	1.1	1.4	**
P	Blade	2.5	2.4	Ns	2.5	2.5	ns	2.2	2.3	ns
	Petiole	3.8	3.1	**	4.3	3.7	**	2.6	2.5	ns
	B. stem	12.4	16.2	**	14.5	22.3	***	12.8	15.2	*
K	Blade	8.6	9.2	*	9.0	10.1	****	7.9	8.4	**
	Petiole	13.9	15.1	Ns	17.0	18.8	*	9.2	11.3	**
	B. stem	2.3	3.3	**	3.1	3.9	*	2.3	3.3	****
Ca	Blade	12.1	10.9	*	12.0	10.7	****	11.7	10.4	**
	Petiole	10.6	8.2	****	9.9	8.5	***	8.5	7.5	*
	B. stem	0.5	0.9	**	0.6	1.1	**	0.7	1.6	****
Mg	Blade	3.0	2.7	**	3.5	3.1	***	2.7	2.4	**
	Petiole	4.5	3.3	****	5.3	4.0	****	4.3	3.7	*
	B. stem	0.4	0.5	*	0.4	0.5	ns	0.4	0.5	ns
S	Blade	2.1	2.1	Ns	2.0	2.0	ns	2.1	2.0	***
	Petiole	1.1	0.8	**	1.2	0.9	***	1.1	1.0	ns
Veraison										
	B. stem							10.6	9.5	*
N	Blade							21.5	22.5	*
	Petiole							6.4	6.2	ns
	B. stem	2.1	2.2	Ns	1.5	1.5	ns			
P	Blade	1.6	1.5	Ns	1.1	1.0	ns			
	Petiole	4.5	3.8	***	2.9	2.7	ns			
	B. stem	25.2	28.4	Ns	8.7	8.6	ns			
K	Blade	3.3	3.4	Ns	5.8	6.4	ns			
	Petiole	24.3	25.3	Ns	7.9	7.9	ns			
	B. stem	4.0	5.3	Ns	2.0	1.9	ns			
Ca	Blade	7.9	7.7	Ns	16.2	15.0	**			
	Petiole	16.3	16.6	Ns	6.9	6.5	ns			
	B. stem	0.5	0.6	Ns	0.3	0.3	ns			
Mg	Blade	2.3	2.2	Ns	3.5	3.2	**			
	Petiole	7.3	6.9	Ns	4.8	4.2	ns			
	B. stem	0.5	0.5	Ns	0.4	0.3	ns			
S	Blade	1.1	1.0	Ns	0.9	0.9	ns			
	Petiole	1.1	1.0	*	1.0	1.0	ns			

**** P value <0.0001, *** P value <0.001, ** P value <0.01, * P value <0.05, Sig[1] Level of significance. Petiole nutrient concentrations are calculated from total nutrient content in the three segments divided by total dry mass of the three segments, and expressed as g/kg. Lower - node of basal bunch, upper- subsequent upper node. n= 36 replicates. Different superscripts show significant difference. ns = not significant.

Supplementary Table 3. The Pearson correlation coefficients (r) of nutrient concentrations between two node positions, opposite to the basal bunch (lower) and the next upper node, at flowering and veraison in three cultivars.

Nutrients	Cabernet Sauvignon		Chardonnay		Shiraz
	Lower vs upper		Lower vs upper		Lower vs upper
	Flowering	Veraison	Flowering	Veraison	Flowering
B.stem					
P	0.582**	0.362*	**ns**	0.813**	0.774**
K	0.648**	0.574**	0.334*	0.685**	0.799**
Ca	0.505**	**Ns**	**ns**	0.765**	0.898**
Mg	0.484**	**Ns**	**ns**	0.726**	0.640**
S	0.614**	**Ns**	0.279*	0.821**	0.897**
B	0.299*	0.643**	**ns**	0.855**	0.827**
Cu	0.519**	**Ns**	**ns**	0.492**	0.698**
Fe	0.509**	**Ns**	**ns**	0.648**	**ns**
Mn	0.586**	0.385*	0.412**	0.778**	0.825**
Mo	**ns**	0.546*	**ns**	0.757**	**ns**
Zn	0.403**	0.492*	**ns**	**ns**	0.546**
Petiole					
P	0.797**	0.919**	0.664**	0.948**	0.824**
K	0.826**	0.663**	0.728**	0.954**	0.812**
Ca	0.816**	0.652**	0.624**	0.957**	0.638**
Mg	0.823**	0.786**	0.631**	0.913**	0.747**
S	0.695**	0.959**	0.490**	0.968**	0.550**
B	0.565**	0.861**	0.831**	0.964**	0.617**
Cu	0.321*	0.577**	0.625**	0.780**	0.748**
Fe	0.549**	0.897**	**ns**	0.882**	0.284*
Mn	0.913**	0.741**	0.773**	0.913**	0.870**
Mo	0.483**	0.879**	**ns**	0.826**	0.558**
Zn	0.347*	0.781**	ns	0.955**	0.400**
Blade					
P	0.699**	0.846**	0.899**	0.712**	0.705**
K	0.544**	0.866**	0.806**	0.428**	0.791**
Ca	ns	0.876**	0.744**	0.413**	0.483**
Mg	0.611**	0.866**	0.607**	0.612**	0.440**
S	0.679**	0.866**	0.689**	0.352*	0.488**
B	0.6341**	0.848**	0.772**	0.725**	0.680**
Cu	0.727*	0.865**	0.708**	0.495**	0.723**
Fe	ns	0.873**	0.543**	ns	0.472**
Mn	0.833**	0.892**	0.912**	0.498**	0.827**
Mo	ns	Ns	ns	ns	ns
Zn	0.514**	0.888**	ns	ns	0.360*

** Correlation is significant at the 0.01 level, * Correlation is significant at the 0.05 level. (n=36).

Petiole segments

The concentrations of all macronutrients varied significantly between the three petiole segments at flowering for Cabernet Sauvignon, Chardonnay and Shiraz (Figure 2) and at veraison for Cabernet Sauvignon and Chardonnay (Figure 3). Differences were less evident for the micronutrients at flowering (Figure 2) and veraison (Figure 3). At flowering, K and Mg concentrations were the lowest in the middle segment of the petiole in all cultivars (Figure 2).

Also, Ca was lowest in the middle segment for Chardonnay and Shiraz but not for Cabernet Sauvignon, and P was the lowest in the middle segment for Cabernet Sauvignon and Chardonnay but not for Shiraz. At veraison, the lowest concentrations for P, K, Ca and Mg were observed in Cabernet Sauvignon but this was not apparent in Chardonnay (Figure 3). N concentration was also lowest in the middle segment in Shiraz at veraison (Figure 1).

Figure 2. Nutrient concentrations in three different petiole segments in three cultivars: Cabernet Sauvignon, Chardonnay and Shiraz at flowering. Macronutrients in Cabernet Sauvignon (a), micronutrients in Cabernet Sauvignon (b), macronutrients in Chardonnay (c), micronutrients in Chardonnay (d), macronutrients in Shiraz (e) and micronutrients in Shiraz (f). Each bar represents mean value of averaged data of two node positions. Petiole segment near blade (blue), middle petiole segment (red), petiole segment near shoot (green). Error bars represent standard error of the mean (n= 36 replicates). Significant differences in nutrient concentrations between petiole segments were determined by performing one way ANOVA (with matching of data from each replicate), followed by comparison of replicate means by Tukey's test ($P<0.05$). Different superscripts show significant difference.

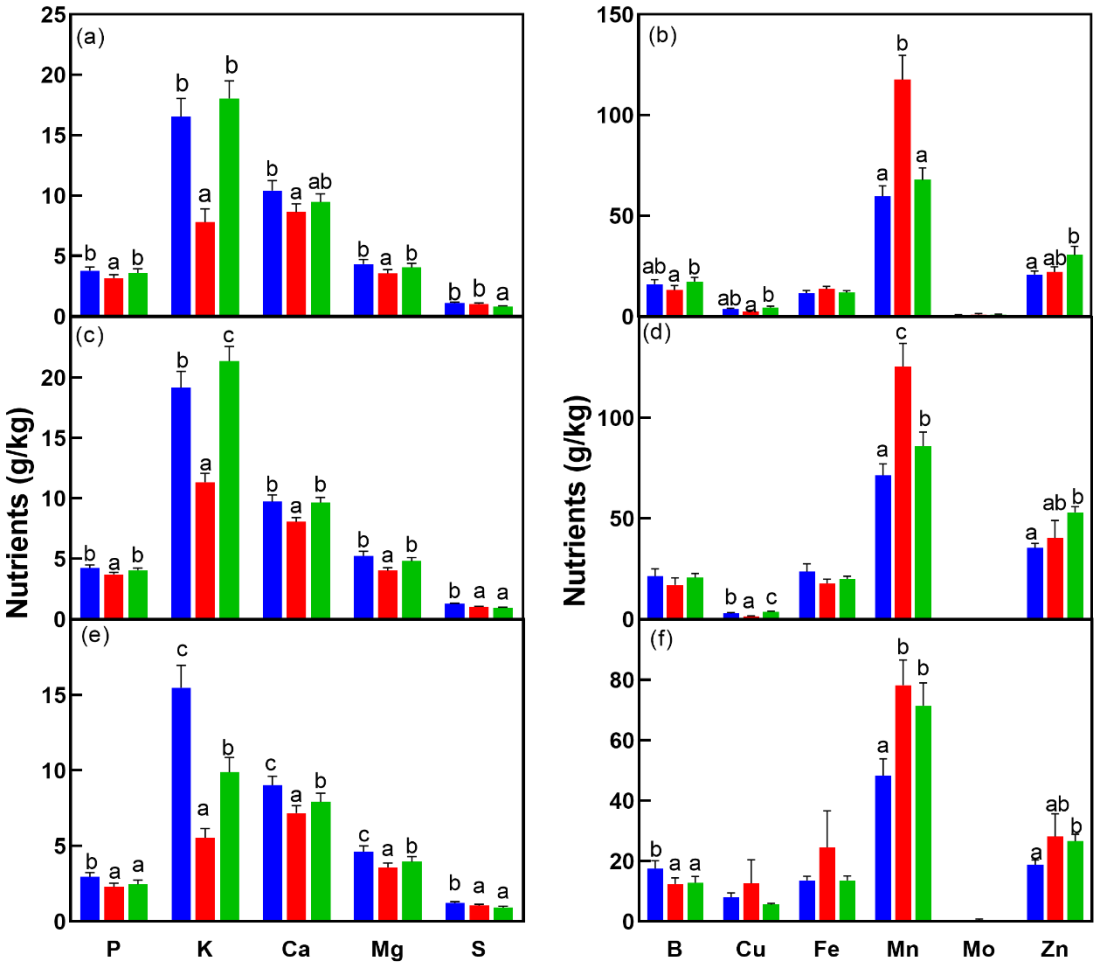
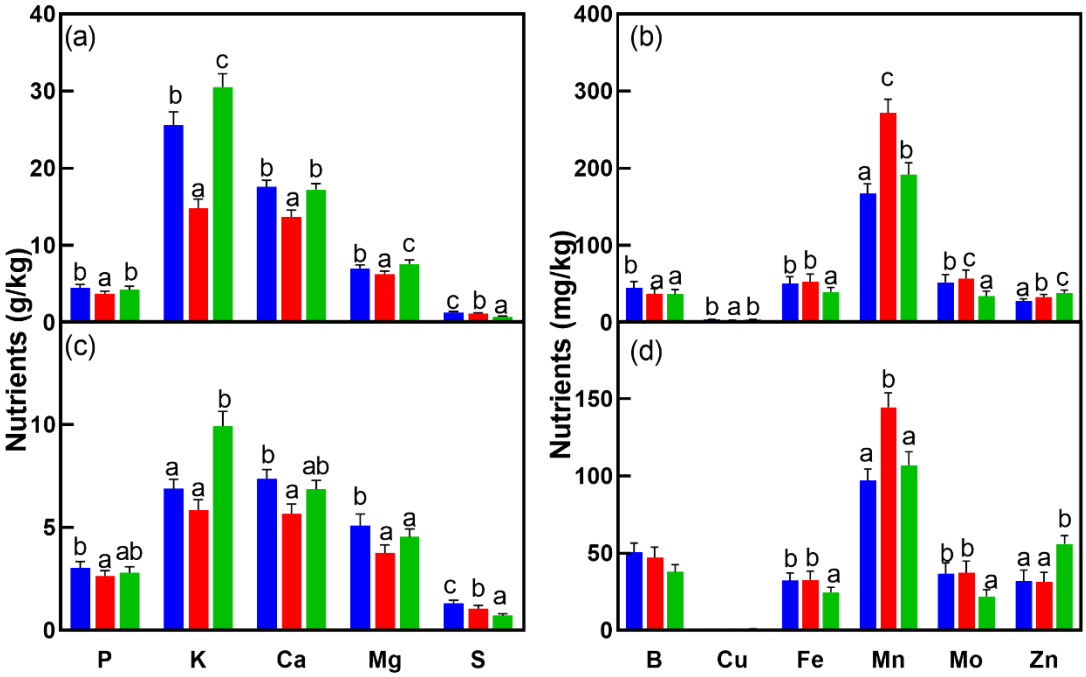


Figure 3. Nutrient concentrations in three different petiole segments in two cultivars: Cabernet Sauvignon and Chardonnay at veraison. Macronutrients in Cabernet Sauvignon (a), micronutrients in Cabernet Sauvignon (b), macronutrients in Chardonnay (c) and micronutrients in Chardonnay (d). Each bar represents mean value of averaged data of two node positions. Petiole segment near blade (blue), middle petiole segment (red), petiole segment near shoot (green). Error bars represent standard error of the mean (n= 36 replicates). Significant differences in nutrient concentrations between petiole segments were determined by performing one way ANOVA (with matching of data from each replicate), followed by comparison of replicate means by Tukey's test (P<0.05). Different superscripts show significant difference.



At flowering, highest concentrations of P, K, Ca and Mg were found in the segment adjacent to the blade in Shiraz, whereas for Cabernet Sauvignon and Chardonnay P, Ca and Mg concentrations were similar in the segments near the blade and near the shoot, but were higher than the concentrations in the middle segment (Figure 2). In Cabernet Sauvignon, K was also similar in the segments near blade and shoot while in Chardonnay the highest level of K was in the segment near shoot. At veraison, highest concentration of Mg was found in the segment near the blade for Chardonnay, but highest in the segment near the shoot for Cabernet Sauvignon (Figure 3). For P and Ca, the concentrations were similar in the segments near the blade and near the shoot in Cabernet Sauvignon and Chardonnay, whereas both were higher than the concentrations in the middle segment in Cabernet Sauvignon but not in Chardonnay. K was highest in the petiole segment adjacent to the shoot in Chardonnay at both flowering and veraison, and in Cabernet Sauvignon at veraison. However, in Shiraz highest concentrations of K were found in the segment adjacent to the blade at flowering. Highest concentrations of S were found in the segment near the blade for Chardonnay and Shiraz at flowering, and at veraison for Cabernet Sauvignon and Chardonnay.

Significant positive correlations were observed between petiole segments for most nutrients at flowering (in all the three cultivars), with the exception of some of the micronutrients (Supplementary Table 4). Similarly, at veraison, significant positive correlations were observed between petiole segments for most nutrients. In Shiraz at veraison, N was also positively correlated between the petiole segments (Supplementary Table 2).

Table 4. Micronutrient concentrations in three different tissue types at two node positions in three cultivars: Cabernet Sauvignon, Chardonnay and Shiraz.

Nutrients (mg/kg)	Tissue	Cabernet Sauvignon			Chardonnay			Shiraz		
		Lower	Upper	Sig[1]	Lower	Upper	Sig[1]	Lower	Upper	Sig[1]
Flowering										
	B. stem	10.1	13.1	Ns	10.4	12.8	ns	6.5	6.9	ns
B	Blade	32.6	28.8	**	18.1	16.7	ns	29.9	24.9	****
	Petiole	16.4	14.7	Ns	21.6	18.1	ns	13.9	14.3	ns
	B. stem	5.2	6.9	**	6.1	6.4	ns	7.4	8.7	*
Cu	Blade	7.8	7.7	Ns	5.8	5.9	ns	12.2	11.4	*
	Petiole	3.5	3.5	Ns	2.9	2.7	ns	9.4	7.2	ns
	B. stem	15.9	16.6	Ns	17.5	18.2	ns	10.3	15.8	ns
Fe	Blade	121.2	106.3	**	101.5	91.9	**	106.5	93.8	****
	Petiole	13.8	10.6	**	21.8	17.8	ns	13.8	19.6	ns
	B. stem	15.3	24.0	***	19.1	30.6	*	13.3	20.0	****
Mn	Blade	126.9	102.1	****	131.0	106.2	****	106.9	88.0	***
	Petiole	89.1	69.5	****	104.8	81.3	***	77.4	54.4	****
	B. stem	1.4	3.1	Ns	0.0	0.0	ns	0.1	1.2	ns
Mo	Blade	0.0	0.0	Ns	0.0	0.0	ns	0.0	0.0	na
	Petiole	0.9	0.7	Ns	0.0	0.0	ns	0.3	0.1	ns
	B. stem	6.7	11.8	**	9.1	13.4	ns	8.5	14.1	***
Zn	Blade	16.5	13.7	**	18.6	14.2	***	17.1	13.7	***
	Petiole	30.4	20.0	*	55.5	33.8	**	27.5	21.7	ns
Veraison										
	B. stem	17.4	19.6	Ns	19.0	16.7	ns			
B	Blade	39.3	41.3	Ns	27.0	29.4	ns			
	Petiole	40.1	36.2	Ns	46.6	41.2	ns			
	B. stem	9.6	12.6	Ns	2.1	1.7	ns			
Cu	Blade	1.6	1.5	Ns	7.7	7.3	*			
	Petiole	3.8	3.5	*	0.8	0.5	ns			
	B. stem	29.8	28.0	Ns	14.3	13.9	ns			
Fe	Blade	80.9	78.2	Ns	163.1	120.5	**			
	Petiole	47.6	42.8	Ns	31.9	25.6	ns			
	B. stem	28.5	38.3	Ns	13.0	14.2	ns			
Mn	Blade	90.2	81.3	Ns	155.5	144.6	ns			
	Petiole	197.6	211.7	Ns	113.1	115.6	ns			
	B. stem	11.5	12.4	Ns	11.7	11.6	ns			
Mo	Blade	0.5	1.5	Ns	1.7	1.0	ns			
	Petiole	47.9	40.3	Ns	33.8	26.2	ns			
	B. stem	6.7	8.2	Ns	5.8	4.1	ns			
Zn	Blade	14.5	11.5	Ns	14.0	10.3	**			
	Petiole	34.0	33.1	Ns	44.5	41.9	ns			

**** P value <0.0001, *** P value <0.001, ** P value <0.01, * P value <0.05, Sig[1] Level of significance. Petiole nutrient concentrations are calculated from total nutrient content in the three segments divided by total dry mass of the three segments, and expressed as mg/kg. Lower - node of basal bunch, upper- subsequent upper node. n= 36 replicates. Different superscripts show significant difference. ns = not significant.

Supplementary Table 4. The Pearson correlation coefficients (r) of nutrient levels between different petiole segments, middle segment (M), segment near blade (L) and segment near shoot (S) at flowering and veraison in three cultivars.

	Cabernet Sauvignon						**Chardonnay**						**Shiraz**		
	M vs L		S vs L		M vs S		M vs L		S vs L		M vs S		M vs L	S vs L	M vs S
	Flow	Verai	Flow	Verai	Flow	Verai	Flow	Verai	Flow	Verai	Flow	Verai	Flow	Flow	Flow
P	.918**	.968**	.885**	.951**	.860**	.961**	.779**	.995**	.798**	.986**	.851**	.983**	.978**	.962**	.967**
K	.699**	.754**	.823**	.822**	.623**	.654**	.818**	.852**	.877**	.878**	.762**	.904**	.868**	.888**	.872**
Ca	.917**	.880**	.858**	.759**	.846**	.697**	.814**	.983**	.811**	.992**	.874**	.971**	.902**	.888**	.898**
Mg	.900**	.871**	.877**	.896**	.846**	.894**	.795**	.986**	.809**	.991**	.880**	.971**	.951**	.923**	.950**
S	.935**	.981**	.867**	.943**	.874**	.960**	.602**	.992**	.592**	.993**	.812**	.989**	.746**	.902**	.736**
B	.857**	.967**	.797**	.976**	.663**	.964**	.937**	.989**	.846**	.966**	.830**	.964**	.928**	.902**	.903**
Cu	ns	ns	.686**	.414*	ns	.466**	.720**	.719**	.796**	.517**	.714**	ns	.950**	ns	ns
Fe	.549**	.990**	.558**	.995**	.728**	.989**	.640**	.982**	ns	.954**	ns	.925**	.528**	.669**	ns
Mn	.925**	.866**	.819**	.829**	.836**	.781**	.810**	.994**	.861**	.988**	.910**	.981**	.846**	.918**	.906**
Mo	.797**	.989**	.795**	.995**	.676**	.985**	ns	.963**	ns	.945**	ns	.962**	.787**	.935**	.767**
Zn	.847**	.941**	0.328	.905**	ns	.909**	ns	.929**	.638**	.962**	.669**	.893**	.678**	.844**	.497**

** Correlation is significant at the 0.01 level, * Correlation is significant at the 0.05 level. In each regression, each data point includes the mean value of upper and lower node positions (n=36 replicates). Flow = flowering; Verai = veraison; ns = not significant.

Discussion

Nutrient concentrations are uneven along the petiole

Nutrient concentrations were not uniform along the length of the petiole with generally lowest concentrations in the central segment (Figures 1, 2, 3). K was particularly low in the middle segment of all three cultivars, sometimes less than 50% of the other two segments (Figures 2, 3). There were some exceptions to this trend, however, which were cultivar specific. As far as we are aware no other studies have examined the nutrient concentrations in different sections of a petiole. Similar to the node itself (Yamaji and Ma 2014), the fleshy basal portion of the petiole adjacent to the shoot may act as a storage hub and exchange site for nutrients. Likewise, we may speculate that the petiole segment near the blade may act as a transient storage pool prior to its partitioning to the various lobes of the blade though this needs to be substantiated. A stem is not merely a support and transport structure but plays a vital role in the storage and release of nutrients (Pate and Jeschke 1995, Furze et al. 2018), and considering that the morphological structure of the petiole is not unlike that of a stem, the petiole may serve similar functions. There is evidence that the petiole can also act as a sequestration site as in the case of chloride (Cl) where the blade appears to be protected from excessive accumulation (Downton 1977). In contrast to the other elements, Mn was consistently higher in the middle segment of the petiole (Figures 2, 3) suggesting that it may be fulfilling its important role in photosynthesis (Alejandro et al. 2020). The presence of nutrient gradients along the petiole has important implications for tissue sampling and confirms that the entire petiole should be tested for consistent results. It is likely that the standards that were developed for Australian viticulture (Robinson 1986) were based on the entire petiole or blade. Parts of the petiole may be inadvertently lost if the petiole is cut rather than broken off the shoot or if the blade is hastily removed by cutting some distance below its junction. Pinching off each blade individually at the junction should overcome this issue.

The concentrations of specific nutrients vary with node position

Node position is important to tissue nutrient assessment at flowering. With the exception of K, blades and petioles positioned opposite the lower bunch had higher nutrients than those collected opposite the upper inflorescence/bunch (Tables 3, 4). The extent of this difference was dependent on the cultivar, sampling time and nutrient itself. A substantial influence of node position was also apparent in Thompson seedless grapevines for some nutrients (K, Ca and Mg) but not others (N, P, B, Zn, Fe and Mn) (Christensen 1969). Unlike our study, however, a wider range of leaf positions from basal leaves to most recently matured leaves and shoot tips were included. In a more recent study in cv. Tempranillo, Romero et al. (2010) found only minor differences in nutrient levels of the blade or petiole collected from opposite to the basal bunch relative to the subsequent upper node. Moreover, this difference decreased as the season progressed. In accordance with their findings, we also noticed a weaker node position effect on nutrient concentrations at veraison compared to that at flowering in Cabernet Sauvignon and Chardonnay (Tables 3, 4). High mobility of K within plants via xylem and phloem could explain the higher concentration of K in the younger tissues at the more distal position (Mpelasoka et al. 2003, White 2012). Christensen (1969) also observed that newly matured leaves had the highest concentration of K with a gradually declining trend along the shoot

towards the older leaves. Taken together, these observations suggest that leaf-sampling position should be consistent, especially earlier in the season due to variability between node positions, and as such sampling leaves only opposite to the basal bunch is advisable. However later in the season either 100% lower, 100% upper, or a 50/50 proportion of each can be adopted.

Tissue nutrient concentrations are dependent on phenological stage and cultivar

As expected, the phenological stage at which the sampling occurred had an important impact on specific nutrient concentrations, but this was dependent on the cultivar and the tissue that was sampled (Table 1). In Cabernet Sauvignon, macronutrient concentrations in leaves (petioles + and blades) and bunchstems were generally higher at veraison than at flowering (with the exception of P and S) but not so in Chardonnay (Table 1). Romero et al. (2010) observed an increasing pattern for Ca and Mg and a decreasing pattern for P and K in both blades and petioles in Tempranillo grapevines between flowering and veraison. In contrast, in our study there was not a consistent relationship in the nutrient concentrations of petioles and blades between flowering and veraison (Table 1). Seasonal changes of nutrient concentrations in both tissues, with a cultivar influence, confirm the importance of developing reference standards for each tissue and each phenological stage (Dominguez et al. 2015), and specific to each cultivar. Under sub-optimal environmental conditions such as water stress, senescence of the basal shaded leaves can be initiated, including those opposite the bunches, and this will need to be considered if sampling at veraison or later in the season.

Significant cultivar differences in the mineral composition of leaves and berries have been previously reported, and this can be explained by differences in absorbing capacity of roots for specific nutrients (Arroyo et al. 1997), root system architecture including depth, vine vigour and vine yield (through bunch number and weight). Cultivar differences in the onset of leaf senescence can also explain the heterogeneity in leaf composition however this was not visually apparent at veraison in the three cultivars examined here.

Blade and petiole nutrients are not always correlated

Various nutrients of the leaf blade correlated well with those of the petiole but this was dependent on the cultivar and the time of sampling (Table 2). This is not too surprising considering that the petiole and leaf blade are dynamic storage sites, with nutrients either accumulating or being remobilised to other sinks. In general, it would be expected that the leaf blade presents a more stable nutrient profile compared to the petiole (Bertoni and Morard 1982) with the petiole a closer reflection of the immediate response to fertilisation considering its greater proportion of vascular tissue. In mature vines with ample storage reserves the extent and direction of mobilisation between perennial components and new vegetative tissues may differ from that of young vines. Our vines were 15 years old with substantial reserves and the relative quantities of a specific nutrient between the petiole and the blade is expected to reflect not only an immediate response to nutrient uptake from the soil but also the dynamic process of remobilisation from various sinks. Romero et al. (2010) observed significant differences between leaf blade and petiole nutrient levels, with higher concentrations of K, Mg, and Zn in petioles and of N, P, Ca, Fe, Mn, Cu, and B in leaf blades in Tempranillo grapevines at different time points throughout the season. Consistent with Romero et al. (2010) our study also showed higher concentration of K and Mg in petioles but higher concentration of Fe and B in leaf blades (Table 1). In Shiraz at veraison, N was more than two fold higher in the leaf blades relative to the petiole (Figure 1). Cultivar differences in

the remobilisation and partitioning of individual nutrients between organs and sinks was apparent despite exposure to the same environmental and cultural conditions. The three cultivars used in this study were all on their own roots and planted at the same time and so rootstock and vine age were not contributing factors to the cultivar differences.

The potential of the bunchstem as an indicator of vine nutrient status

The nutrient concentrations of the bunchstem were more closely correlated to that of the leaf petiole than the blade (Table 2). The closer association with the petiole than the blade is logical because like the petiole the bunchstem forms a transport pathway for nutrients. Bunchstems had generally lower concentrations of most nutrients than relative to petioles or blades, with the exception of K, Cu, Fe and Mo at specific time points (Table 1). It is well known that grapes are the major sink for K (Mpelasoka et al. 2003, Rogiers et al. 2017). High concentration of K in the bunchstem was also apparent in cv. Viosinho Blanc (Arrobas et al. 2014) and can be explained by its role in the transport of assimilates from leaf to berry as well as loading of K itself as a mineral ion into the berries (Mpelasoka et al. 2003, Hawkesford et al. 2012, Rogiers et al. 2017). It will need to be determined if the bunchstem is more representative of the crop's nutrient requirements than the leaf tissues, especially for K in the context of grape composition and quality. If so, bunchstems themselves may be sampled as an indicator of nutrients available for reproductive growth but standards will need to be developed. Any tissue that is targeted for sampling should be easy to identify, collect and handle in large numbers (Wolpert and Anderson 2007), and as such the bunchstem at flowering may be a good choice. However, the impact on yield in low cropping vineyards will need to be considered.

5 Conclusions/Outcomes

I. Diagnostic App:

Grapevine nutritional disorders can result in low productivity and poor quality fruit. After speaking with members of the wine industry it is clear that a diagnostic app would be of great value to them; it addresses symptom confusion and the reluctance to use slow and expensive diagnostic labs. We developed a hydroponic method to create various nutritional deficiency and toxicity symptoms. A comprehensive set of leaf image features form the basis of machine and deep learning algorithms which are subsequently transferred to a mobile phone platform. Models have been developed for healthy, N, Mg, K and Ca deficient leaves that are able to correctly identify the symptom at a 90% or higher accuracy using the same glasshouse leaves. The file size is small enough to fit in the storage space of standard smart phones and the processing time is currently less than 1 second. Further development is however required to improve the accuracy of field vine diagnosis. The project brought together expertise in plant physiology, image recognition, machine learning and deep learning and involved collaborators from Charles Sturt University's School of Computing and Mathematics, the National Wine and Grape Industry Centre and CSIRO.

II. Hyperspectral Imaging:

Based on our preliminary studies, hyperspectral imaging for rapid, cost-effective analysis of plant nutritional status appears to be a promising avenue for further research. Hyperspectral images can potentially facilitate early nutrient disorder detection as the spectral wavelength bands reach beyond the visible range. Early indicators of stress, invisible to the human eye, may be captured so that rapid management responses can be implemented. The advantage of using this technique include the ability to sample and assess more frequently and more precisely within a specific block, potentially allowing the formation of nutritional maps at several points across the season. In the future, hyperspectral cameras mounted on a tractor could potentially acquire these images during normal vineyard maintenance.

III. Refined Tissue Nutrient Sampling Protocols:

A nutrient analysis of leaves is an invaluable tool for determining vine nutritional status and managing vineyard nutrition. Our study aimed to optimise the tissue sampling protocol and to explore the differences in nutrient levels between grape varieties and tissue types. The main findings were that (1) cultivars grown under identical conditions differ in tissue nutrient levels, (2) node position has an impact on tissue nutrient levels, and (3) nutrient levels are not uniform along the leaf petiole.

6 Recommendations

Future R&D directions:

I. Diagnostic app for visual symptom assessment

Recommended Practise Change: No recommendations yet as the tool requires further development. In conjunction with a chemical diagnostic analysis based on appropriate tissue sampling, in future the app may be used to carry out a rapid in-field assessment of unusual visual symptoms.

Potential Benefits: Faster, more accurate diagnosis relative to traditional field manuals

Further Research: Develop methods to optimise diagnosis of field vines under natural conditions. In the long term, broaden app's capabilities to assess micronutrients, assess symptoms for two or more combined nutrient deficiencies, and broaden app's scope to encompass diseases, pests and abiotic stresses.

II. Hyperspectral Imaging for pre-visual symptom assessment

Recommended Practise Change: No recommendations yet as the method requires further research

Potential Benefits: Rapid on-farm decision making for corrective action

Further Research: Trial imaging using portable equipment with a broader wavelength range

III. Tissue sampling protocols for chemical analysis

Recommended Practise Change: Sample the entire petiole at the right location on the shoot. The petiole should be broken off the shoot and the leaf blade pinched from the very end of the petiole. Since node position is important, consistent sampling of a particular node or combination of nodes should be adopted corresponding with the same node(s) used to develop the reference standards. We recommend to build a historical database of a particular cultivar in a particular block to use as a reference standard targeted at the desired berry composition/yield. This practise change has been recommended in four NSW growing regions.

Potential Benefits: Appropriate application of correct formulations, amounts and timing of fertilisers and other soil amendments to optimise yield and fruit quality, reduced waterway pollution, improved soil health.

Further research: Defining the best tissue(s) to sample and the best time(s) to sample during the growing season for maximum benefit to productivity and/or quality.

7 Appendix 1: Communication

Refereed Publications:

1. Debnath S, Paul M, Rahaman DM, Debnath T, Zheng L, Baby T, Schmidtke L, Rogiers SY. 2021. Identifying individual nutrient deficiencies of grapevine leaves using hyperspectral imaging. Remote Sensing 13,3317 https://doi.org/ 10.3390/rs13163317
2. Baby T, Moroni FJ, Gascon-Aldana P, Moroni NC, Holzapfel BP, Schmidtke LM, Walker RR, Rogiers SY. 2021. Characterising leaf petiole, blade and bunchstem nutrient concentration across three cultivars. Australian Journal of Grape and Wine Research 27, https://doi.org/10.1111/ajgw.12496
3. Rogiers SY, Greer DH, FJ Moroni, Baby T. 2020. Potassium and magnesium mediate the light and CO_2 photosynthetic responses of grapevines. Biology 9, 144; doi:10.3390/biology9070144
4. Debnath S, Debnath T, Paul M, Rogiers SY, Baby T, Rahaman DM, Zheng L, Schmidtke L. 2020. Hyperspectral imaging to detect age, defects and individual nutrient deficiency in grapevine leaves. Sensors 20, 1-24: arXiv:2007.05197
5. Rahaman DMM, Baby T, Oczkowski A, Paul M, Zheng L, Schmidtke LM, Holzapfel BP, Walker RR, Rogiers SY. 2019. Grapevine nutritional disorder detection using image processing. PSIVT 2019: Image and Video Technology pp 184-196. Available: https://doi.org/10.1007/978-3-030-34879-3_15

Industry articles:

1. Baby T, Rogiers SY. 2021. Leaf nutrient analysis: a consistent sampling protocol is the key. Practical Winery and Vineyard (USA). In review
2. Baby T, Rogiers SY. 2020. Correct petiole sampling for accurate vine nutrient analysis. Grapevine Management Guide. 2020-2021 , p.52
3. Rogiers SY. Baby T, Oczkowski A, Rahaman M, Zheng L, Paul M, Holzapfel B, Schmidtke L, Walker R. 2020. Smartphone app to assess grapevine nutrient disorders. Grapevine Management Guide. 2020-2021 , p.54-55
4. Baby T, Rogiers SY. 2020. Leaf nutrient analysis – do we need to refine the current sampling protocol? Wine & Viticulture Journal 35 (2) 33-35

Conference proceedings:

1. Baby T, Holzapfel BP, Oczkowski A, Rahaman DMM, Paul M, Zheng L, Schmidtke LM, Walker RR, Rogiers SY. 2019. Vine Nutrition: A Diagnostic Smartphone App for Vine Nutritional Disorders. 17th Australian Wine Industry Technical Conference (AWITC 2019), Adelaide, Australia.

Seminars and Workshops:

1. Face to face- Swanhill (1/08/19) and Mildura (2/08/19) as part of the AWRI Pre-season Pest and Disease Workshop. Vine Nutritional Disorders: Assessing Elemental Status Accurately- Dr Suzy Rogiers
2. Face to face- Griffith (13/08/19) and Tumbarumba (24/09/19) as part of the NSW DPI Spring Grapevine Health Field Days. Vine Nutritional Disorders: Assessing Elemental Status Accurately- Dr Suzy Rogiers

3. Online- NSW DPI Spring Grapevine Health Field Days on 08/09/2020: The development of a smartphone app to identify and manage nutrient deficiency in grapevines - Dr Suzy Rogiers. https://youtu.be/6W0iBJl4G7M. There were about 40 people registered for this event.
4. Online- NWGIC Research Update on 28/10/2020: The development of a smartphone app to identify and manage nutrient deficiency in grapevines - Dr Suzy Rogiers. https://youtu.be/u-agjqhhmXc. There were 100 people registered for this event.
5. Online-NWGIC Research Update on 11/08/2021: Identifying individual nutrient deficiencies of grapevine leaves using hyperspectral imaging - Dr D M Motiur Rahaman. https://youtu.be/b5oR7GvDuT8

Media:

1. NWGIC research sheds new light on petiole sampling. December 2019. Decanted, the NWGIC newsletter.https://www.csu.edu.au/nwgic/about-us/news/feature-stories/stories/2019/nwgic-research-sheds-new-light-on-petiole-tissue-sampling
2. App to help assess and manage nutrient disorders. July 2020. Wine Australia News. https://www.wineaustralia.com/news/articles/app-to-help-assess-and-manage-nutrient-disorders
3. New prototype app plots vine nutritional status. September 2021. Wine Australia News. https://www.wineaustralia.com/news/articles/new-prototype-app-plots-vine-nutritional-status

8 Appendix 2: Intellectual Property

New IP produced by the project include:

1. A grapevine diagnostic app
2. Datasets of RGB images for healthy and nutrient deficient leaves with matching ground-truthed data
3. Data processing pipelines and algorithms for diagnosing nutrient disorders
4. Hyperspectral datasets and indexes for assessing nutrient deficiencies
5. New knowledge on nutrient gradients within the grapevine petiole

9 Appendix 3: References

References for Chapter 2

1. Bhange, M., Hingoliwala, H.A. Smart Farming: Pomegranate Disease Detection Using Image Processing. In: James, A.P., Al-Jumeily, D., Thampi, S.M. Second International Symposium on Computer Vision and the Internet (VisionNet'15) 2015, Procedia Computer Science, vol. 58, pp. 280 – 288. ScienceDirect (2015).

2. Dey, A.K., Sharma, M., Meshram, M.R. Image Processing Based Leaf Rot Disease, Detection of Betel Vine (Piper BetleL.). In: Ibrahim, S.A., Mohammad, S., Khader, S.A. In-ternational Conference on Computational Modelling and Security (CMS 2016) 2016, Proce-dia Computer Science, vol. 85, pp. 748-754. ScienceDirect (2016).

3. Pujari, D.J., Yakkundimath, R., Byadgi, A. Image Processing Based Detection of Fungal Diseases in Plants. In: Samuel, P. Proceedings of the International Conference on Information and Communication Technologies (ICICT 2014) 2014, Procedia Computer Sci-ence, vol. 46, pp. 1802-1808. ScienceDirect (2015).

4. Bravo, C., Moshou, D., West, J., McCartney, A., Ramon, H. Early Disease Detection in Wheat Fields using Spectral Reflectance. Biosystems Engineering 84(2), 137-145 (2003).

5. Stone, C., Chisholm, L., McDonald, S. Effect of Leaf Age and Psyllid Damage on the Spectral Reflectance Properties of Eucalyptus Saligna Foliage. Australian Journal of Botany 53 (1), 45-54 (2005).

6. Jaillais, B., Roumet, P., Pinson-Gadais, L., Bertrand, D. Detection of Fusarium Head Blight Contamination in Wheat Kernels by Multivariate Imaging. Food Control 54, 250-258 (2015).

7. Lu, J., Ehsani, R., Shi, Y., De Castro, A., Wang, S. Detection of Multi-Tomato Leaf Diseas-es (Late Blight, Target and Bacterial Spots) in Different Stages by Using a Spectral-Based Sensor. Scientific Reports 8, Article 2793, 1-11 (2018)

8. Xie, C., Shao, Y., Li, X., He, Y. Detection of Early Blight and Late Blight Diseases on To-mato Leaves Using Hyperspectral Imaging. Scientific Reports 5, Article 16564, 1-11 (2015)

9. Barbedo , J. G.A., Tibola, S.C., .Fernandes, J. M.C. Detecting Fusarium Head Blight in Wheat Kernels Using Hyperspectral Imaging. Biosystems Engineering 131, 65-76 (2015).

10. Wang, D., Vinson, R., Holmes, M., Seibel, G., Bechar, A., Nof, S., et al. Early Detection of Tomato Spotted Wilt Virus by Hyperspectral Imaging and Outlier Removal Auxiliary Classifier Generative Adversarial Nets (OR-AC-GAN). Scientific Reports 9, Article 4377, 1-14 (2019).

11. Lowe, A., Harrison, N., French, A. Hyperspectral Image Analysis Techniques for the De-tection and Classification of the Early Onset of Plant Disease and Stress. Plant Methods, 13(1). 80-92 (2017).

12. Kishore, M., Kulkarni, S.B. Hyperspectral Imaging Technique for Plant Leaf Identification. In: 2015 International Conference on Emerging Research in Electronics, Computer Science and Technology (ICERECT), pp. 209–213. IEEE, Mandya, India (2016).

13. Ariana, D.P., Lu, R. Hyperspectral Waveband Selection for Internal Defect Detection of Pickling Cucumbers and Whole Pickles. Computers and Electronics in Agriculture 74 (1), 137–144 (2010).

14. Ayala-Silva, A., Beyl, C.A. Change in Spectral Reflectance of Wheat Leaves in Response to Specific Macronutrient Deficiency. Advance in Space Research, 35, 305-317 (2005).

15. Pacumbaba Jr.,R.,O., Beyl, C.A. Change in Hyperspectral Reflectance Signatures of Lettuce Leaves in Response to Macronutrient Deficiencies. Advance in Space Research, 48, 32-42 (2011).

16. ABC News Australia, https://www.abc.net.au/news/rural/2019-01-22/aussie-wine-exports-grow-by-10-per-cent/10737050, last accessed 2020/02/19.

17. Liakopoulos, G., Nikolopoulos, D., Karabourniotis, G.: The First Step from Light to Wine: Photosynthetic Performance and Photoprotection of Grapevine (Vitis vinifera L.) Leaves. Functional Plant Science and Biotechnology 1(1), 112-119 (2007).

18. Poni, S., Intrieri, C.: Grapevine Photosynthesis: Effects Linked to Light Radiation and Leaf Age. Advances in Horticultural Science 15(1-4), 5-15 (2001).

19. Greer, D., Weedon, M. Modelling Photosynthetic Responses to Temperature of Grapevine (Vitis vinifera cv. Semillon) Leaves on Vines Grown in a Hot Climate. Plant Cell and Environment 35(6), 1050-64 (2011).

20. Knoll, L., Redl, H. Gas Exchange of Field-grown Vitis Vinifera L. cv. Zweigelt Leaves in Relation to Leaf Age and Position Along the Stem. International journal of vine and wine sciences, 46(4), 281-295 (2012).

21. Martinelli, F., Scalenghe, R., Davino, S., Panno, S., Scuderi, G., Ruisi, P. Advanced Methods of Plant Disease Detection. A review. Agronomy for Sustainable Development 35(1), 1–25 (2015).

22. Mahlein, A.K. Plant Disease Detection by Imaging Sensors – Parallels and Specific Demands for Precision Agriculture and Plant Phenotyping. Plant Disease 100(2), 241-251 (2016).

23. Junges, A.H., Lampugnani, C.S., Almança, M.A.K. Detection of Grapevine Leaf Stripe Disease Symptoms by Hyperspectral Sensor. Phytopathologia Mediterranea 57(3), 399−406 (2018).

24. Lagorio, M.G., Cordon, G.B., Iriel, A. Reviewing the Relevance of Fluorescence in Biological Systems. Photochemistry Photobiology Science 14(9), 1538-59 (2015).

25. Kume, A. Importance of the Green Color, Absorption Gradient, and Spectral Absorption of Chloroplasts for the Radiative Energy Balance of Leaves. Journal of Plant Research 130(3), 501–514 (2017).

26. Terashima, I., Fujita, T., Inoue T., Chow, W.S., Oguchi, R. Green Light Drives Leaf Photosynthesis More Efficiently than Red Light in Strong White Light: Revisiting the Enigmatic Question of Why Leaves are Green. Plant Cell Physiology 50(4), 684–697 (2009).

27. Merzlyak, M.N., Chivkunova, O.B., Melø, T.B., Naqvi, K.R. Does a Leaf Absorb Radiation in the Near Infrared (780–900 nm) Region? A new approach to quantifying optical reflection, absorption and transmission of leaves. Photosynthesis Research 72(3), 263-70 (2002).

28. Ahmed, C.B., Rouina, B.B., Boukhris, M. Changes in water relations, photosynthetic activi-ty and proline accumulation in one-year-old olive trees (Olea europaea L. cv. Chemlali) in re-sponse to NaCl salinity. Acta Physiologiae Plantarum 30(4), 553-560 (2008).

29. Fabre, S., Lesaignoux, A., Olioso, A., Briottet, X. Influence of Water Content on Spectral Reflectance of Leaves in the 3–15- Domain. IEEE Geoscience and Remote Sensing Letters 8(1), 143-147(2011).

30. Dillena, S.Y., Beeck, M.O., Hufkens,K., Buonanduci, M., Phillips, N.G. Seasonal Patterns of Foliar Reflectance in Relation to Photosynthetic Capacity and Color Index in Two Co-occurring Tree Species, Quercus Rubra and Betula Papyrifera. Agricultural and Forest Meteorology 160, 60-68 (2012).

31. Bielczynski, L.W., Łącki, M.K., Hoefnagels, I., Gambin, A., Croce, R. Leaf and Plant Age Affects Photosynthetic Performance and Photoprotective Capacity. Plant Physiology 175(4), 1634-1648 (2017).

32. Liu, L., Huang, W., Pu, R., Wang, J. Detection of Internal Leaf Structure Deterioration Using a New Spectral Ratio Index in the Near-Infrared Shoulder Region. Journal of Integrative Agriculture 13(4), 760–769 (2014).

33. Neuwirthová, E., Lhotáková, Z., Albrechtová, J. The Effect of Leaf Stacking on Leaf Reflectance and Vegetation Indices Measured by Contact Probe during the Season. Sensors 17 (6), 1202-1224 (2017).

34. Gazala, I.F., Sahoo, R.N., Pandey, R., Mandal, B., Gupta, V.K., Singh, R., et.al. Spectral Reflectance Pattern in Soybean for Assessing Yellow Mosaic Disease. Indian Journal of Vi-rology 24 (2), 242-249 (2013).

35. https://mgofmc.org/docs/nutrientdeficiency.pdf. Last Accessed on 18th February 2020.

36. Yuan, F., Bauer, M., E. Comparison of Impervious Surface Area ond Normalized Differ-ence Vegetation Index as Indicators of Surface Urban Heat Island Effects in Landsat Image-ry. Remote Sensing of Environment 106(3), 375-386 (2007).

37. Jayakumar, D. M., Kumar, S. D., Thendiyath, R. Spatiotemporal Variability of Soil Mois-ture and Drought Estimation Using a Distributed Hydrological Model. In: Samui, P., Kim, D., Ghosh, C. Integrating Disaster Science and Management, pp. 451 – 460. ScienceDirect (2018).

38. Choubin, B., Soleimani, F., Pirnia, A., Sajedi-Hosseini, F., Alilou, H., Rahmati, O., Me-lesse, A. M., Singh, V. P., Shahabi, H. Effects of Drought on Vegetative Cover Changes: Investigating Spatiotemporal Patterns In: Melesse, AM, Abtew, W and Senay,G. Extreme Hydrology and Climate Variability: Monitoring, Modelling, Adaptation and Mitigation, pp. 213 – 222. Elsevier (2019).

39. Shahrokhnia, H., Ahmadi,. S.H. Remotely Sensed Spatial and Temporal Variations of Veg-etation Indices Subjected to Rainfall Amount and Distribution Properties In: Pourghasemi, H.R., Gokceoglu, C. Spatial Modeling in GIS and R for Earth and Environmental Sciences, pp. 21-53. Elsevier (2019).

40. Siciliano, D., Wasson, K., Potts, D.C., Olsen, R.C. Evaluating Hyperspectral Imaging of Wetland Vegetation as a tool for Detecting Estuarine Nutrient Enrichment. Remote Sensing of Environment 112, 4020-4033(2008).

41. Mutanga, O., Skidmore, A.K. Red edge shift and biochemical content in grass canopies. ISPRS Journal of Photogrammetry and Remote Sensing 62(1). 34-42 (2007).

References for Chapter 3

Alejandro, S., Höller, S., Meier, B. and Peiter, E. (2020) Manganese in plants: from acquisition to subcellular allocation. Frontiers in Plant Science 11, 300.

Amiri, M.E. and Fallahi, E. (2007) Influence of mineral nutrients on growth, yield, berry quality, and petiole mineral nutrient concentrations of table grape. Journal of Plant Nutrition 30, 463-470.

Arroyo, M., Garcia-Escudero, E., Zaballa, O. and Chavarri, J. (1997) Variety influence in vine (Vitis vinifera L.) nutritional status and must and wine potassium contents. Acta Horticulturae 448, 133-136.

Arrobas, M., Ferreira, I.Q., Freitas, S., Verdial, J. and Rodrigues, M.Â. (2014) Guidelines for fertilizer use in vineyards based on nutrient content of grapevine parts. Scientia Horticulturae 172, 191-198.

AWRI (2010) Grapevine Nutrition. Petiole Analysis. Research to Practise Viti-Notes.

Baby, T., Hocking, B., Tyerman, S.D., Gilliham, M. and Collins, C., 2014. Modified method for producing grapevine plants in controlled environments. American Journal of Enology and Viticulture, 65(2), pp.261-267.

Benito, A., Romero, I., Domínguez, N., García-Escudero, E. and Martín, I. (2013) Leaf blade and petiole analysis for nutrient diagnosis in Vitis vinifera L. cv. Garnacha Tinta. Australian Journal of Grape and Wine Research 19, 285-298.

Bertoni, G. and Morard, P. (1982) Blade or petiole analysis as a guide for grape nutrition. Communications in Soil Science and Plant Analysis 13, 593-605.

Brunetto, G., Ceretta, C.A., Kaminski, J., Melo, G.W.B.d., Lourenzi, C.R., Furlanetto, V. and Moraes, A. (2007) Application of nitrogen in grapevines in the campaign of the Rio Grande do Sul: productivity and chemical characteristics of the grape must. Ciência Rural 37, 389-393.

Christensen, P. (1969) Seasonal changes and distribution of nutritional elements in Thompson Seedless grapevines. American Journal of Enology and Viticulture 20, 176-190.

Christensen, P. (1984) Nutrient level comparisons of leaf petioles and blades in twenty-six grape cultivars over three years (1979 through 1981). American Journal of Enology and Viticulture 35, 124-133.

Christensen, P. and Kearney, U. (2000) Use of tissue analysis in viticulture. Cooperative Extension Work in Agriculture the University of California 10, 1-9.

Clarke, S.J., Lamont, K., Pan, H., Barry, L., Hall, A. and Rogiers, S.Y. (2015) Spring root-zone temperature regulates root growth, nutrient uptake and shoot growth dynamics in grapevines. Australian Journal of Grape and Wine Research 21, 479-489.

Conradie, W. (1981) Nutrient consumption by Chenin Blanc grown in sand culture and seasonal changes in the chemical composition of leaf blades and petioles. South African Journal of Enology and Viticulture 2, 15-18.

Davenport, J.R., Lunden, J.D. and Winkler, T. (2012) Wine grape tissue nutrient concentrations in the inland Pacific Northwest. Communications in Soil Science and Plant Analysis 43, 21-27.

Dominguez, N., García-Escudero, E., Romero, I., Benito Bermejo, A. and Martín Rueda, I. (2015) Leaf blade and petiole nutritional evolution and variability throughout the crop season for Vitis vinifera L. cv. Graciano. Spanish Journal of Agricultural Research 13, 1-17.

Downton, W.J.S. (1977) Influence of rootstocks on the accumulation of chloride, sodium and potassium in grapevines. Australian Journal of Agricultural Research 28, 879-889.

Fallahi, E., Shafii, B., Stark, J.C., Fallahi, B. and Hafez, S.L. (2005) Influence of wine grape cultivars on growth and leaf blade and petiole mineral nutrients. HortTechnology 15, 825-830.

Furze, M.E., Trumbore, S. and Hartmann, H. (2018) Detours on the phloem sugar highway: stem carbon storage and remobilization. Current Opinion in Plant Biology 43, 89-95.

García-Escudero, E., Romero, I., Benito, A., Domínguez, N. and Martín, I. (2013) Reference levels for leaf nutrient diagnosis of cv. Tempranillo grapevine in the Rioja appellation. Communications in Soil Science and Plant Analysis 44, 645-654.

Garcia, M., Gallego, P., Daverede, C. and Ibrahim, H. (2001) Effect of three rootstocks on grapevine (Vitis vinifera L.) cv. Négrette, grown hydroponically. I. Potassium, calcium and magnesium nutrition. South African Journal of Enology and Viticulture 22, 101-103.

Guo, W., Nazim, H., Liang, Z. and Yang, D. (2016) Magnesium deficiency in plants: an urgent problem. The Crop Journal 4, 83-91.

Hawkesford, M., Horst, W., Kichey, T., Lambers, H., Schjoerring, J., Møller, I.S. and White, P. (2012) Functions of macronutrients. In: Marschner's Mineral Nutrition of Higher Plants (Elsevier) pp. 135-189.

Holzapfel, B.P., Smith, J.P. and Field, S.K. (2019) Seasonal vine nutrient dynamics and distribution of Shiraz grapevines. OENO One 53, 363-372.

Keller, M. (2005) Deficit irrigation and vine mineral nutrition. American Journal of Enology and Viticulture 56, 267-283.

Kliewer, W.M. (1991) Methods for determining the nitrogen status of vineyards. Proceedings of the International Symposium on Nitrogen in Grapes and Wine: Seattle, Washington, USA 18-19 June 1991, (American Society for Enology and Viticulture, ASEV) pp. 133-147.

Laibarra, I.R., Bermejo, A.B., Miguel, N.D., Domínguez, E.G.-E. and Rueda, I.M. (2014) Leaf blade and petiole nutritional diagnosis for Vitis vinifera L. cv. Tempranillo by deviation from optimum percentage method. Spanish Journal of Agricultural Research, 206-214.

Lehoczky, E. and Kocsis, L. (1998) Nutrient content of grapevine leaves in various graft combinations. Communications in Soil Science and Plant Analysis 29, 1983-1989.

Mpelasoka, B.S., Schachtman, D.P., Treeby, M.T. and Thomas, M.R. (2003) A review of potassium nutrition in grapevines with special emphasis on berry accumulation. Australian Journal of Grape and Wine Research 9, 154-168.

Pate, J.S. and Jeschke, W.D. (1995) The role of stems in transport, storage, and circulation of ions and metabolites by the whole plant. In: Plant stems, Ed. B. Gartner. (Academic Press: San Diego, CA) pp 177–204.

Porro, D., Stringari, G., Failla, O. and Scienza, A. (2001) Thirteen years of leaf analysis applied to Italian viticulture, olive and fruit growing. Acta Horticulturae 564, 413–420.

Robinson, J.B., Treeby, M.T. and Stephenson, R.A. (1997) Fruits, vines and nuts. Reuter, D.J. and Robinson, J.B., eds. Plant analysis: An interpretive manual (CSIRO Publishing: Collingwood, Vic., Australia) pp. 249–382.

Robinson, J. (1986) Fruits, vines and nuts. In: Plant Analysis, Ed. D.J. Reuter, Robinson, J.B. (Inkata Press: Melbourne, Sydney, pp. 12) pp. 120-147.

Robinson, J. (1988) Grapevine Nutrition. In: Viticulture Practices, Ed. B. Coombe, Dry, P. (Winetitles: Adelaide, South Australia) pp. 178-208.

Robinson, J., Nicholas, P. and McCarthy, J. (1978) A comparison of three methods of tissue analysis for assessing the nutrient status of plantings of Vitis vinifera in an irrigated area in South Australia. Australian Journal of Experimental Agriculture 18, 294-300.

Rogiers, S.Y., Coetzee, Z.A., Walker, R.R., Deloire, A. and Tyerman, S.D. (2017) Potassium in the grape (Vitis vinifera L.) berry: transport and function. Frontiers in Plant Science 8, 1629.

Romero, I., García-Escudero, E. and Martín, I. (2010) Effects of leaf position on blade and petiole mineral nutrient concentration of Tempranillo grapevine (Vitis vinifera L.). American Journal of Enology and Viticulture 61, 544-550.

Schaller, K. (2006) Evaluation of the nutritional status of perennial crops–possibilities and pitfalls of leaf analysis. Bulletin of University of Agricultural Sciences and Veterinary Medicine Cluj-Napoca. Horticulture 63, 5-10.

Schreiner, R.P. and Scagel, C.F. (2017) Leaf blade versus petiole nutrient tests as predictors of nitrogen, phosphorus, and potassium status of 'Pinot Noir'grapevines. HortScience 52, 174-184.

Stellacci, A., Armenise, E., Caliandro, A. and Rubino, P. (2010) Relationships between soil characteristics and leaf nutrient concentrations in grapevine. Acta Horticulturae 868, 135-142.

Tandonnet, J.P., Soyer, J.P., Gaudillère, J.P., Decroocq, S., Bordenave, L. and Ollat, N. (2008) Long term effects of nitrogen and water supply on confered vigour and yield by SO4 and Riparia Gloire de Montpellier rootstocks. OENO One 42, 89-98.

Treeby, M.T., Goldspink, B.H. and Nicholas, P.R. (2004) Vine nutrition. In: Grape Production Series No. 2. Soil, irrigation and nutrition, Ed. B.P. Nicholas (South Australian Research and Development Institute: Adelaide, South Australia) pp. 173-197.

Uchida, R. (2000) Essential nutrients for plant growth: nutrient functions and deficiency symptoms. Plant Nutrient Management in Hawaii's Soils, 31-55.

White, P.J. (2012) Long-distance transport in the xylem and phloem. In: Marschner's Mineral Nutrition of Higher Plants (Elsevier) pp. 49-70.

Wolpert, J.A. and Anderson, J.M. (2007) Rootstock influence on grapevine nutrition: minimizing nutrient losses to the environment. In: Proceedings of the California plant and soil conference, Sacramento, CA, USA. Ed. California Chapter of the American Society of Agronomy (California Chapter of the American Society of Agronomy: Davis, CA) pp. 77–83.

Yamaji, N. and Ma, J.F. (2014) The node, a hub for mineral nutrient distribution in graminaceous plants. Trends in Plant Science 19, 556-563.

10 Appendix 4: Staff

Name	Organisation	Role
Suzy Rogiers	NSW Department of Primary Industries	Project Lead
Lihong Zheng	Charles Sturt University	Principal Investigator
Manoranjan Paul	Charles Sturt University	Principal Investigator
Bruno Holzapfel	NSW Department of Primary Industries	Principal Investigator
Leigh Schmidtke	Charles Sturt University	Principal Investigator
Rob Walker	CSIRO	Principal Investigator
Tintu Baby	Charles Sturt University	Postdoctoral Fellow
Alex Oczkowki	Charles Sturt University	Programmer
Motiur Rahaman	Charles Sturt University	Postdoctoral Fellow
Sourabhi Debnath	Charles Sturt University	PhD Student
Tanmoy Debnath	Charles Sturt University	PhD Student
Francesca Moroni	Charles Sturt University	Technical Assistant
Nicholas Moroni	Charles Sturt University	Technical Assistant
Pedro Gascon-Aldana	Charles Sturt University	Technical Assistant
Dewatage Perera	Charles Sturt University	Technical Officer
Di Hubbard	Charles Sturt University	Technical Officer
Helen Pan	Charles Sturt University	Technical Officer
Krista Mentjox	NSW Department of Primary Industries	Project Officer- Business Development

11 Appendix 5: Survey questions

- How do you currently diagnose grapevine nutritional disorders, diseases and pests? (Field Manuals/Google/Diagnostic Labs/Experience/Other)
- Have you ever sent soil or petiole samples to a diagnostic lab for nutritional information? If so, how often?
- Have you ever sent diseased tissue or pests for diagnosis to pathology/entomology labs?
- Would you consider using a Smartphone App to help with pest/disease/ nutritional diagnosis?
- Are you currently using any Smartphone Apps in decision making on pest/disease/ nutritional disorders management in your vineyard? If yes, which one? What are the features you like / dislike?
- Please rank the following issues with (1) being the highest priority for your operation:

Nutrition Disease Pest Other

- What is the minimum accuracy for a correct diagnosis that you will tolerate?
- How long are you prepared to wait for the processing to take place on the phone?
- Would you prefer to take images in the vineyard or would you prefer to take the samples inside and take images of them inside?
- Do you want to be able to tag the geolocation of the disorder for future reference?
- Do you want to have links to fact sheets and potential treatments of the disorder?
- Would you like to have access to real time incidence information of the disorder for your region?
- Do you want to have the capacity to create a historical database of the disorders for your site?
- How do you rate your network connection of your vineyard? (poor, good, super)?
- Are there any functions you would like us to add in the App?
- Would you like us to get in touch with you via email to learn more about the new App? If so, please leave contact details here:
- What other goals can we help you achieve?

12 Appendix 6: Acknowledgements

This research was supported by funding from Wine Australia. Wine Australia invests in and manages research, development and extension on behalf of Australia's grape growers and winemakers and the Australian Government.

We would like to thank all participants from the wine industry who took out time to complete the survey, undertake user testing and participate in the interviews.

Technical assistance by Francesca Moroni, Pedro Gason-Aldana, Di Hubbard, Dewatage Perera, Helen Pan and staff from CSU's diagnostic lab is greatly appreciated.

Thanks to Krista Mentjox, NSW DPI Business Development at the GATE for leading the commercialisation process.